NASA CR-2592
Vol. II of III

RADAR DERIVED SPATIAL STATISTICS OF SUMMER RAIN

DATA REDUCTION AND ANALYSIS

by

T.G. Konrad and R.A. Kropfli

Prepared by

APPLIED PHYSICS LABORATORY
THE JOHNS HOPKINS UNIVERSITY
Johns Hopkins Road
Laurel, Maryland 20810

for Goddard Space Flight Center

NATIONAL AERONAUTICS AND SPACE ADMINISTRATION • WASHINGTON, D. C. • SEPTEMBER 1975

TECHNICAL REPORT STANDARD TITLE PAGE

1. Report No.	2. Government Accession No.	3. Recipient's Catalog No.
NASA CR 2592		

4. Title and Subtitle	5. Report Date
Radar Derived Spatial Statistics of Summer Rain - Data Reduction and Analysis, Volume II of III	September 1975
	6. Performing Organization Code
7. Author(s) T. Konrad and R.A. Kropfli	8. Performing Organization Report No.
9. Performing Organization Name and Address Applied Physics Laboratory The Johns Hopkins University Johns Hopkins Road Laurel, Maryland 20810	10. Work Unit No.
	11. Contract or Grant No. Agree. S-70248AG NASA/DOD
12. Sponsoring Agency Name and Address National Aeronautics & Space Administration Washington, D.C. 20546	13. Type of Report and Period Covered Contractor Report
	14. Sponsoring Agency Code

15. Supplementary Notes

16. Abstract

This is Volume II of the three volumes constituting the final report on the rain statistics program. In this volume, the data reduction and analysis procedures are discussed along with the physical and statistical descriptors used. The statistical modeling techniques are outlined and examples of the derived statistical characterization of rain cells in terms of the several physical descriptors are presented.

Recommendations concerning analyses which can be pursued using the data base collected during the experiment are included.

17. Key Words (Selected by Author(s))	18. Distribution Statement
Precipitation, radar, radar-weather, space communications, rain scatter, rain modeling, rain cell statistics, rain cell descriptions	Unclassified - Unlimited Cat 47

19. Security Classif. (of this report)	20. Security Classif. (of this page)	21. No. of Pages	22. Price*
UNCLASSIFIED	UNCLASSIFIED	187	$7.00

For sale by the National Technical Information Service, Springfield, Virginia 22161

EXECUTIVE SUMMARY

The experimental program designed to provide the basic radar data for the statistical modeling of summer rain storms is described in a companion report, (Volume I) entitled, "Radar Derived Spatial Statistics of Summer Rain -- Experiment Description," NASA CR-2592. In that report, the equipment used, including the radar, signal processing and recording instrumentation, the data collection procedures and other aspects of the experiment itself were discussed. In this report the data reduction and analysis procedures are discussed along with results of the statistical modeling analysis. Examples of the derived statistical characterization of rain cells in terms of several physical descriptors are presented.

Primary data for the reduction and analysis phases of the program were on the computer-compatible digital magnetic tapes containing the integrated log power received in each of 871 range gates recorded during PPI raster scans through the field of rain cells. The first step in the reduction process was to identify the peaks or local maxima in power received for each sweep in a scan. All the data for a given sweep were read into core memory of the NASA/GSFC IBM 360/95 computer as a two-dimensional array. The computer then performed a search routine in this array to find the maxima of log power received. Although all the data for a sweep were read into core, only those areas which contained rain cells were searched. Thus, areas which contained no rain or areas of known ground clutter were eliminated. Having identified the peaks or core locations, the computer then generated specific contours of reflectivity about each peak using a point-by-point, compare-and-minimize algorithm. The reflectivity referred to in this report is in fact the equivalent reflectivity factor. No attempt was made to account for the state of the precipitation, i.e., ice vs water. Two types of contours may be generated: (1) contours relative to the peak value; and (2) contours in absolute terms, e.g., 30, 40, 50 dBZ. In the present analysis only the relative contours were used.

The following parameters were then calculated:

a. Area within the specified contour

b. Length and width of each contour through the centroid

c. Orientation of the major axis through the centroid

d. Altitude at the location of the peak

e. All inter-peak distances.

These parameters along with the value of the reflectivity factor and coordinates of the peaks make up the physical descriptors calculated for each peak.

The next step was to identify those peaks in each scan which make up a rain cell. The computer assigned a number to each peak found in a sweep. Although the same areal search pattern was following by the computer, the peak numbers associated with a given cell are not necessarily the same from sweep to sweep, for example, due to spurious local maxima. The following procedure was used to identify those peaks in each sweep of a scan which made up the same cell. The location, range and azimuth of all peaks found in a scan were plotted. The cells were identified based on the fact that those peaks associated with the same rain cell are clustered together. A cell was defined as an identifiable cluster of peaks with consecutive sweep numbers. All cell identification was performed by one individual so that the same set of criteria was used, subjective though they may be.

In order to ensure that the cells used in the statistical analysis were (essentially) independent, only those raster scans separated by one half hour were used. This eliminated those scans which were taken very rapidly for time history and cell development analysis. The assumption was that although the cell itself may be the same for scans separated by one half hour, the characteristics have changed sufficiently so that the cells may be treated as independent.

With the foregoing restriction on the data, a total of 185 scans through fields of rain cells on 21 days during the four-month observation period were included in the statistical analysis with a total of 1141 identifiable cells. These cells were classified and categorized as follows. Those cells whose peak reflectivity was above 30 dBZ at the lowest elevation angle were classified as rain-on-the-ground cells or ROG cells. The lowest elevation angle of the PPI sweeps was 0.5 deg and at the maximum range of observation, 70 nmi, corresponds to an altitude of 2 km. Those cells whose radar return began at altitudes above 2 km were classed as Virga. (Note that this definition differs from that commonly used in meteorology.) The reflectivity threshold of 30 dBZ was chosen to restrict the analysis to those cells with high core reflectivities which represent a problem for communications from the standpoint of attenuation and interference caused by scattering. The cells in the ROG class were further subdivided into reflectivity categories according to their reflectivity value at the lowest elevation angle. Categorizing the cells in this manner allows a comparison with ground-based measurements of rainfall rate from rain gages and provides a means for extrapolating the data from this experiment to other locations based on the frequency of occurrence of rain intensities at ground level.

Frequency distributions of the peak or core reflectivities, areas of the 10 dB down contour about the peak, the contour length-to-width ratio and the orientation of the contour major axis were formed for each class and category of cells as a function of altitude. Two profile-shape parameters and their distributions were compiled; the reflectivity ratio which is the ratio of the maximum reflectivity factor in a cell to that at the lowest elevation angle; and the altitude of the maximum reflectivity. The arithmetic mean, mode, median, and standard deviation for all the foregoing distributions were also calculated.

The distributions of the number of cells were compiled in two ways: (1) according to category for a given altitude interval, and (2) at each altitude for a given category. Of particular interest is the distribution of cells in the lowest altitude interval since this distribution may be compared with ground-based rainfall rate data from other locations for extrapolation purposes.

The question of cell spacing is of importance in siting terminals of communication networks. One technique for improving communication link reliability is via space diversity. The spacing of diversity terminals to minimize the effects of the rain is directly related to the distribution of distances between the rain storms. The distance between all identified cells used in this study, taken two at a time, were measured. The population of scans, sweeps and cells was the same as that used in the other investigations discussed earlier. The resulting frequency distribution and cumulative frequency show the most probable spacing to be 12 nmi with a median value of approximately 18 nmi.

Statistical descriptions of rain cells in terms of a variety of physical cell parameters have been generated along with the probability of occurrence and altitude extent for various storm classes and categories. The various frequency distributions, cumulatives and conditional probabilities have been cast in a way which is most useful from the communications standpoint and may not be directly applicable in other disciplines. It is emphasized, however, that the data accumulated during the experiment represents a general data base which can be used again in the future to answer different questions than those dealt with to date.

VOLUME II--DATA REDUCTION AND ANALYSIS

CONTENTS

CONTENTS (Continued)

CONTENTS (Continued)

CONTENTS (Continued)

CONTENTS (Continued)

ILLUSTRATIONS

ILLUSTRATIONS (Continued)

ILLUSTRATIONS (Continued)

TABLES

1. GENERAL DESCRIPTION OF RADAR DATA REDUCTION PROCEDURE

Primary radar data for the rain cell analysis are the digital tapes containing integrated log power received from PPI sweeps through rain storms as described in the companion report, Volume I, entitled, "Radar Derived Spatial Statistics of Summer Rain -- Experiment Description," NASA CR-2592. The data reduction plan set forth here and in Ref. 1, results in printed listings and card output containing the following rain cell descriptors:

a. Peak equivalent reflectivity factor (Z_e value) and coordinates of the peak

b. Area, direction, height, length, and width of specified contours

c. Spacings between cells.

Note that hereafter in this report, the equivalent reflectivity factor will be referred to simply as the reflectivity or reflectivity factor.

This information forms the basic input data for the data processing program which determines statistical descriptions of the rain cell descriptors.

The flow chart in Figure 1.1 indicates the data reduction plan. Video signals, either real time or from the playback of a video tape, are processed by the radar video processor as described in Volume I. The result is a computer-compatible, digital magnetic tape containing integrated log power received from 871 range bins. The data tapes are the input to the "first pass" program as indicated in Figure 1.1.

An entire data file, i.e., all recorded data from a single sweep, is read into core of the IBM 360/95. Only particular areas specified by the "analyst" indicated in Figure 1.1 are processed by the first pass program. The analyst examines the PPI for regions of interest and specifies range and angle limits for as many as 10 areas by means of control cards. The first pass program then searches the areas for local maxima of log power received and generates the desired contours about those peaks.

Contours are specified by an identification number unique to the contour. Each sweep is identified by the following information: year, day of year, scan number of day and sweep number of scan. Each peak is labeled consecutively by the first pass program in the order in which the peaks were found. Thus, a unique contour identification

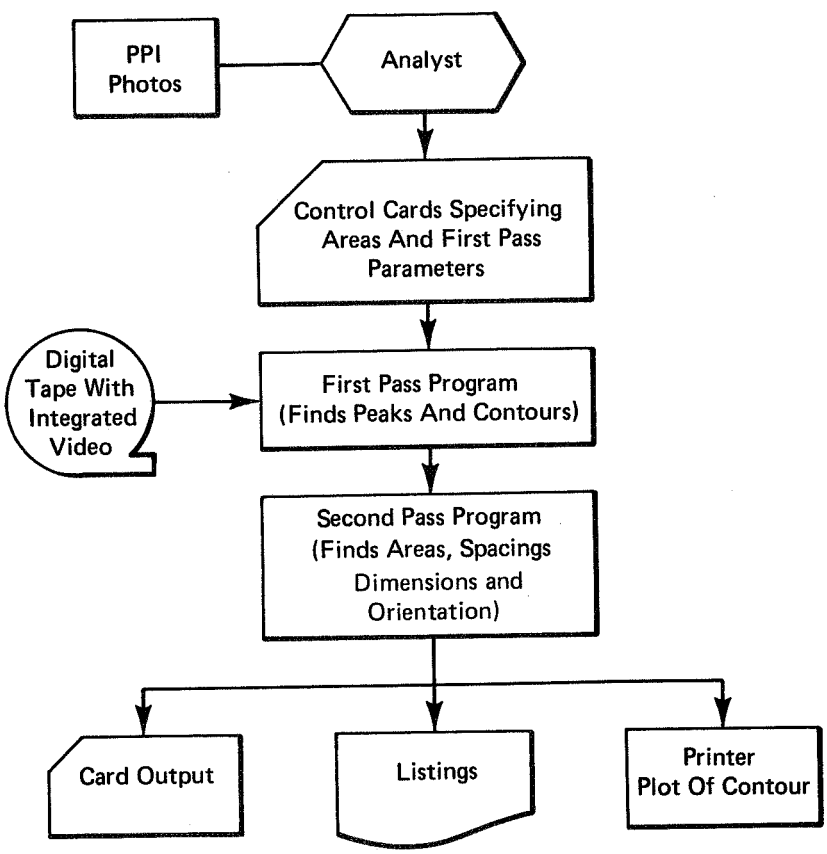

Figure 1.1. Data Reduction Flow Diagram

number is possible with this information plus the contour value. An example might be as follows: 3/220/37/5/2/6. This would represent (right to left) the 6 dB contour about peak #2 in sweep #5 of scan #37 on day 220 in 1973.

The second pass program calculates the area of each contour, the maximum and minimum dimension through the centroid of the area, the orientation of the maximum dimension and the distance between all peaks. Output is on cards containing all the peak and contour information, a listing of all the foregoing and a printer plot of the contour itself.

The discussion in the next two major sections concerning the First and Second Pass data reduction computer programs is taken from References 2, 3 and 4.

2. FIRST PASS PROGRAM

2.1 GENERAL DESCRIPTION

Figure 2.1 indicates the relationships between the various arrays referred to as "areas," "range intervals," and the "Z array" used by the program. These terms and others used in the following discussion are defined as follows:

- Raw data or Z array: The two dimensional array representing integrated log power received from a radar pulse volume at a particular range and angle.

- Summed array: A two dimensional array of each value representing the sum of many independent radar pulse volumes.

- Area: One of several regions of interest within the Z array which will be processed by the computer. The boundaries of these areas are specified by control parameters. Data outside of the areas are not considered in peak search and contouring routines.

- Range interval: A block of data from the raw data array in which equal numbers of azimuth and range elements are summed to form elements of the summed array. These summed elements

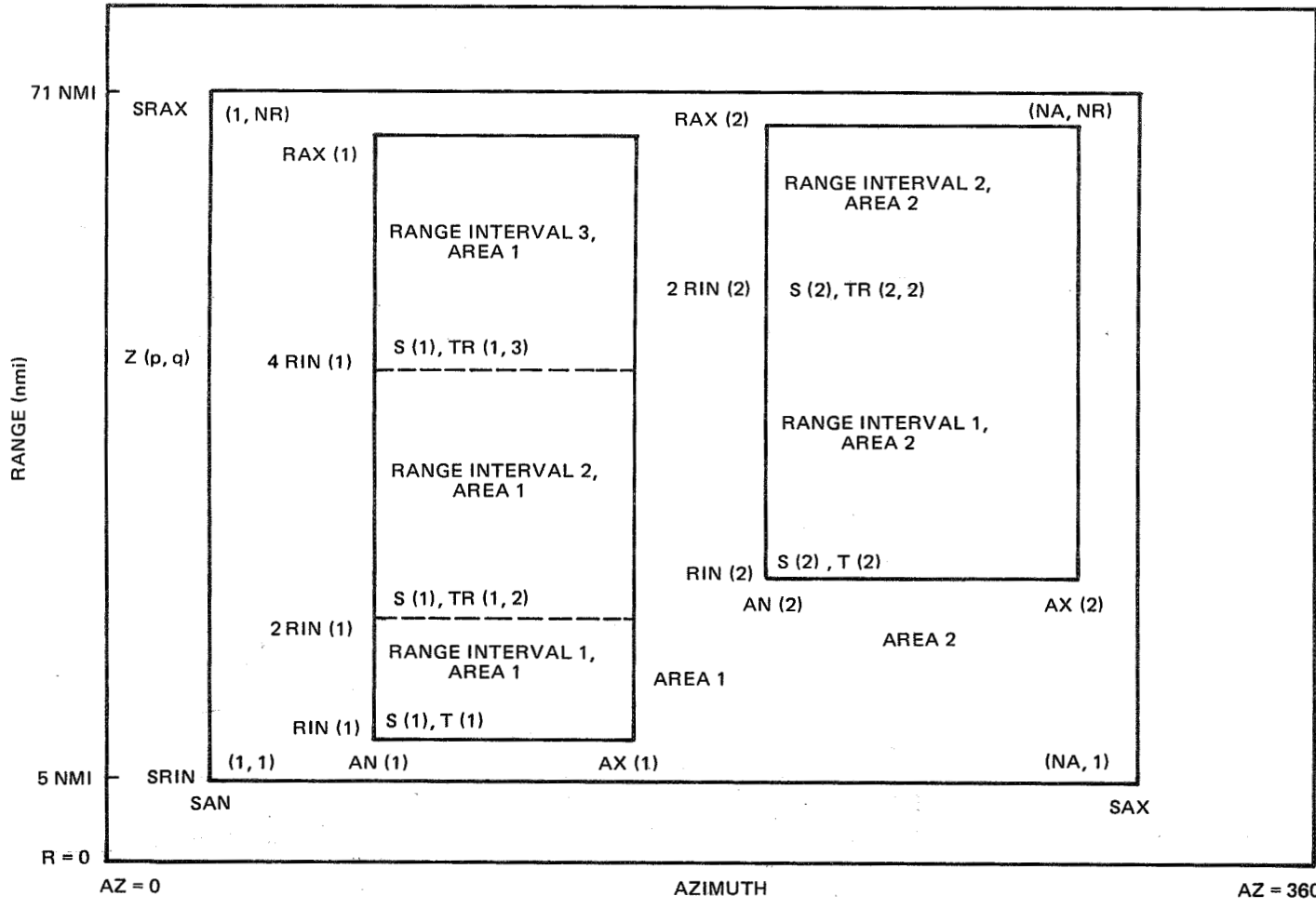

Figure 2.1. Areas, Data Arrays, and Range Intervals

represent log power received, averaged over an area having the approximate dimensions specified by the input parameter DEL. The number included in the average decreases with increasing range interval number because of the increase in the sample volume with range.

- Range bin number: The range coordinate referred to the origin of the Z array.

- Angle bin number: The angle coordinate referred to the origin of the Z array.

- Complete range interval: Range interval with twice the number of points as the preceding interval. Such an interval ends at a range 2^J RIN(I) where J is the range interval number.

Generally, an entire PPI sweep was not stored since angle limits were specified for the radar video processor to limit recorded data during the experiment. Each element of the Z array is an 8 bit byte representing log power received. In Figure 2.1, out of the possible maximum scan of 360^o in azimuth, only the data specified by the azimuth interval (SAX, SAN) were stored on tape. The range limits of the recorded data were fixed by the radar video processor. Data between 5 nmi and 71 nmi were recorded for a 1 μs radar pulse (the outer limit is halved if a 0.5 μs pulse is used). All data during this experiment were acquired using a 1 μs pulse.

Although all recorded data are core-loaded, only the areas specified by the analyst will be processed. Control cards are used to specify azimuth and range limits for area (I), namely, AX(I), AN(I), RAX(I), and RIN(I). (See Figure 2.1.) These limits were determined by an analyst who selected areas within the stored regions from PPI photographs made during the experiment. Each area was divided by the program into as many as four range intervals. Figure 2.1 shows two areas, one having three range intervals and the other having two range intervals. Any number of areas up to ten may be specified; each area may extend over an angle not to exceed 120^o.

The basic sequence of operations performed by the program is shown in Figure 2.2. After a complete file of data containing one sweep has been read into core as the two-dimensional Z array, coordinates defining the areas of interest within the Z array are computed from

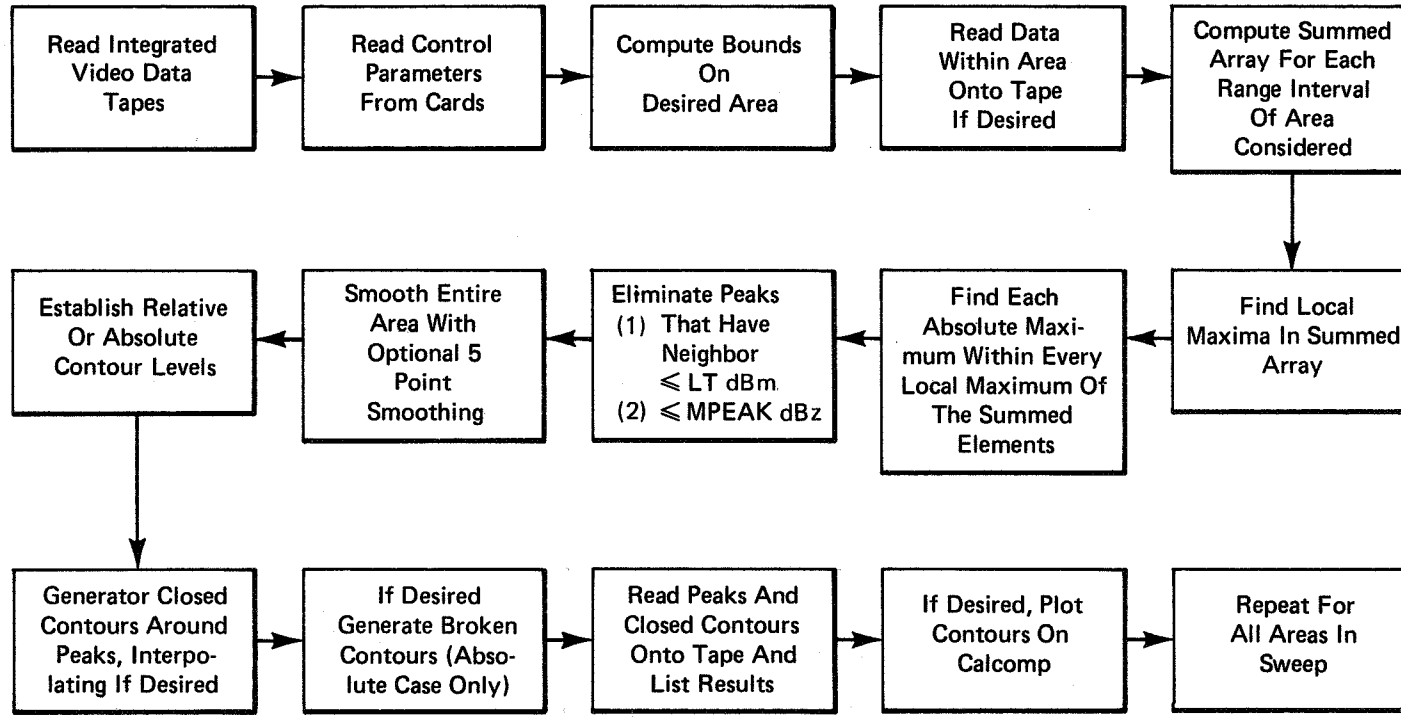

Figure 2.2. Peak Search and Contouring Program — First Pass Program

range and angle limits specified on input cards. These coordinates are computed in terms of bin numbers referenced to the origin of the Z array (SRIN and SAN in Figure 2.1). All bin numbers are referred to the origin of the Z array unless otherwise stated. Note that the program uses a table that relates angle bin number to angle, in degrees, and therefore the generated contours are not distorted by variations in the scan rate. The angle used in the table is taken directly from each record on the data tape. Although the entire Z array is read into core, no further consideration is given to data outside of these areas.

The first step in the peak search routine is to form a summed array out of the raw data within an area. The summed array is described in more detail in Section 2.3. The peak search is thus carried out in a more efficient manner on this summed array. Each area is divided into range intervals within which the numbers of points constituting a summed element are the same. The intervals are chosen by the program in a way that makes the azimuth distance between summed elements vary from DEL/2 up to a maximum of DEL where DEL is an input parameter in meters. The number of range bins included in each summed element is determined by the program so that the range distance between summed elements is DEL for all range intervals. Thus the area represented by each summed element varies from $(DEL)^2/2$ to DEL^2, and each element can contain from 48 to 336 raw data points if the pulse length is 1 μs and DEL = 2000 m. These operations are performed on the raw data representing unnormalized log power received.

Next, local maxima in the summed array are found for each range interval of the area under consideration. This is done simply by finding all summed elements which are larger than each of their four nearest neighbors. No range normalizing or thresholding is performed up to this point. After these local maxima are found in the summed array, the absolute maxima of the raw data constituting these sums are found. To be considered a true maximum each of these selected raw data points must pass two further tests: They must not have any of their four nearest neighbors at or below the specified input threshold, LT (dBm); and they must be greater than the minimum reflectivity MNPEAK (dBZ) when transformed from log power received to reflectivity factor. These tests eliminate echoes from point targets and radar interference, and also eliminate from consideration weak reflecting cells, i.e., peaks less than some specified reflectivity.

The next step is to smooth the data within the areas with a five-point smoothing technique, the amount of smoothing and the number of repetitions being controlled by input parameters. Note that smoothing is restricted to the specified areas and is performed on the unnormalized log power received.

The calculation of the contour level or levels is now performed if levels relative to the previously determined peaks are desired. If absolute contours are desired, the absolute input values are used directly.

Closed contours, i.e., contours that are contained within an area, are now generated. Only points being considered for the contour are range-normalized instead of all points within the area. Any contour that passes out of the area is terminated and the next peak is considered. For this reason the contours must be requested in decreasing order, otherwise some contours might not be considered by the program. As an option, the program provides for linear interpolation between data points.

The program will also generate contours that pass through the area boundary. This option is available only if absolute contours are requested. All closed contours are generated first and then, if desired, an area boundary search is performed to determine the existence of "broken" contours. Once the end points are established, the "broken" contours are generated in a manner similar to that used to generate the closed contours.

The results of the first pass program consist of a listing of the peaks and their coordinates, and the contour values and their coordinates.

2.2 INPUT TO FIRST PASS PROGRAM

2.2.1 Tape Input

Three different input tape formats, depending on the data source, can be read by the program. The "real time" format is for digital tapes recorded during the experiment, i.e., summer 1973, the "early video" format is for data processed from video tapes from the summer of 1972, and the "late video" format is for data taken from all video tapes subsequent to 1972. These three formats are listed in Tables 2.1, 2.2 and 2.3, respectively. Parameters common to all three formats include year, day of year, scan number of day, scan type, and angle limits of recorded data. Other real-time tape input parameters contained in the header records are the sweep number of the scan, pulse width, and the value of the high level signal. All these parameters can be overridden with card input if necessary.

No parameters other than the common parameters listed above are read from the "early video" formatted tapes. Conversely, the "late

Table 2.1

Tape Format I - Real-Time Runs

	Byte #1	Data	Range
Header:	1	Record Type = 1	1
	2,3	Day of Year	1-365
	4	Year	0-99
	5	Scan # of Day	0-255
	6	Scan Type	1-3
	7,8	Initial Az	$0-(2^{16}-1)$
	9,10	Initial El	$0-(2^{16}-1)$
	11,12	Final Az (El)	$0-(2^{16}-1)$
	13,14	Angle Difference	$0-(2^{16}-1)$
	15,16	Data Angle #1	$0-(2^{16}-1)$
	17,18	Data Angle #2	$0-(2^{16}-1)$
	19	Sweep # of Scan	0-255
	20,21	Scan Rate	$0-(2^{16}-1)$
	22	Scan Direction	0-1
	23	PRF	1-3
	24	Pulse Width	1-2
	25	Integration Cycle	1-4
	26	High Level Cal.	0-99
	27	Error Flag-Antenna Vel.	0-3
	28	Error Flag-Antenna Pos.	0-3

Table 2.1 (Continued)

	Byte #1	Data	Range
	29	Flag - Noise	0-1
	30	Flag - Low Cal.	0-1
	31	Calibration Level	0-99
RVP Rec #1	32	Data Flag	
	33-35	Time	
	36-37	Start Az	
	38-9	Start El	
	40-910	Integ Video	
	911	Zero	
	912-914	High Level Cal.	
	915	Zero	
	916-920	Noise	
	921	Zero	
	922-930	Low Level Cal.	
RVP Rec #2	931-1829		
RVP Rec #3	1830-2728		
RVP Rec #4	2729-3627		

Total Length 3627

Table 2.2

Tape Format II - Early Video

	Byte #	Data
Header	1	Record Type = 2
	2,3	Day of Year
	4	Year
	5	Scan # of Day
	6	Scan Type
	7-14	Unused
	15,16	Data Angle #1
	17,18	Data Angle #2
	19-31	Unused
RVP Rec #1	32	Data Flag
	33-53	Digital Data
	54-1013	960 Bytes Integ Video
RVP Rec #2	1014-1995	
RVP Rec #3	1996-2977	
RVP Rec #4	2978-3959	

Total Length 3959

Table 2.3

Tape Format III - Later Video

	Byte #	Data
Header	1	Record Type = 3
	2-31	Same As Early Video, Format II
RVP Rec #1	32	Data Flag
	33-53	Digital Data
	54-924	Integ Video
	925	Zero
	926-928	High Level Cal.
	929	Zero
	930-934	Noise
	935	Zero
	936-944	Low Level Cal.
RVP Rec #2	945-1857	
RVP Rec #3	1858-2770	
RVP Rec #4	2771-3683	

Total Length 3683

video" format requires the pulse length and the high level calibration level to be read from tape.

2.2.2 Card Input

Information and control instructions are input to the first pass program via cards. Each set of cards as described below designates a "run" which processes data from one particular file, i.e., a PPI sweep on the input tape. Each run sets forth its own set of options, area limits, etc. At the end of one set of data (run), the program returns to the initial point, ready to read more cards for the next run. This run is processed, and all subsequent runs, until the card denoting format type and file number has a format designation greater than 3. This terminates the job ('END OF RUN' is printed on a page following the last page of regular output).

A detailed description of the input control cards is given below since it graphically demonstrates the variables, their definitions and values which go into the first pass program. There are three types of cards containing three types of information and instruction. These will be described in the order in which they appear in the card deck.

Information on the first card is as follows:

Column	Format	Identification
1-6	Integer	Format designation (1=real-time, 2=early video, 3=late video) (A format designation greater than 3 terminates the run)
7-12	Integer	File number of data on input tape

The second set of cards read by the program contains values of parameters shown below. The first card in this set must have the 5 characters &PARM in columns 2-6, then at least one blank column. Next follow the names and values of parameters, using as many cards as needed. Only the first card needs the characters &PARM; all subsequent cards may be filled, i.e., columns 2-80 may be used for names and values of parameters. After the last parameter and a comma (or blank) the 4 characters &END must be punched.

Variable Name	Format	Pre-set Value	Definition
MAXC	Integer	1000	Maximum number of points/contour.
NA	Integer	--	Number of angle bins. This value must be supplied for early and late video tapes and is computed for real-time tapes.
NR	Integer	871	Number of range bins (Formats I&III).
		960	Number of range bins (Format II).
SAN	Real	--	Minimum angle of data (deg). This value is computed from header information.
SAX	Real	--	Maximum angle of data (deg). This value is computed from information in the 31 bytes of header.
DELTA	Real	--	Angular span of data (deg). This value is computed from header information.
IDIR	Integer	0	Indicates direction of scan (0= clockwise; 1=counterclockwise).
IPCHCD	Integer	1	Punch phase 2 (areas, etc.), on cards for good contours (0 to delete).

The third set of cards to be read are the same format as that for the second set except that the characters &CARDS must be in columns 2-7 on the first card.

Variable Name	Format	Pre-set Value	Definition
DEL	Real	4000	Peak search parameter (m)
LT	Integer	-95	Low level test value (dBm)
LW	Integer	-92*	Low calibration level (dBm)

Variable Name	Format	Pre-set Value	Definition
TP	Integer	-20*	High calibration level (dBm)
CALO	Integer	--	Low calibration level (tape units)
CALU	Integer	--	High calibration level (tape units)
RANGE	Real	30	Normalizing range (nmi)
MNPEAK	Integer	30	Minimum value of peaks (dBz)
RADARC	Real	76.3	Radar constant (dB)
NOA	Integer	1	Number of areas ($\leq$10)
AN(1), AN(2), ..., AN(NOA)	Real	0	Minimum angle limits on areas (deg)
AX(1), AX(2), ..., AX(NOA)	Real	0	Maximum angle limits on areas (deg)
RIN(1), RIN(2) ..., RIN(NOA)	Real	0	Minimum range limits on areas (nmi)
RAX(1), RAX(2) ..., RAX(NOA)	Real	0	Maximum range limits on areas (nmi)
SRIN	Real	5.1	Minimum range of data (nmi) Formats I and III
		0	Minimum range of data (nmi) Format II
SRAX	Real	75.5	Maximum range of data (nmi) Formats I and III
		77.65	Maximum range of data (nmi) Format II
IABCNT	Integer	0	Contours are relative to peaks (=1 if absolute)

Variable Name	Format	Pre-set Value	Definition
C(1) - C(10)	Integer	C(1)=6 C(2)-C(10)=2	Contour values (max. 10) (dB if IABCNT=0; dBz if IABCNT=1) [Values should be decreasing order (from peak)]
INTP	Integer	1	Interpolation on contours (=0 for no interpolation)
NSMTH	Integer	2	Initial number of smoothings
MAXSMO	Integer	4	Maximum number of smoothings
CSMTH	Real	0.2	Smoothing constant
CALCMP	Integer	0	Indicates plotter options (0=print-plot only (1=Calcomp plot only (2=both
LINTYP	Integer	500	Frequency of plot symbol for Calcomp plots of closed contours
ITOL	Integer	5	Maximum amount (dBz) by which contour points are allowed to deviate from the contour value.
CTAPE	Integer	1	Compute areas, etc., for good contours. These are printed at the end of the sweep (0 to delete).
XC	Real	-0.0	Set the Calcomp plotter continuation option for Goddard Space Flight Center (=999. at APL).

*For Format I (real time) these values are obtained from the header record, bytes 31 and 26, respectively.

Note that the "real-time" format data requires the low level calibration signal and the minimum range stored to be read from cards. The "early video" tapes require the pulse width, the two-point calibration values, and the minimum range to be specified on cards. Finally,

the "late video" format requires the low-level calibration and the minimum range to be on cards. Note that any tape input parameter may be overridden with card input for any of the three formats.

2.3 PEAK SEARCH

In order to reduce the number of steps required in the peak search routine and to smooth out inconsequential fluctuations that may introduce false peaks, points in the raw data array are summed to form a new array, SUM, having resolution limited to the input parameter DEL. This summing should be distinguished from the five-point smoothing done prior to the contouring discussed below. A separate summed array is temporarily formed only to expedite the peak search and in no way reduces the ultimate resolution of the contours.

The spatial volume represented by each element in the array SUM is approximately equalized by dividing the area into range intervals, each interval starting at twice the range of the preceding interval. The number of points in a summed element is fixed within an interval so that the azimuthal distance changes by no more than a factor of two within each interval. The largest azimuthal distance of an element with any range interval is specified by the input parameter DEL. The value of DEL should be at least 2000 m. This parameter also specified the range distance between summed elements which is constant for all range intervals. Thus the area covered by an element of SUM varies from $(DEL)^2/2$ to $(DEL)^2$ within each range interval.

Once the summed array has been established, each of its elements is in turn compared to its four neighbors to find the relative maxima. The absolute maxima of the raw data comprising these summed elements are then determined. Next, points are rejected that have one or more nearest neighbors below the threshold (power received) input parameter, LT (dBm). This test rejects point targets and interference from other radars. Finally, a test is performed that eliminates all local maxima which, when converted to dBZ values, are smaller than the minimum reflectivity, MNPEAK (dBZ). Data points passing these tests are considered legitimate peaks and their values and coordinates are stored for future use by the program.

2.4 SMOOTHING

A five-point smoothing operation can be applied to all points within the areas. The following equation is used:

$$Z_0' = cZ_0 + \frac{(1-c)}{4}(Z_1 + Z_2 + Z_3 + Z_4)$$

Z_0' is the smoothed value, Z_0 is the unsmoothed value, Z_1 through Z_4 are the unsmoothed values for the four nearest neighbors to the point being smoothed, C is the smoothing parameter that can take on values from 0 to 1. Note that C = 1 produces no smoothing, C = 0.2 produces equal weighting for all five points and C = 0 replaces the unsmoothed value by the average of the four neighbors. This procedure is carried out in a way such that smoothed values are unaffected by other smoothed values. Repeated applications of the smoothing operation bring additional neighbors into the average. For this reason the area boundary must not be on the boundary of the Z array. The area should lie at least 1 nmi and 2 deg within the Z array. The maximum number of repeated smoothings is specified via an input parameter. The computer will systematically increase the number of smoothings until (a) a successful contour is found, or (b) the maximum number of smoothings is reached. It then proceeds to the next peak.

2.5 CONTOUR GENERATION

2.5.1 Closed Contours

To establish the first contour point, the contour generation routine performs a comparison of Z values along an azimuth equal to the azimuth of the peak. The comparisons start at the coordinates of the peak and proceed along the peak azimuth, increasing range until the first point at which the Z value is less than the desired contour. It must then be determined if this point, or the preceding point is closer to the desired contour. The closer of these points is used as the initial point on the contour. Nearest neighbors are then examined and the one that minimizes the difference between the value at a point and the desired contour value is selected as the next point.

The process is repeated with the last point found on the contour being eliminated from the test. Before the test is repeated a check is performed to see if the generated contour has reached the starting point. If so, the contour generation is terminated. The procedure is also terminated if an excessively large number of contour points, specified by an input parameter, has been generated. In that event an appropriate statement is printed and the next peak is considered.

The program range-normalizes only the points being considered for the contour instead of all points within the area. The desired contour test value in dBZ is transformed to log power received at the normalizing range in tape units. To determine the contour points, a comparison is made between the normalized log power and the test value transformed to the normalizing range.

Several constraints on the contour path were found to be necessary during the test cases that have been run. The forbidden paths are depicted in Figure 2.3.

The constraints shown in Figures 2.3(a) and 2.3(b) reduce the number of points to be tested to five. In the figures, point B was generated after point A. Only the five points indicated by an X are considered after point B; points C and D are forbidden. Figure 2.3(c) shows an additional constraint without which contours were frequently found to double back and return to the initial point without enclosing the peak. Furthermore, the obvious constraint has been added which forbids the selection of any previously selected contour point. Termination occurs if the last point is surrounded by previously selected contour points.

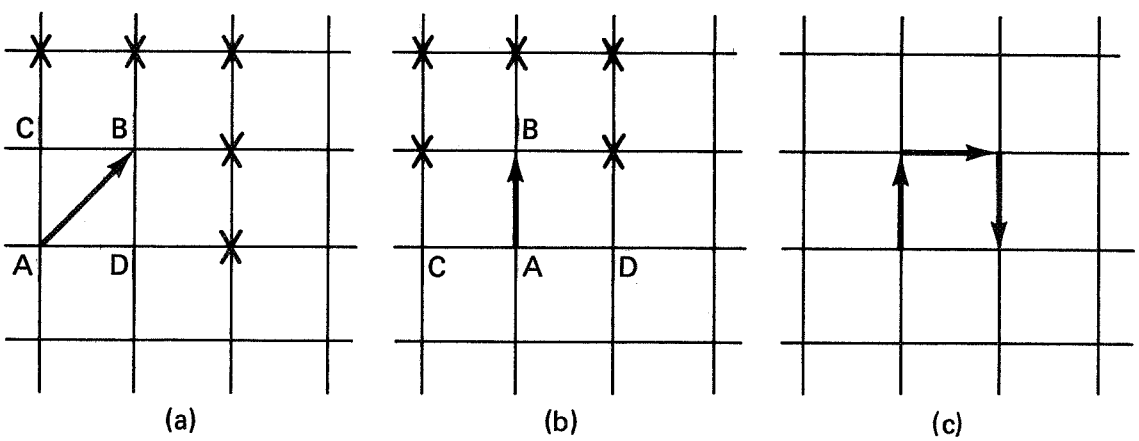

Figure 2.3. Constraints on Contour Generation

The program terminates the contour if the contour crosses the boundary of the designated area. The test for a boundary crossing is efficiently accomplished by computing the minimum number of bins to the nearest boundary, M, after the first contour point has been found. The contour is then generated for the next M points. If M<0 the boundary has been crossed, the contour is terminated, and the next peak is considered. If M>0 then M more points are generated on the contour before another boundary check is made. The procedure is repeated until the contour is closed, crosses the boundary, or is terminated for any of the above reasons. Note that this procedure requires that contours be requested in descending order for all contours to be generated.

Finally, termination of the contour occurs if the difference between the dBZ value of the contour point and the test value exceeds an input tolerance (TOL). The following list is given to summarize the conditions for which the contour is terminated:

a. First point is outside area

b. Contour starts within area but extends outside

c. It is impossible to find the next contour point due to the constraints imposed, e.g., point is surrounded by previously chosen points

d. Number of contour points found exceeds some specified maximum, MAXC

e. Contour point found is more than a prescribed tolerance (TOL in dB) away from desired contour value.

In each case, an appropriate statement is printed out and the program goes on to the next peak in the case of the closed contour mode, or the next boundary point in the case of the broken contour mode (discussed in the following paragraph). Conditions a and b do not apply, however, to boundary search mode, i.e., broken contour mode.

An option included in the program allows for absolute contours to be specified in dBZ rather than contours relative to each peak. The procedures for contour generation are identical except that the input dBZ values are used directly for the contour values instead of being computed from the peak dBZ value. As in the case of relative contours, the contour generation begins from a local maximum.

The optional interpolation is performed only in the proximity of the last point generated on the contour; and the interpolated points are considered along with the measured data points as the program seeks the next contour point. In Figure 2.4 the measured data points (squares) and the interpolated points (circles) are shown along with the interpolation equations.

2.5.2 Broken Contours

When absolute contours are generated an option is available to generate contours that cross the area boundary. This is particularly useful in processing RHI's where structures frequently extend off the

data array. When this option is requested, the program first generates the closed contours, if any, and then initiates an area boundary search to find the contour crossings. The crossings are detected by testing for sign changes in the difference between the boundary data point and the desired contour value. When a sign change is detected a contour has been crossed and the first contour point is established. The contour is generated from this point as usual until it reaches another boundary. The entire area boundary is examined in this way with end points from previously generated contours being skipped in the search.

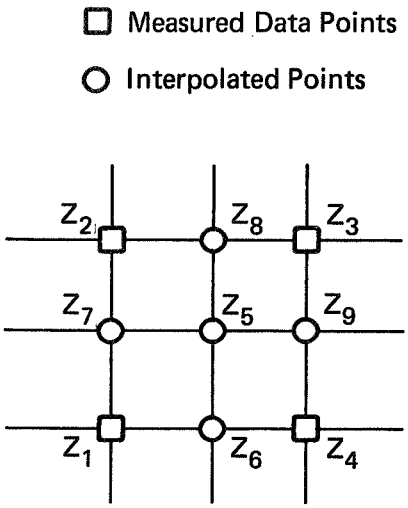

$$Z_5 = \tfrac{1}{4}(Z_1 + Z_2 + Z_3 + Z_4)$$

$$Z_6 = \tfrac{1}{2}(Z_4 + Z_1)$$

$$Z_7 = \tfrac{1}{2}(Z_1 + Z_2)\text{, etc.}$$

Figure 2.4. Sketch and Equations of Interpolation Method

2.6 CALIBRATIONS

A two-point calibration relating tape units (0 to 255) to log power received (dBm) is used. Data tapes processed in real time have high- and low-level calibration signals on each RVP record. Data processed from "late format" (Table 2.3) video tapes also have high- and low-level signals. However, the "early format" tapes (Table 2.2) have only the high-level signals and the two-point calibrations must be supplied to the program by cards. The "real time" program (Table 2.1) takes

an average of these samples over the entire sweep and uses the results in the calibration. These average values may be overridden with cards if necessary. The standard deviation is also computed and listed to indicate any calibration changes during the sweep.

As indicated earlier, not all raw data points in the area are run through the two-point calibration that relates log power to tape units. The calibration is used a minimum number of times since only the following data are transformed by means of this calibration procedure:

a. All local maxima

b. The range normalization correction for potential contour points

c. The desired contour value.

An input parameter, RCON in dB, is used to account for all constant radar parameters and corrections to the data. The radar "K factor" is included in this constant as well as the corrections for log averaging and quantization of the integrator input and output data.

A detailed discussion of the radar calibration program, the corrections to the data and resulting equations used to calculate the equivalent radar reflectivity are contained in Volume I of this report and in Ref. 5.

2.7 CORRECTION FOR ATMOSPHERE ABSORPTION

This section describes the atmospheric attenuation correction term added to the radar equation to compensate for the absorption due to collision-broadened resonances of the oxygen and water vapor molecules. A more detailed treatment is given in Goldhirsh and Kropfli, Ref. 5.

In Figure 2.5 is plotted the total two-way integrated attenuation at a frequency of 3 GHz as a function of range for a family of elevation angles. These curves were calculated for ray paths in accordance with the CRPL exponential reference atmosphere refraction model with Ns = 313. Note that at zero elevation and ranges of 70 nmi and 35 nmi the total attenuation is 1.8 and 1.0 dB, respectively. At an elevation angle, θ_e, of 10^o or greater the absorption is less than 0.5 dB for all ranges. Furthermore, for ranges less than 15 nmi the attenuation is also less than 0.5 dB for all elevation angles. The correction term is applied to the interval.

$$\theta_e \leqslant 10^o$$

$$15 \text{ nmi} \leqslant R \leqslant 70 \text{ nmi}$$

where the total absorption is for the most part greater than 0.5 dB.

For computational simplification, each of the curves in Figure 2.5 has been approximated by the linear form

$$A = m(\theta_e)R + b(\theta_e) \quad \text{(dB)}$$

where m and b are θ_e dependent. The best fit values of these parameters are given in Figure 2.6 where the indicated values introduced an error $\leqslant \pm$ 0.1 dB in the curves of Figure 2.5.

A table giving the values of m and b was programmed for the first pass program at 0.5^o elevation intervals up to 10^o, resulting in 21 values for m and 21 values for b, where each θ_e defines given values for m and b, respectively, over the range interval. The value for A may be added directly to the radar equation (expressed in dB). Again, see Volume I and Ref. 5. Outside the interval defined above, no correction was made, resulting in an error less than 0.5 dB.

3. SECOND PASS PROGRAM

3.1 GENERAL DESCRIPTION

The purpose of the second pass program (Ref. 4) is to take cell locations and cell contours generated by the first pass program and calculate a few cell descriptors that are input to the third and fourth pass statistical analysis programs. The output is a printed listing of the calculated quantities and cards which are used as input to the third pass program (Section 7).

The following quantities are calculated in the second pass program:

a. Areas within the computed contours

b. All inter-peak spacings

c. Length and width of each contour through the centroid

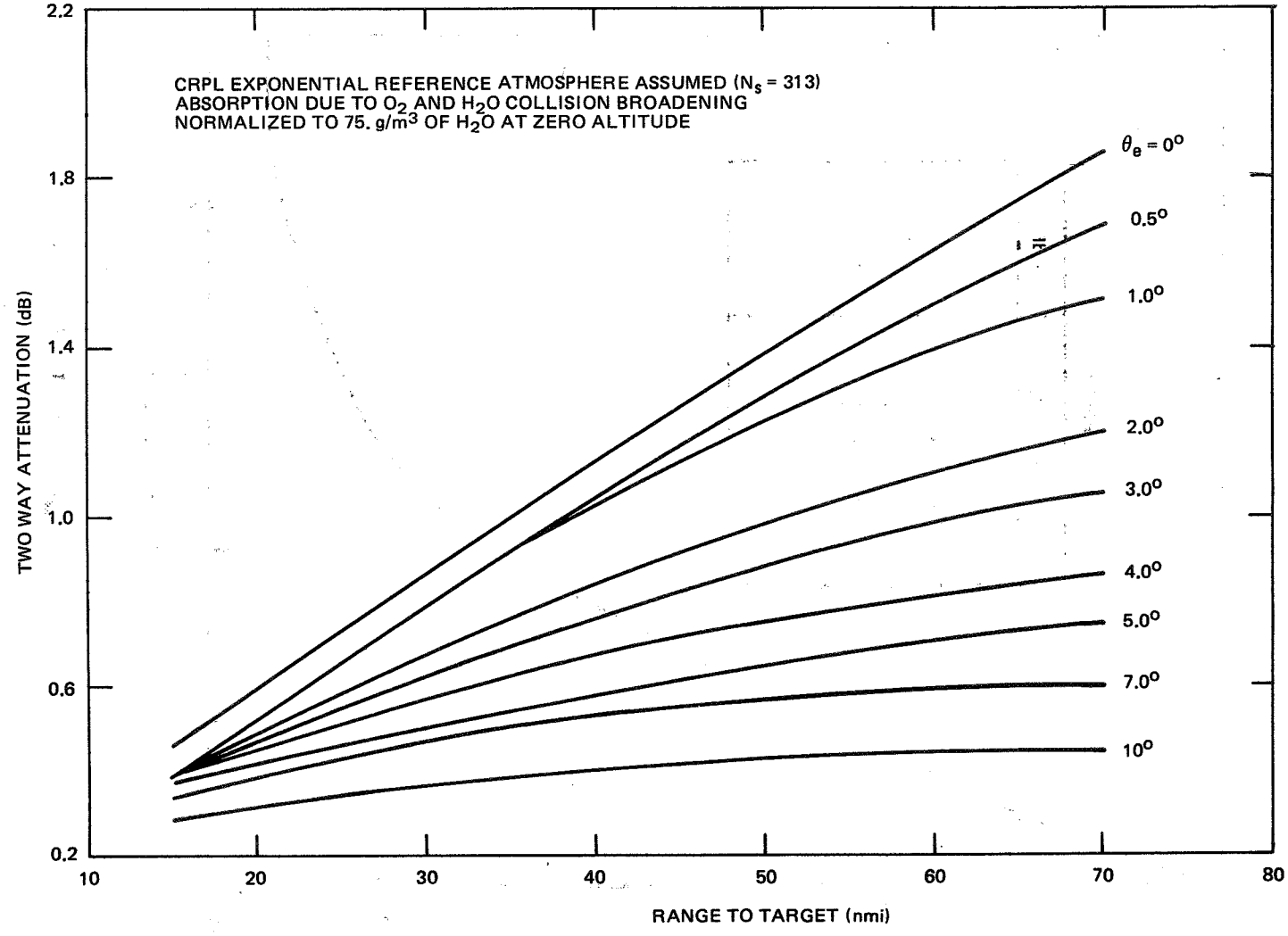

Figure 2.5. Two Way Attenuation Due to Atmospheric Absorption (f = 3 GHz)

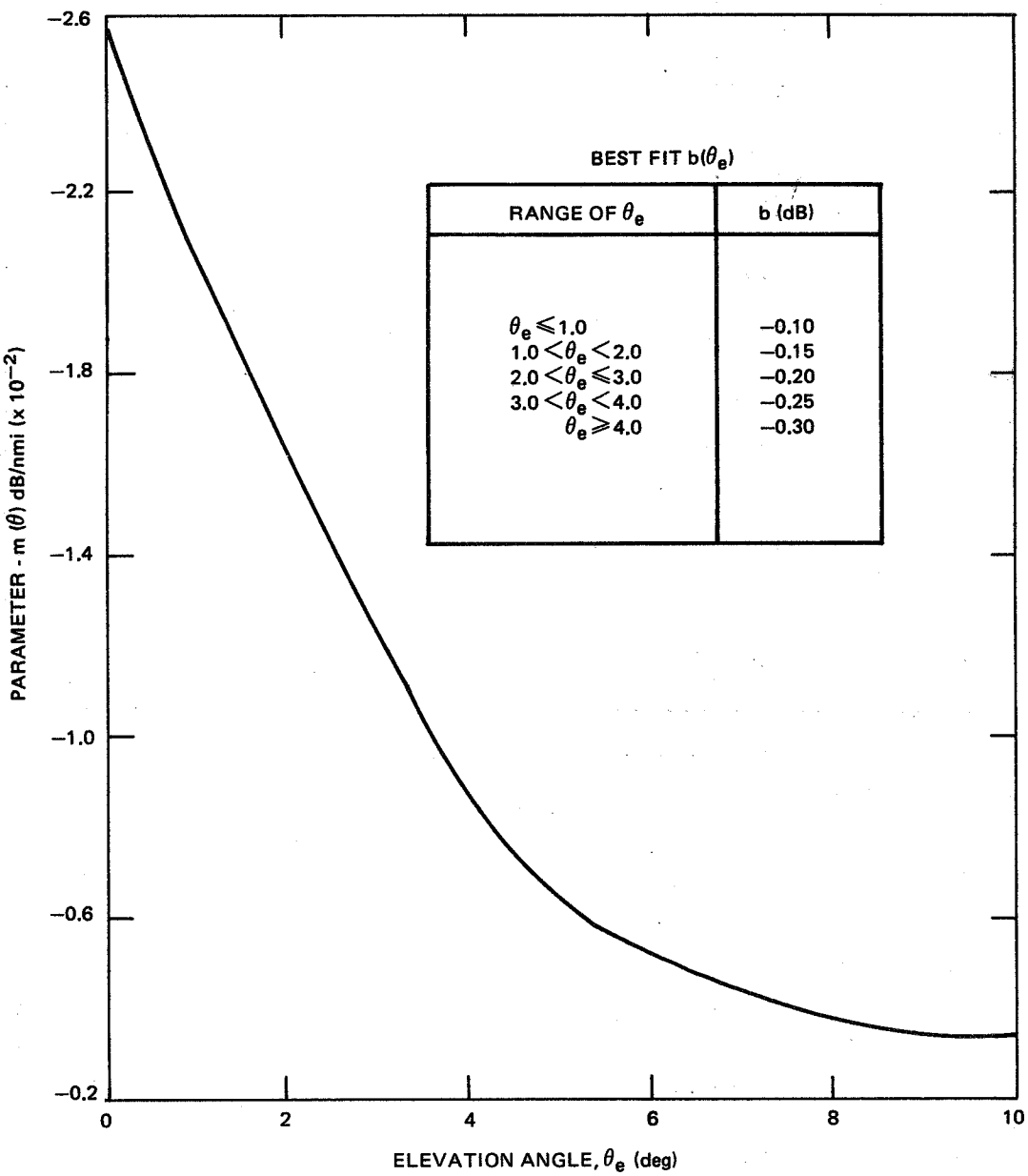

Figure 2.6. Best Fit Parameter

d. Orientation of cell major axis

e. Height of cut through peak.

Figure 3.1 illustrates these various cell and field descriptive parameters.

3.2 ALGORITHMS AND PROCEDURES

3.2.1 Cell Areas

The polar plot in Figure 3.2 indicates the method used to sum the incremental triangular elements.

The total triangular area described by the origin and points n and n + 1 is added to a running sum, but the smaller area defined by the origin and points m and m + 1 is subtracted. The decision to add or subtract is based on the sign of the azimuth difference between the pairs of points. Although some contours will be generated in the opposite direction, i.e., counterclockwise, the magnitude will always be correct. Absolute values are taken to produce a positive result.

3.2.2 Cell Spacings and Relative Directions

The second pass program calculates the distance R(n,m), the distance between peaks n and m, for all $m \neq n$. The angle from North made by a line between peaks n and m is also calculated. The number of calculated distances is not large for typical numbers of peaks in a scan; for example, 8 peaks would have 28 distances computed.

3.2.3 Contour Length, Width and Orientation

The algorithm used to calculate the contour maximum and minimum dimensions and orientation involves a computation of the distance between opposite sides of the contour through the centroid of the area. Maximum and minimum distances ending on the contour are determined. Lines from the centroid to each contour point are extended through the centroid to a point on the opposite side of the contour and the length is computed. Values are examined for a maximum and minimum until all points have been considered. The maximum and minimum values of the dimensions and the direction are printed out for each contour and read onto cards. Figure 3.3 illustrates the technique.

3.2.4 Cell Height

The height of the radar measurement at the location of the peak is calculated for each peak. The procedure outlined by Blake

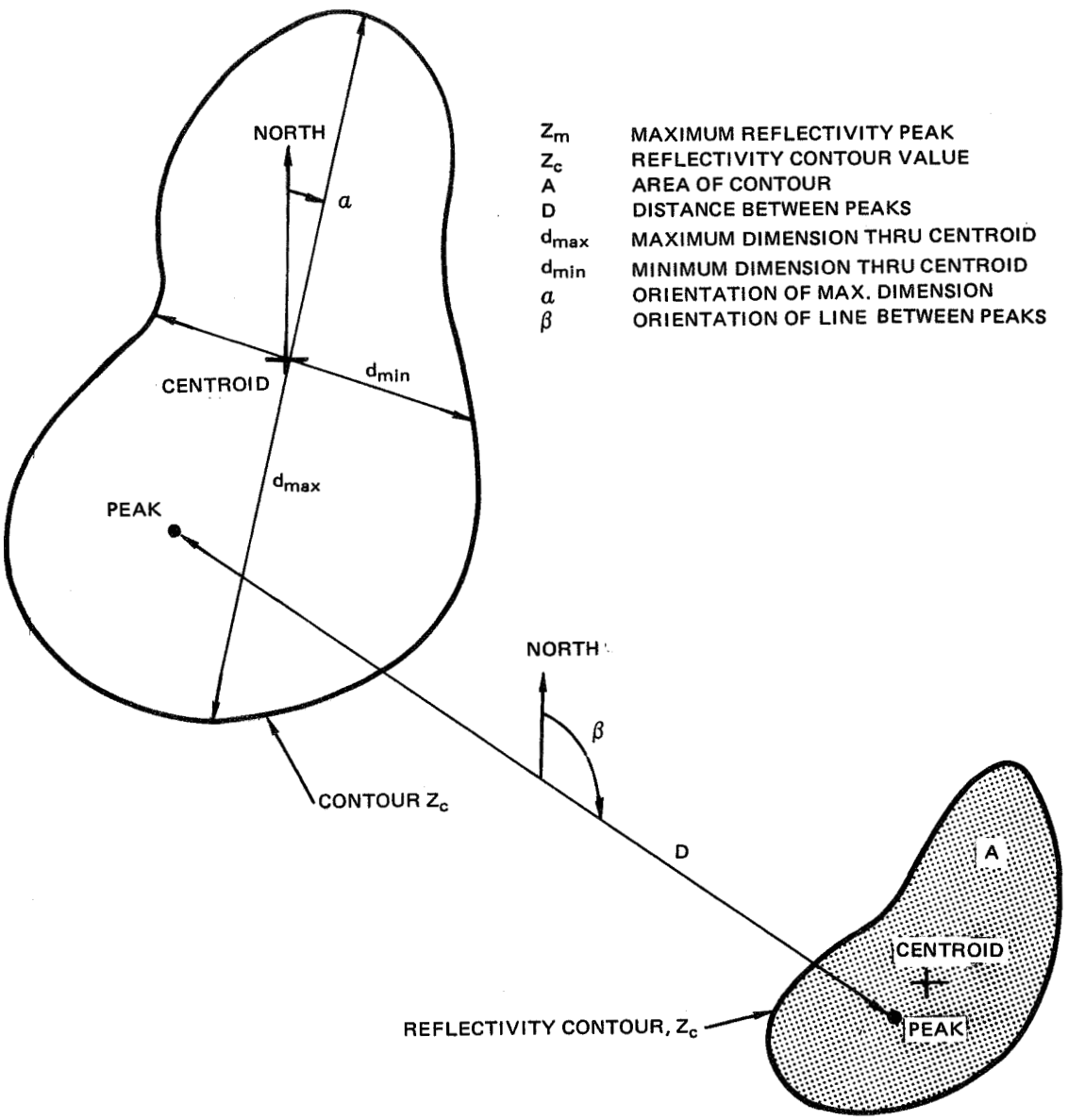

Figure 3.1. Sketch of Cell Parameters Calculated in the Second Pass Program

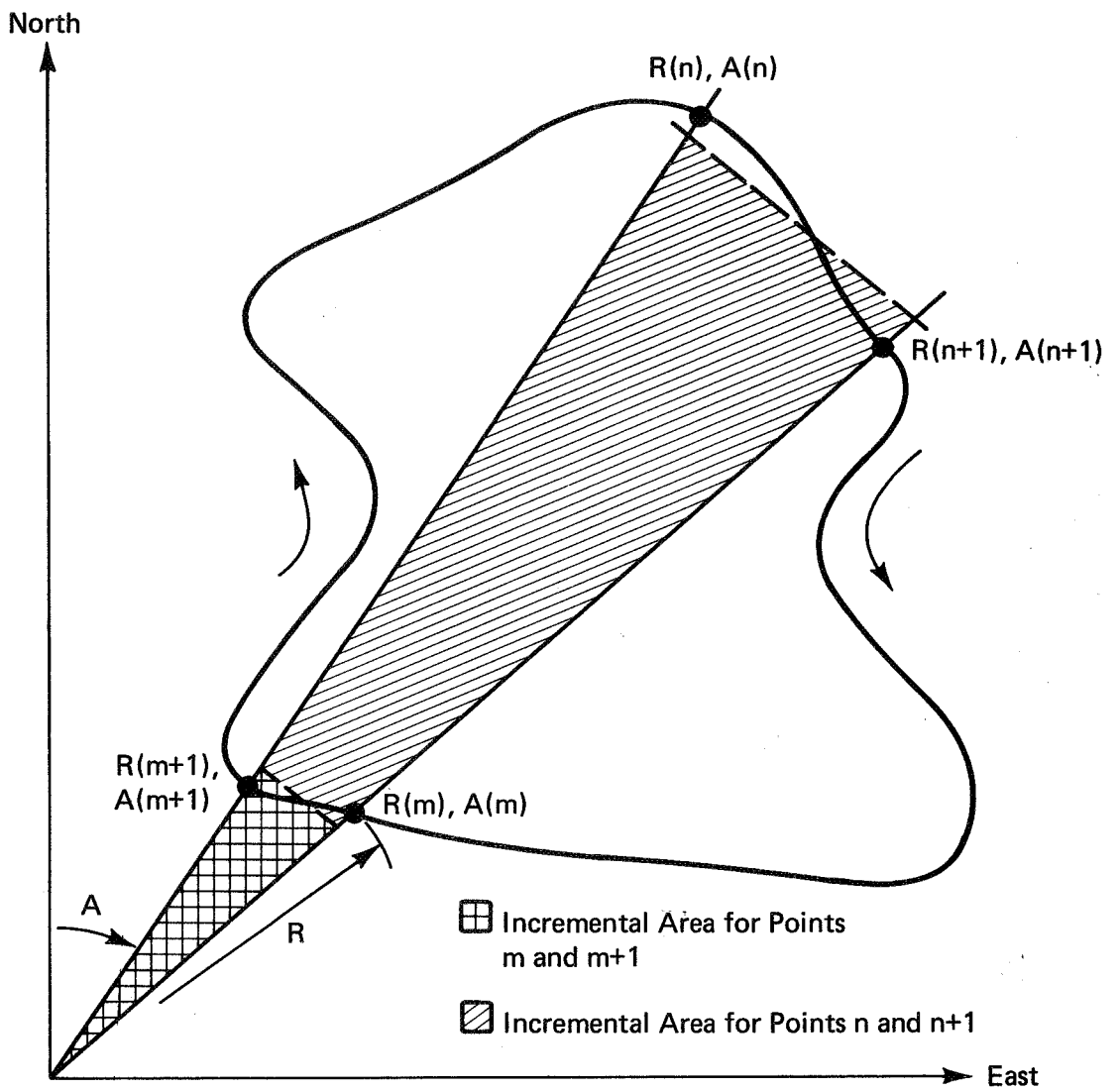

Figure 3.2. Sketch Showing Area Calculation Method

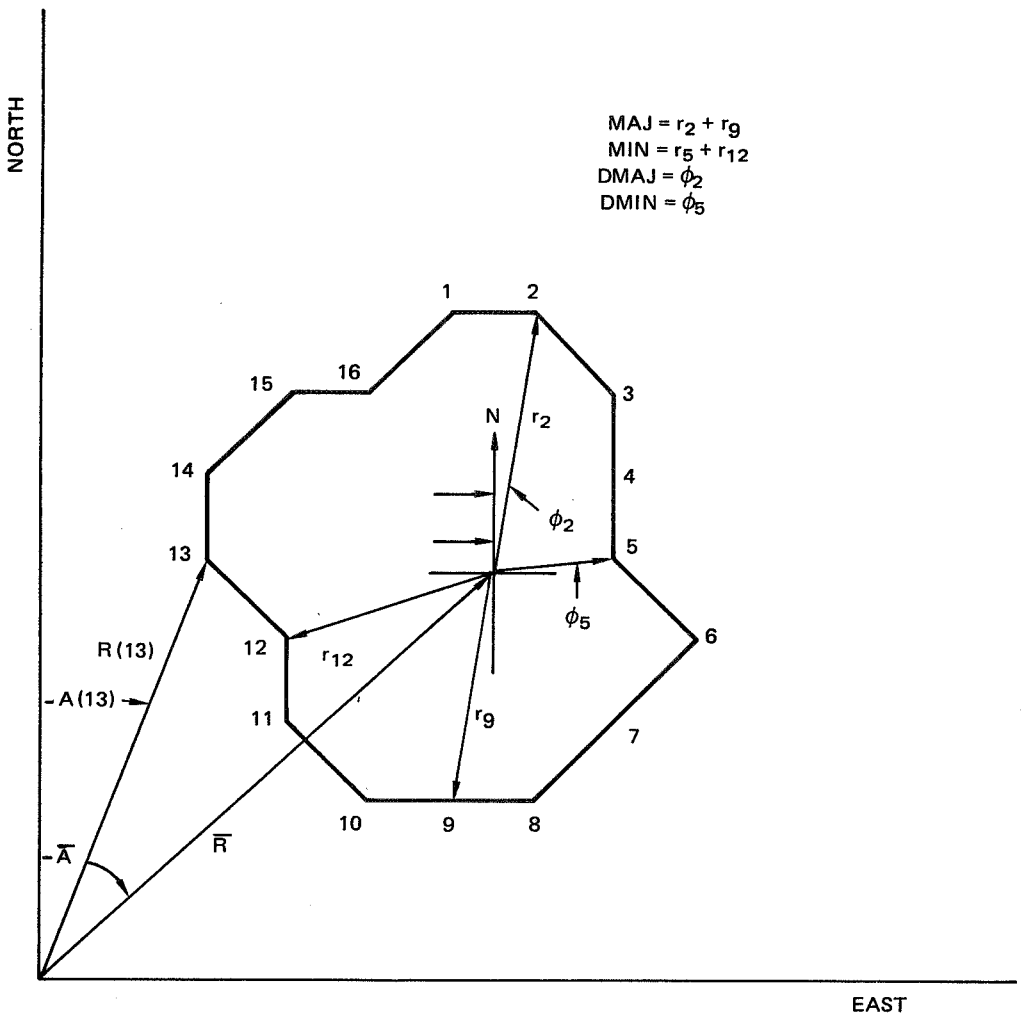

Figure 3.3. Sketch Indicating Cell Length, Width, and Direction

(Ref. 7) for an exponential atmosphere was used to calculate height from range and elevation of the sweep. A FORTRAN IV program was obtained from the author (Blake) which computes the height of a peak given its range and the initial elevation angle of the radar. The program was revised to function as a subroutine of the main computer program.

3.3 OUTPUT

Output of the first and second pass programs is in two forms, cards and printer listings including a printer plot of the contour.

3.3.1 Card Output

There are two types of card output from the second pass program since the information is too extensive to be contained on a single card. There is one Type I card for each sweep in a scan. The format of this card is as follows:

Column	Description of Contents
1-2	Last two digits of the year
4-6	Day number (1,2,...,365)
8-9	Scan number
11-12	Sweep number
14-15	Number of good peaks (kk) for which data was computed
18-19	Hours } Time of Sweep
21-22	Minutes } Time of Sweep
24-27	Seconds (xx.x) } Time of Sweep
30-31	Identification number for peak n_1
33-34	Identification number for peak m_1
36-40	Distance (km) between peaks n_1 and m_1
43-53	Same as columns 30-40 for the next pair of peaks

Column	Description of Contents
56-66	Same as columns 30-40 for the next pair of peaks
69-79	Same as columns 30-40 for the next pair of peaks

If this information exceeds one card, subsequent cards will contain a maximum of 6 pairs of peaks and distances in columns 4-14, 17-27, 30-40, 43-53, 56-66 and 69-79.

The Type II cards contain the information for each peak and its contour for the 'kk' peaks (see columns 14-15 on card Type I).

Column	Format	Description
1-2	xx	Peak identification (1,2,...,kk)
4-7	xx.x	Reflectivity value (dBz)
8-12	xxx.x	Azimuth of peak (deg)
13-16	xx.x	Range of peak (nmi)
17-20	xx.x	Height of peak (km)
22-23	xx	Value of contour (dB)
24-29	xxxx.x	Area within contour (km^2)
30-33	xx.x	Length of contour (km)
34-37	xx.x	Width of contour (km)
38-40	xxx	Direction of major axis (deg from North)
42-60		Same as columns 22-40 for next contour
62-80		Same as columns 22-40 for next contour

If this information exceeds one card, subsequent cards will have a maximum of four contours per card, the first in columns 2-20, the second in columns 22-40, the third in columns 42-60 and the fourth in columns 62-80.

3.3.2 Printer Output

For each successful contour about a peak there is one page of printer output which presents a printer-plot of the contour and lists pertinent data concerning the location and reflectivity of the peak, contour level, the number of points on the contour, the mean of the reflectivity values of contour points, and the standard deviation. An example of the contour plot is shown in Figure 3.4. The plot is in B-scope format and as such, the contour is distorted somewhat. Note the peak located in the hook in the lower right-hand corner of the contour.

At the end of each sweep search, the computer lists all its findings, i.e., all the peaks found. Figure 3.5 shows an example of the printer listing for each sweep. The first line gives identification information. The second line shows the status of the contour. The status refers to the success the computer had in completing a specified contour. Status 2, 3, 4, 5, and 6 were discussed earlier in paragraph 2.5.1 on the constraints imposed on the contour search routine. Section A of Figure 3.5 is a listing of all the peaks found, their reflectivity value (ZMAX), their location (RMAX and AMAX), the contour requested, the standard deviation of these points, the total number of points on the contour, the status (see above), and the number of smoothings applied to the data. Note that the contour search for peaks 1, 3, and 4 were unsuccessful with two smoothings because the contour point became surrounded (status 3), i.e., one of the constraints discussed in paragraph 2.5.1 was imposed. Contours for peaks 2 and 5 were successfuly found (status 1).

The computer proceeded to smooth the data for peaks 2, 3, and 5 once more (3 smoothings) and was successful in finding the contour for peaks 1 and 3. Data for peak 4 was smoothed once more (4 smoothings) but the computer was still unsuccessful (status 3). Since the maximum number of smoothings allowed on this run was 4, the computer stopped trying to generate a contour for peak 4.

Section B of Figure 3.5 presents the peak and contour data for the successful contours only. Note that peak 4 does not appear in the listing. The contour level (6 dB), the peak reflectivity (ZMAX), the range and azimuth of the peak (RMAX) and AMAX) are repeated from Section A. Next are listed the contour descriptors: area, length of major and

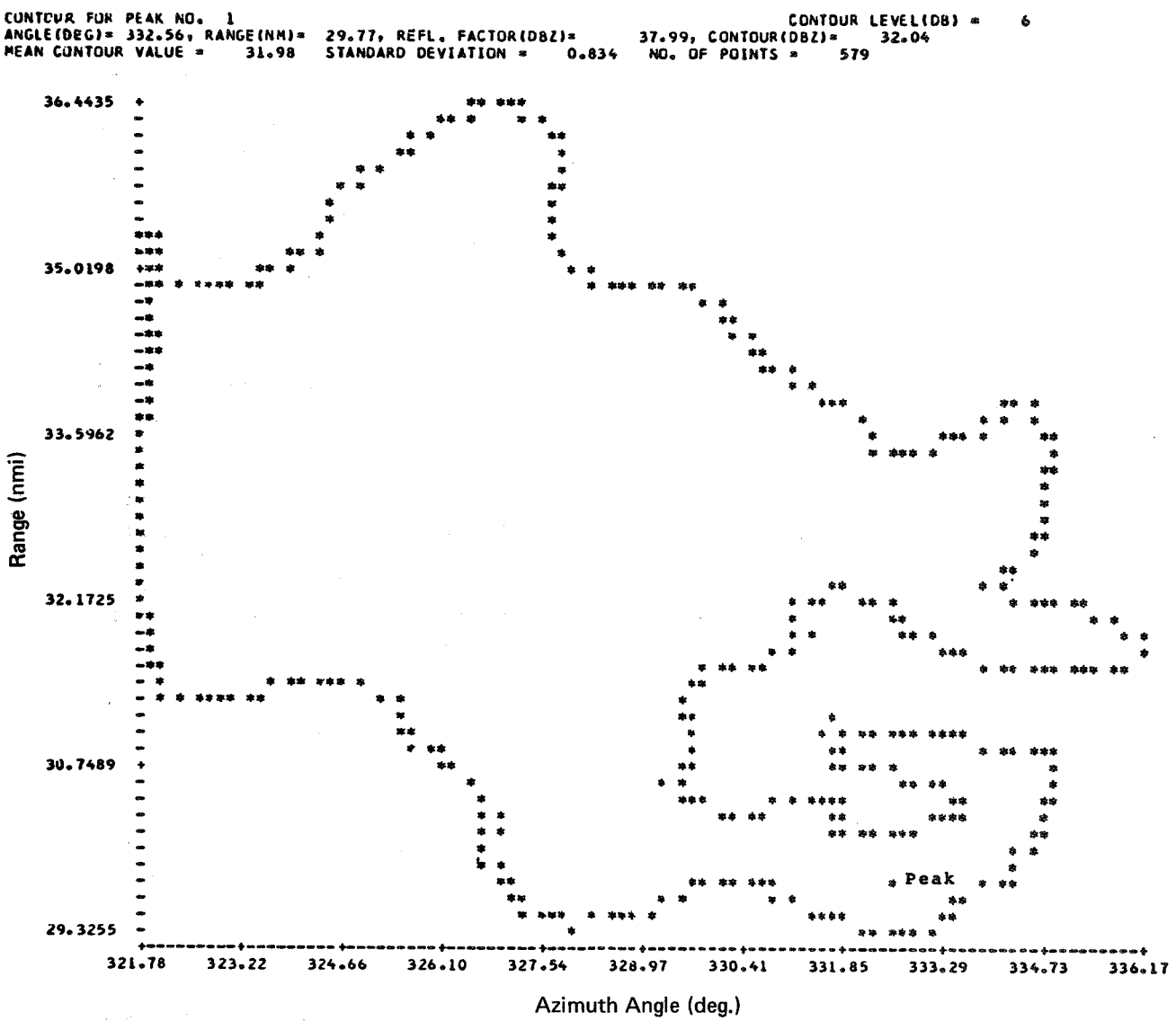

Figure 3.4. Printer Plot of Relative Contour About Peak

SUMMARY OF CONTOURS FOR DAY 149 OF 1973, SCAN 21, SWEEP 4
STATUS: 1 = SUCCESSFUL, 2 = EXCEEDS ITOL, 3 = SURROUNDED, 4 = RAN OFF AREA, 5 = FIRST POINT NOT FOUND, 6 = MAXC EXCEEDED

PEAK NO.	ZMAX	RMAX	AMAX	CONTOUR	MEAN CONTOUR VALUE	S. D.	NO. PTS	STATUS	NO. SMOOTHINGS	
1	37.99	29.77	332.56	6	32.03	0.270	209	3	2	Section A
2	50.24	31.39	327.78	6	44.21	0.512	68	1	2	
3	32.74	37.62	335.38	6	26.88	0.325	244	3	2	
4	58.29	30.26	371.30	6	51.84	1.336	238	3	2	
5	49.54	36.40	378.31	6	43.31	0.838	88	1	2	
1	37.99	29.77	332.56	6	31.98	0.834	579	1	3	
3	32.74	37.62	335.38	6	26.84	0.243	92	1	3	
4	58.29	30.26	371.30	6	52.31	0.357	135	3	3	
4	58.29	30.26	371.30	6	52.39	0.413	282	3	4	

PEAK	CONTOUR (DB)	ZMAX (DBZ)	RMAX (NM)	AMAX (DEG)	AREA (KM**2)	MAJOR AXIS (KM)	MINOR AXIS (KM)	DIRECTION (DEG)	HEIGHT (KM)	ABAR (DEG)	RBAR (NM)	
2	6	50.2	31.4	327.8	3.7	2.8	1.5	20	2.2	327.9	31.7	Section B
5	6	49.5	36.4	378.3	2.0	2.8	0.4	56	2.6	377.4	35.8	
1	6	38.0	29.8	332.6	105.8	16.3	7.8	91	2.1	328.8	32.5	
3	6	32.7	37.6	335.4	5.5	5.6	1.2	51	2.7	335.4	37.9	

DISTANCES(KM) BETWEEN THE 4 PEAKS.

2	5	54.2	Section C
2	1	5.6	
2	3	14.3	
5	1	49.0	
5	3	50.2	
1	3	14.8	

Figure 3.5. Computer Listing of Peaks and Descriptors

minor axes, the orientation of the major axis and the altitude of the peak. The final two columns list the azimuth and range of the centroid of the area. All the information in Section B with the exception of the centroid location is punched on cards (see paragraph 3.3.1).

The next listing, Section C, presents the distance between the peaks. Note that only one distance is listed for each combination of two peaks. The data in this table are also punched on cards. See paragraph 3.3.1 for format.

In summary, the output of the second pass program consists of a printer plot contour of each peak in a sweep and a summary sheet listing all the peaks found in that sweep along with contour data. These data and the contour plot are examined by the analyst prior to the third pass program. This is discussed in Section 5.

4. RESULTS OF FIRST AND SECOND PASS DATA REDUCTION

The results of the first and second pass computer reduction are listings, printer plots, and punch cards containing the peaks found by the search routine and the descriptive parameters of the contour. In all cases the 10 dBZ down contour relative to the peak was requested. Not all the data taken during the summer 1973 observation period were processed through the first and second pass and computer reduction. In some cases the data were bad on the digital and/or video tapes. This was especially true during the first month of the experiment (May) when the equipment and techniques had not been completely shaken down. In other cases there were too few scans taken during the day to warrant reducing the data: for example, on several days there appeared one or two very weak cells. Only a few (2 or 3) scans were taken and the cells disappeared. In other cases, the data on tape were good but unretrievable for some reason, e.g., lack of End-of-File marks so that the computer could not locate the data properly on the digital tape. On several days, the rain system was very extensive and extremely complex as shown by the contoured-video PPI photographs. It was felt that the use of the algorithms for peak search and contour generation would not yield good results in those situations. These algorithms work best in the case of isolated cells. In light of the plentiful data available, it was decided not to process or reduce the data for those days.

On one occasion the military engaged in chaff drops within our area of observation, unknown to us. To the radar, these chaff clouds resembled rain showers albeit with peculiar characteristics. A number of scans were taken but were discarded after learning of the chaff problem. No data on this day were used.

Table 5.1 in the companion report, Volume I, entitled "Radar Derived Spatial Statistics of Summer Rain - Experiment Description," NASA CR-2592 lists all the data taken. In Table 4.1 a portion of Table 5.1 is reproduced with the number of scans reduced by the first and second pass. Needless to say the computer output of the first and second pass is voluminous and is not included as part of this final report. The printouts have been preserved and filed at the Applied Physics Laboratory, The Johns Hopkins University. They are available for inspection or further analysis at APL/JHU.

5. GENERAL DESCRIPTION OF THE DATA PROCESSING PROCEDURE

The purpose of the data processing procedure is to compile the statistical distributions of the cell descriptors calculated in the Data Reduction section leading to statistical models which characterize the variation of the peak reflectivity, area, cross-sectional shape and number of cells with altitude for defined classes and categories of rain cells. Figure 5.1 shows the general flow of data and the statistical processing procedure.

The output of the second pass computer program as outlined in Section 3.3 contains the following information:

a. Value of peak reflectivity factor and coordinates of all the peaks, along with identification in terms of scan, sweep and peak number

b. The area, length, width, and direction of major axis for specified contours, e.g., 10 dB down from peak value

c. Spacings between all peaks.

The details of the second pass output format, etc., may be found in Section 3.3. This information, then, forms the basic input for the statistical processing program.

The first step was to identify those peaks in a scan which make up a rain cell. Each sweep of a scan was at a different elevation angle. In the second pass program, the computer examined each sweep separately to find the peaks and their contours. It was given no information, or criteria, however, on which to decide which peaks in each sweep of a scan go together to make up a cell. This cell identification was performed by an analyst. The location, range and azimuth of each

Table 4.1

Data Reduced in First and Second Pass Computer Programs

Day	Total Number of Scans Taken	Number of Scans Reduced (1st and 2nd Pass)	Comments
May 9	5	0	Bad data tape
14	5	0	Bad data tape
15	4	0	Bad data tape
17	7	0	Bad tape and widespread
23	8	5	
24	13	6	
29	13	12	
Jun 13	13	10	
18	13	12	
20	2	0	Two few scans
21	17	11	
22	27	18	
26	2	0	Two few scans
27	7	0	Widespread
28	4	0	
29	31	26	
Jul 3	15	12	
5	6	5	
10	21	18	

Table 4.1 (Continued)

Day	Total Number of Scans Taken	Number of Scans Reduced (1st and 2nd Pass)	Comments
11	17	0	Widespread
18	4	0	
20	4	0	
27	15	13	
31	12	10	
Aug 1	16	11	
2	13	6	
3	19	0	Widespread
13	27	18	
14	11	6	
15	16	14	
16	16	15	
20	10	9	
21	9	9	
Total	402	246	

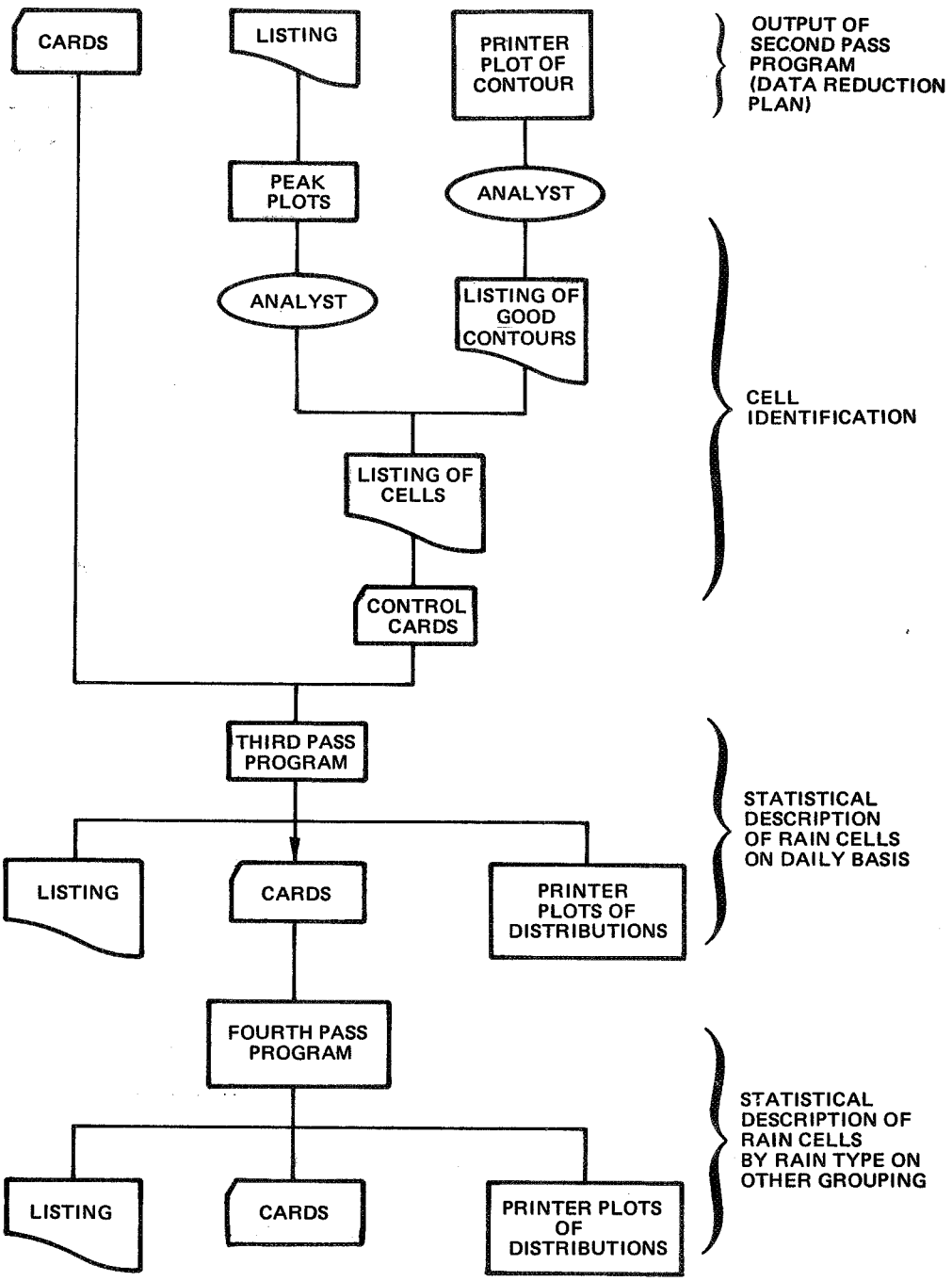

Figure 5.1. General Data Processing Procedure

peak found in a scan was plotted. The analyst, then, identified the individual cells based on the fact that those peaks associated with the same rain cell are grouped in a cluster. The other function of the analyst was to check the printer plot of each contour and confirm that the contour was good. Contours which were excessively complex due to noisy data or had a high standard deviation about the desired contour value, for example, were rejected at this point. Essentially the analyst ensured that those peaks and contours which were included in the subsequent statistical processing were reasonable and did not violate some criteria which were not covered by the first pass contour search algorithm. A listing was made of the scan, sweep, and peak numbers for each cell identified along with control cards to be used in the subsequent computer programs.

The third pass computer program uses the data on cards produced by the second pass program along with the control cards described above for each day and compiles the following statistical information:

a. Frequency distributions of peak reflectivity, area, length-to-width ratio and direction according to cell class and category for various altitude intervals along with the mean, median, mode and standard deviation for each distribution.

b. Frequency distributions of the reflectivity ratio and altitude of the maximum reflectivity as a function of cell class and category along with the mean, median, mode and standard deviation for each distribution.

c. The distributions of the number of cells by cell class and category for each altitude along with the mean, mode, median and standard deviation.

d. The distribution of the numbers of cells by height for each cell class and category; again with the mean, mode, median, and standard deviation of each distribution.

The output of the third pass program contains a listing of all the data described above, printer plots of the distributions and punched cards.

Note that the third pass program uses data for only one day at a time. The various distributions are for the cells which were identified on a single day.

The fourth pass computer program was designed to accumulate the data for a number of days and to produce the same type output as described above for the third pass. Output cards from third pass (one deck for each day) are assembled and used as input to the fourth pass. No control cards are required. The analyst is free to assemble the fourth pass input deck according to any criteria he chooses, e.g., all days with air-mass showers or every other Tuesday if desired. Note, however, that the fourth pass uses the daily statistics from third pass and merely accumulates the data for a number of days. As such the categories, height intervals etc., for fourth pass must correspond to those used in the third pass or daily program. This point will be expanded further in a subsequent section on the detailed description of both programs.

This completes the data processing procedure. The procedures are, in fact, quite versatile in that the choice of cells to be included in a population, the cell classes and categories to be used, the intervals for the various parameters in the frequency distributions, etc., are all left to the discretion of the analyst via the control cards for the third pass computer program and via the input parameters.

6. CELL IDENTIFICATION PROCEDURE

6.1 CONTOUR CULLING AND SELECTION CRITERIA

The output of the first and second pass programs includes a printer plot of the contour about each peak for which a contour is found. An example is shown in Figure 3.4. As described earlier in the Data Reduction section, only those contours which were successfully completed are included in Section B of the printout listing, Figure 3.5. In some cases, however, the contour was classified as "successful" by the computer according to the criteria and algorithms it used but was unacceptable for other reasons not known to the computer, i.e., based on criteria which were not contained in the computer program. The following are some examples of this situation.

The first pass contour program did not require that the peak be contained within the contour. Thus, the computer, on occasion, found a closed, well behaved contour (as far as it was concerned) which did not contain the peak. This situation was generally found where the reflectivity gradient was low about the peak.

Another reason for rejecting the peak was an excessively high standard deviation of the contour value. The program calculated the mean contour value and the standard deviation of the individual values

on the contour from the desired contour value. Where the standard deviation exceeded 1 dBZ the contour was rejected by the analyst.

The program did not contain any provision which would prevent the contour from crossing itself. That is, a closed contour in the form of a figure eight, for example, was acceptable to the computer. However, the algorithm for calculating the area of the contour is such that when this happens the area calculated is the difference between the areas of the two loops. When the two loops were of similar size, the contour was rejected; where one was very much smaller than the other so that the resulting area was not significantly affected, the contour was included in the subsequent analysis.

On some occasions, the contour as found by the computer was extremely complex. This typically occurred in regions where the reflectivity gradient was very flat, and the computer in its efforts to find the contour, wanders about. Rejection of this type of contour was based solely on the judgment of the analyst.

In summary, each printer-plot contour was examined and questionable contours were culled based on the analyst's judgment and criteria not contained in the computer contour program (first and second pass).

6.2 CELL IDENTIFICATION PROCEDURE

As the various peaks in a given sweep were found, the first pass computer program assigned a number to each peak. Thus, each peak was identified by a scan, sweep, and peak number. Although the computer followed the same areal search pattern in locating the peaks, the peak numbers associated with a given cell from one sweep to the next were not necessarily the same. This was caused, for example, by spurious local maxima at some altitude in the sweep not associated with an identifiable cell and also when all the cells did not reach the same altitude. Thus, a procedure was developed to identify the peaks in each sweep of the scan which make up the same rain cell.

The location of each peak for each sweep in a given scan was plotted. An example is shown in Figure 6.1. Notice that the peak locations cluster. A cell was defined as an identifiable cluster of peaks with consecutive sweep numbers. On some occasions a sweep may be missing from the consecutive set of sweep numbers indicating that, for some

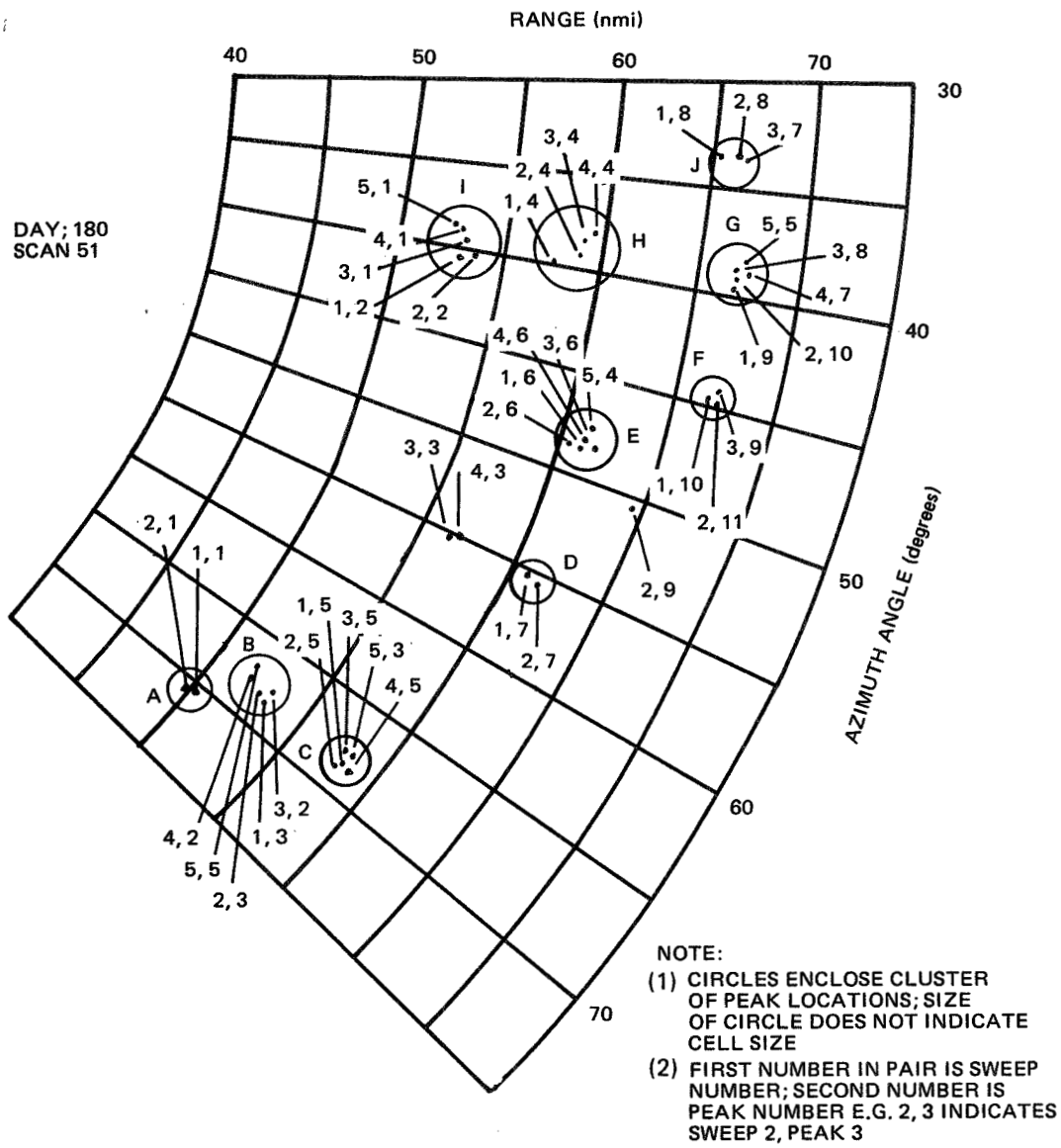

Figure 6.1. Peak Locations for Complete Scan

reason the computer algorithm did not find a peak. No attempt was made to interpolate data for such a missing peak. The cell remained in the population as is. Where more than one sweep was missing from a set of sweep numbers, the cell was discarded.

All the peaks found by the computer were plotted, including those peaks where the computer was unsuccessful in finding a contour and those peaks where the contour was discarded by the analyst. The contour data for the latter were not included in the statistical analysis, however, as will be discussed below.

Using the plots of peak locations for each scan, then, the cells were identified and listings were made as shown in Table 6.1, for the cells in Figure 6.1.

The cell identification procedure relied heavily on the judgment of the analyst. All cell identification was performed by one individual so that the same set of criteria, subjective though they may be, would be applied to all the data. No rigid rules were applied such as, "all the peak locations must be contained within a circle of x miles diameter" or "consecutive peak locations must be within some distance of each other." The use of such rigid rules was rejected early in the cell identification process. If applied they would have resulted in the culling of many legitimate cells. For example, on occasion the set of consecutive sweep numbers was strung out in a line as opposed to being tightly clustered. Such a pattern of points indicated that the rain cell was not vertical but leaning in some direction. In other cases, what appeared to be two cells at the lower altitudes (low sweep numbers) combined at the higher altitudes into a single cell or turret. Cells of this type were not included in the cell listings.

7. THIRD PASS COMPUTER PROGRAM

7.1 GENERAL DESCRIPTION

The third pass program (Ref. 8) was designed to process data on a day-by-day basis only. It uses the output data from the second pass program for each cell as determined by the control cards, compiles frequency distributions of reflectivity, area of a selected contour, the contour length-to-width ratio, the direction of the major axis of the contour, the number of cells, the reflectivity ratio and height of the maximum reflectivity for various cell classes and categories (Section 7.2) as a function of altitude. The mean, mode, median and standard deviation are calculated for all the above frequency distributions.

Table 6.1

Example of Cell Identification List

Day 180

Scan	Cell	Sweep	Peak	Scan	Cell	Sweep	Peak
51	A	1	1	51	F	1	10
		2	1			2	11
						3	9
	B	1	3				
		2	3		G	1	9
		3	2			2	10
		4	2			3	8
		5	5			4	7
						5	5
	C	1	5				
		2	5		H	1	4
		3	5			2	4
		4	5			3	4
		5	3			4	4
	D	1	7		I	1	2
		2	7			2	2
						3	1
	E	1	6			4	1
		2	6			5	1
		3	6				
		4	6		J	1	8
		5	4			2	8
						3	7

Figure 7.1 shows the general flow of data and the basic sequence of operations performed by the program. Preset values of the various program parameters designate bounds to be used in establishing bin size for the sorting of data to obtain the frequency distributions, e.g., upper and lower bounds of the altitude and altitude interval. These parameters can all be overridden via input at execution. Control cards containing information from the cell identification procedure (Table 6.1), are read into the program. The control information (cell, scan, sweep and peak identifiers organized by cell) is read into the computer core memory a scan at a time. After the data for one scan has been stored, the cell class and category of each cell is determined using the reflectivity value from the first sweep, i.e., the first elevation angle. The classification and categorization of cells is discussed in detail in Section 7.2. The program then performs a bin sort of reflectivity at the altitude of each succeeding sweep. At this point the computer determines the maximum reflectivity for the cell and the altitude of that maximum and saves this information for processing later in the program.

As noted in Section 6.2, the location of peaks for which no contour was found and peaks for which the contour was bad, were plotted in the cell identification procedure. The reflectivity of those peaks associated with a cell for which the contour was bad or nonexistent was included in the reflectivity distributions at each altitude, although the contour information was ignored by the program (Section 7.4). For this reason, the number of cells in the reflectivity distributions will be larger than the number of cells in the other distributions such as for area, or direction, etc.

Contour area is the next parameter to be sorted. The contour to be used is established by input selection, e.g., the 10 dBZ down contour. Using the class and category established earlier, the program sorts the area at each altitude.

In the second pass program the maximum dimensions through the centroid of the specified contour were calculated. The ratio of the length-to-width (L/W) is calculated in the third pass program and a bin sort procedure performed.

Next, the program compiles the distribution of the direction of the major axis of the contour. Prior to sorting, however, the program transposes all angles into the $0\text{-}180^{\circ}$ sector to remove the ambiguity in the direction.

The bin sort procedure described above is repeated for each sweep in the cell. At this point, both the maximum reflectivity in the

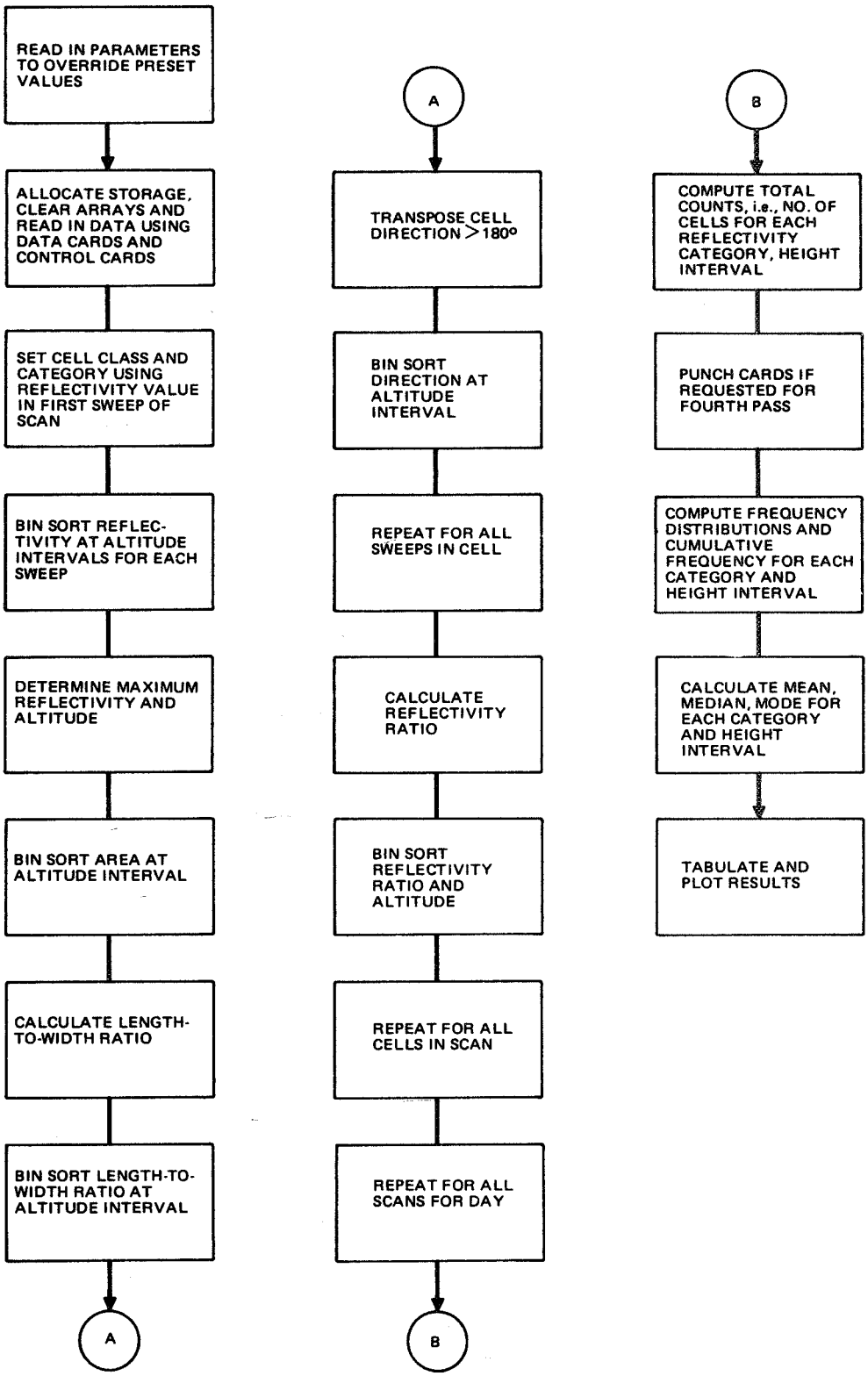

Figure 7.1. General Description of 3rd Pass Program

cell is known and the altitude at which it occurs. The reflectivity ratio, i.e., the ratio of the maximum reflectivity to that at the lowest elevation angle, is calculated and a bin sort is performed on the ratio and altitude of maximum reflectivity. Figure 7.2 illustrates the reflectivity ratio parameters. Note that the reflectivity ratio was not calculated for those cells which did not have a detectable return below 2 km. Such cells were placed in a special "Virga" category. This is described further in the subsequent section on classification and categorization.

The bin sort procedure is repeated for all cells in a scan and then for all scans in a day. When all scans have been processed, the frequency counts and the mean, mode and standard deviation are punched on cards for use in the fourth pass program. The frequency distribution and cumulative frequency distribution are then determined. Means and standard deviations are calculated using the raw input data. The mode(s) is established as the bin or interval with the highest frequency count; and the median is computed by a linear interpolation for the 50 percent point in the cumulative frequency distribution.

Finally, the results for each parameter are tabulated for each combination of cell class, category and altitude interval, and plotted. The output is organized into the following groups:

a. Frequency distributions of reflectivity, area, length-to-width ratio and direction as a function of cell class, category and altitude interval.

b. Summary results of the means, medians, modes, and standard deviations of reflectivity, area, length-to-width ratio and direction as a function of altitude for each cell class and category.

c. Frequency distributions of the reflectivity ratio and altitude of maximum reflectivity according to cell class and category.

d. Summary results of the means, medians, modes, and standard deviations of the reflectivity ratio and altitude at maximum reflectivity.

e. Distribution of the number of cells by class and category for a given altitude.

f. Distribution of the number of cells by height for a given cell class and category.

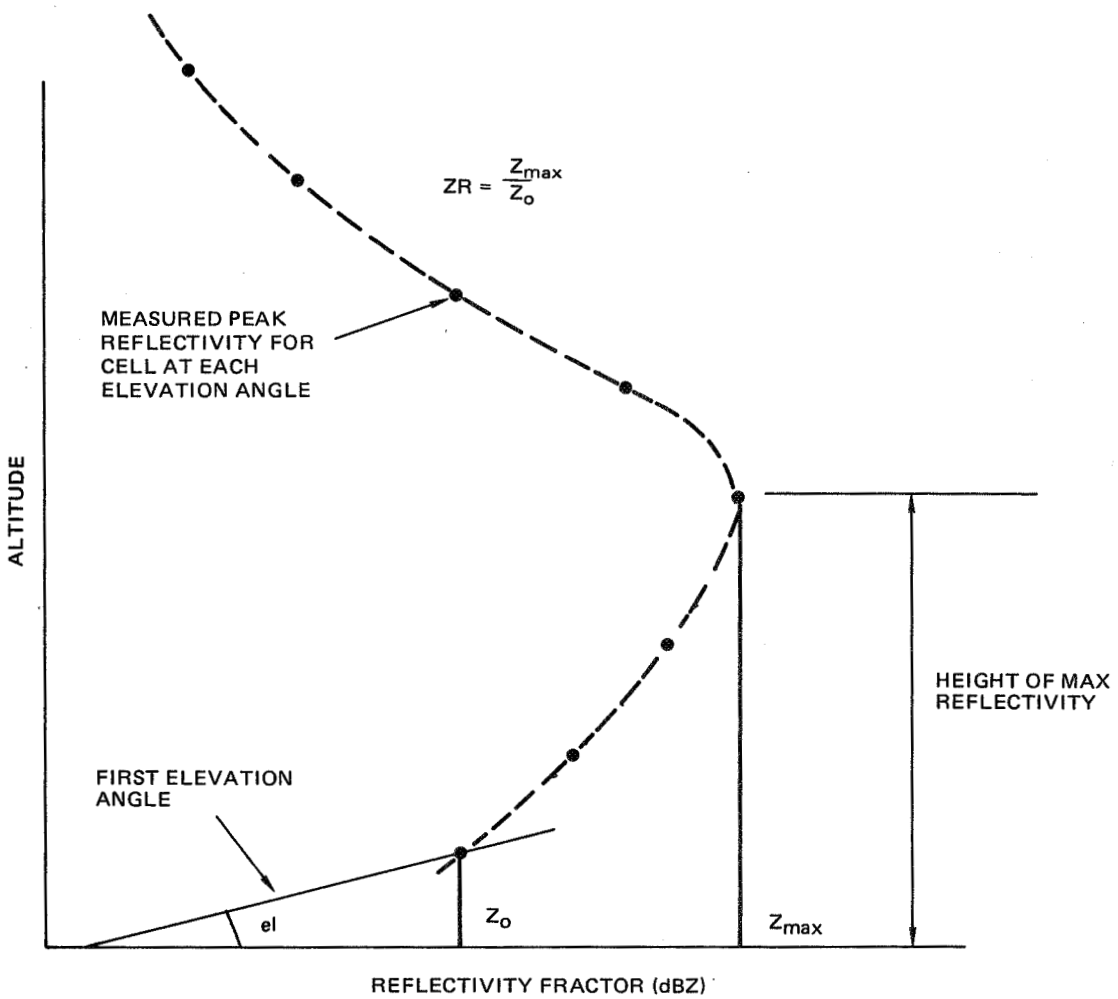

Figure 7.2. Definition of Reflectivity Ratio and Height of Maximum Reflectivity

The above output is in the form of both listings and printer plots. Examples are shown in the section dealing with the detailed description of the third and fourth pass output (Section 7.6.1).

7.2 CLASSIFICATION AND CATEGORIZATION OF CELLS

Cells were divided by the computer into two general classes: (1) those whose peak reflectivity was greater than a given threshold at the lowest elevation angle, referred to as "rain-on-the-ground" or ROG cells, and (2) those whose peak reflectivity at the lowest elevation angle were below the threshold, referred to as "Virga." The lowest elevation angle for which data were taken in any PPI raster scan was 0.5 deg; at 70 nmi this corresponds to an altitude of approximately 2 km. If the upper limit of the lowest altitude interval were chosen less than 2 km, e.g, at 1 km, then all those cells at ranges greater than roughly 40 nmi would be classified as Virga. On the other hand, with a 2 km upper limit, the rain from those cells at long range, e.g., 60-70 nmi, may not in fact reach the ground. The upper bound of the lowest altitude limit is an input parameter in the third pass program and may be changed. All calculations performed and results reported herein, however, are for a 2 km upper bound. The reflectivity threshold is an input and was chosen as 30 dBZ in the present study. Therefore, cells classified as "rain-on-the-ground" or ROG cells have returns greater than 30 dBZ at altitudes less than 2 km in altitude. All cells classified as "Virga" have no returns above the threshold of 30 dBZ at altitudes below 2 km. The base of a Virga class cell may occur at any altitude above 2 km, but no subdivision of the Virga cells in terms of the altitude of their respective bases was attempted. The computer program as written does not have this capability. The program simply tests the altitude of the first sweep for each cell to determine whether it is greater than or less than the upper bound of the first altitude interval, i.e., 2 km.

It should be recalled that the lower threshold of 30 dBZ was originally imposed on the peak reflectivities in the second pass program. Peaks with a reflectivity less than 30 dBZ were not considered. It is possible therefore that a cell classified as Virga does in fact have rain which reaches the ground, but the radar returns at altitudes below 2 km are less than 30 dBZ. The reflectivity threshold was chosen so as to concentrate the investigation on those cells which have high reflectivities. Cells with low peak reflectivities, e.g., 30 dBZ and below, were not considered to be a serious problem for communications.

The cells in the ROG class were further subdivided into categories according to the reflectivity value at the lowest elevation

angle, i.e., at the lowest altitude in the scan. Cell categories were chosen based on 5 dB intervals in the peak reflectivity, e.g., 30-35, 35-40, 40-45, etc. The reflectivity interval, however, is an input parameter and can be changed at execution. A category referred to as the "all" category includes all cells in the ROG class regardless of their reflectivity at the lowest elevation angle, i.e., all cells for which the peak reflectivity is within the reflectivity range of 30 to 70 dBZ with rain below 2 km. Thus, the data labeled as "all" in fact are the data for the ROG class.

The classification and categorization of rain cells according to their reflectivity values at the ground (lowest altitude observed below 2 km) was chosen so that the statistics of the occurrence of rain cells of various intensities determined in the present program could be compared directly with the statistics of rainfall rate on the ground accumulated by the Weather Service and others. Such statistics are available for a large number of locations for long periods of time. Extrapolation of rain cell occurrence statistics along with the statistical description of the profile of the cells from one location to another must be done using the ground based observations of rain distribution and rainfall rate statistics. Defining the rain cell classes and categories in terms of the cell reflectivity at (essentially) ground level then allows a direct comparison of their probabilities of occurrence with these ground measurements.

7.3 INPUT TO THIRD PASS COMPUTER PROGRAM

Input to the third pass computer program consists of three parts: (1) the output data from the second pass computer program containing information concerning the reflectivity of each peak found and the results of the contour search routine, namely the area, height of the peak, maximum and minimum dimensions of the contour through the centroid, and the direction of the maximum dimension, identified in terms of day, scan, sweep, peak number and contour value; (2) the control instructions that identify which peaks in each sweep of a given scan constitute a cell; and (3) the input program parameters. All the foregoing information is in the form of punch cards. No provisions are made for tape input.

7.3.1 Input Data

The basic data used in the third pass consist of the peak reflectivities and contour information generated by the second pass computer program. The format for this data on punch cards is covered in Section 3.3, Second Pass Program.

There are two limitations built into the third pass program: (1) the number of cells in a scan is limited to 25; and (2) the number of sweeps in a scan is limited to 28. There is no limit to the number of scans in a day.

7.3.2 Data Control

The procedure for identifying the peaks and sweeps which make up a cell was described in Section 6.2. This procedure results in a listing of cells according to the day, scan, sweep and peak numbers; Table 6.1. Control cards containing this information are read into the third pass program which select the proper combination of peak, sweep and scan. The format for these cards is shown in Table 7.1.

7.3.3 Input Parameters

The input parameters set the bounds for the various parameters and the intervals to be used, i.e., bin sizes. Table 7.2 is a listing of the input parameters and a description of each, the program name, format and initial or preset value. Note that the preset values can be overridden by card input at execution.

7.4 BIN SEARCH AND COMPILATION OF HISTOGRAMS

The control information, i.e., sweep and peak numbers organized by cells, is brought into core a scan at a time and a subsequent search is made through the data (from second pass) to select the appropriate reflectivity area, altitude, length, width and direction. As discussed in Section 7.1, each contour was visually examined by the analyst to confirm that the contours were good. Those contours which were "bad" for whatever reasons are identified in the control card; see Table 7.1, Column 11. The reflectivity and altitude of the peak are always passed on, but the contour data, namely, area, length, width and direction, are passed on only if the control card requests the use of contour data. The assumption here is that the peak reflectivity and location found by the second pass program are correct, but the contour is in error or was not found by the computer for reasons discussed earlier. Inclusion of reflectivity peaks with bad and nonexistent contours in the reflectivity population is based on the fact that such peaks are, in fact, part of the clusters of peak locations defining a cell. One result of this decision is that the number of cells contributing to a reflectivity frequency distribution in some category and altitude interval, for example, will be larger than the number of cells in the area, length-to-width and direction distributions. This is not considered a problem, however, since the results are cast in frequency distributions and cumulative distributions.

Table 7.1

Data Control Card Format

All cards have the same format. All values are positive integers, right-justified.

Columns	Description
1-3	Day number
4-6	Scan number
7-10	Cell identification (alpha)
11	Blank=use contour data; 1=ignore contour data
12-13	Sweep number (if any)
14-15	Peak number (if any)
16-20	Same description as 11-15
21-25	Same description as 11-15
.	
.	
.	
76-80	Same description as 11-15

If there are more than fourteen sweeps and peaks associated with a given cell, the second card for that cell repeats day, scan, and cell identification.

Table 7.2

Description of Input Parameters for Third Pass Program

Description	Initial Value	Program Name	Format
Reflective Category			
Lower bound of lowest category	30 dBZ	ZCLO	Float
Upper bound of highest category	70 dBZ	ZCHI	Float
Category interval or bin size	5 dBZ	DZC	Float
Reflectivity			
Lower bound of lowest interval	30 dBZ	ZLO	Float
Upper bound of highest interval	70 dBZ	ZHI	Float
Reflectivity interval size	5 dBZ	DZ	Float
Altitude			
Upper bound of lowest altitude interval	2 km	HLO	Float
Upper bound of highest altitude interval	20 km	HHI	Float
Altitude interval for all except the first interval, i.e., 0 to HLO	1 km	DH	Float
Area			
Lower bound of lowest interval	0 km^2	ALO	Float
Upper bound of highest interval	5000 km^2	AHI	Float
Area interval or bin size	100 km^2	DA	Float

Table 7.2 (Continued)

Description	Initial Value	Program Name	Format
Length-to-Width Ratio			
Lower bound of lowest interval	1	ELO	Float
Upper bound of highest interval	10	EHI	Float
L-to-W interval size	1	DE	Float
Direction of Maximum Contour Dimension			
Lower bound of lowest interval	0 deg	PHILO	Float
Upper bound of highest interval	180 deg	PHIHI	Float
Angle interval size	5 deg	DPHI	Float
Reflectivity Ratio			
Lower bound of lowest interval	1	ZRLO	Float
Upper bound of highest interval	101	ZRHI	Float
Reflectivity ratio interval size	5	DZR	Float
Altitude of Maximum Reflectivity			
Lower bound of lowest interval	0 km	BHLO	Float
Upper bound of highest interval	20 km	BHHI	Float
Altitude interval size	1 km	DBH	Float
Contour Value	10	CONTOUR	Fixed
Card Output Request	Yes	PUNCH	Char.
Identification of Run	49 Characters	IDENTIFICATION	Char.

After the data for one scan have been stored, they are processed a cell at a time. As described above, a bin sort is performed on each of the various parameters for a cell class, category and altitude interval. If a value exceeds the maximum value allowed for that parameter, the value is placed in the highest bin and a record is kept of that occurrence. In the output listing an asterisk is placed next to the number count to indicate that the maximum value was exceeded. For example, a maximum altitude of 20 km was preset in the program (see Table 7.2, HHI = 20 km). If the altitude of a peak in a sweep is greater than 20 km, the data for that peak would be placed in the 19 to 20 km altitude interval and an asterisk placed in the listing to indicate that the maximum altitude was exceeded.

When all cells in a scan have been processed, the program reads in the data for the next scan. When all scans have been processed, the number count in each bin may be punched out on cards if desired. Next, the number count for the "all" category, i.e., the ROG class cells, is compiled by combining the data for all reflectivity categories in the ROG class cells in a given altitude interval.

The number count data thus compiled may be considered as a set of histograms and form the basis for the statistical modeling discussed in the next section. In the case of the ROG class cells there is (potentially) one histogram for each of the six parameters (peak reflectivity, area of the contour, length-to-width ratio, direction, reflectivity ratio and height of the maximum reflectivity) for each combination of category, altitude interval, and local reflectivity. In addition, histograms of the number of cells in each class and category at a given altitude and, conversely, the number of cells at each altitude for a given class and category are also constructed. These histograms are the first step in the statistical modeling procedure.

A similar set of histograms for the foregoing parameters, with the exception of the reflectivity ratio and altitude of maximum reflectivity, at each altitude, may be constructed for the Virga class cells.

A detailed description of the statistical modeling procedure is contained in Section 7.5.

7.5 STATISTICAL DESCRIPTIONS

Statistical descriptions in the form of frequency distributions, cumulative frequency distributions and the mean, mode, median and standard deviations were calculated for all the histograms described in the previous section. The general data flow, procedures and interpretation of the distributions are discussed in the following sections.

7.5.1 Distributions of Peak Reflectivity

In Figure 7.3 the statistical modeling or data flow diagram for the peak reflectivity is shown. The figure applies to both the ROG and Virga class cells. The right hand column lists the type of curve produced and the number of such curves for the various combinations of cell class, category and altitude interval.

The first step is the calculation of the frequency distribution. Although not strictly correct, the frequency distribution may be thought of as a conditional probability, e.g., the probability that a cell has a peak reflectivity of some value given that the cell is from a given category and class and at some given altitude. In Figure 7.3 this probability is labeled p(Z/ZC,h) where Z is the peak reflectivity, ZC is the reflectivity category and h indicates the altitude interval. The probability that a peak reflectivity of some value will be encountered at a given altitude regardless of the cell category, i.e., for the class of cells, is given by the distribution p(Z/ZC,h) where the category ZC is the "all" category, i.e., all ROG cells regardless of their peak reflectivity below 2 km are lumped together as a class of cells. This probability might also be written p(Z/h) where no mention of cell category is made but simply refers to all cells of the ROG class. See Section 7.5.4 for further discussion of this distribution and its interpretation.

The cumulative frequency distribution may be interpreted as a cumulative probability. It is the probability that the peak reflectivity is less than or equal to some value, given a cell class, category, and altitude. In Figure 7.3 this probability is labeled P(Z/ZC,h). The median value was determined by a linear interpolation of the cumulative frequency distribution to find the 50 percent point.

The mean of the reflectivity in dBZ and standard deviation were calculated using standard techniques. Note that taking the mean dBZ, however, is not equal to the mean reflectivity in mm^6/m^3. No correction for this difference was made.

The mode(s) was established as the bin or interval with the highest frequency count in the histogram. In many cases, multiple values of the mode occur since no curve fitting was performed on the histograms or frequency distributions.

Finally, profiles of the mean, mode, and median reflectivity values were accumulated as a function of altitude.

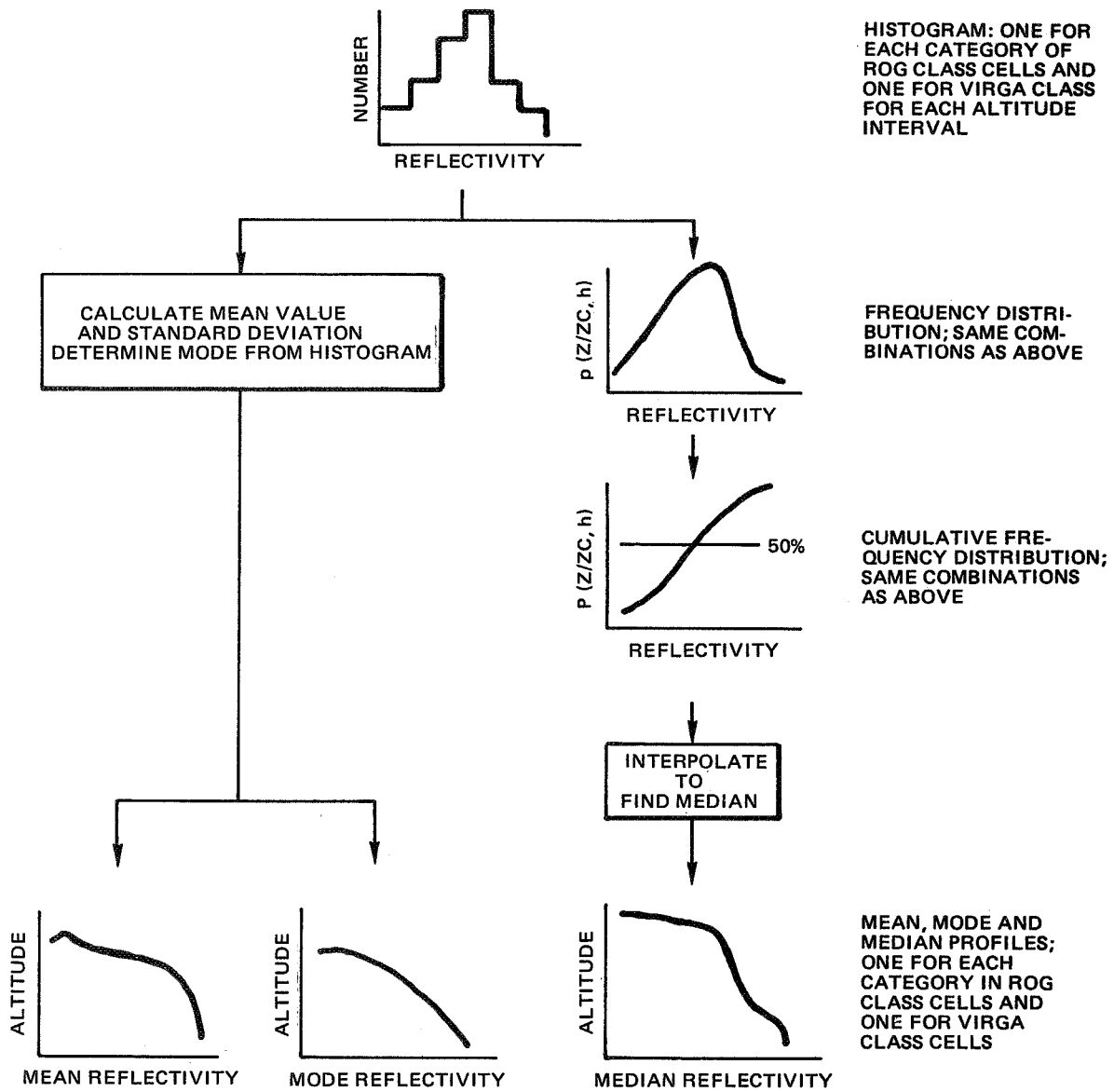

Figure 7.3. Statistical Modeling Flow Diagram for Reflectivity

7.5.2 Distributions of Contour Area, Length-to-Width Ratio and Orientation

The distributions of contour area, length-to-width ratio (L/W) and orientation (ϕ) are somewhat more complicated than those for peak reflectivity. In addition to being sorted in terms of cell class, category and altitude, the area, L/W ratio and orientation are further sorted according to the local peak reflectivity value (Z) at the particular altitude. That is, the distributions or probabilities are based on three conditions, ZC, h and Z. The reason for this is apparent by considering Figure 7.4 in which the area of the 10 dB contour is used as an example. In the figure are shown the peak reflectivity profiles for four cells, all of which belong to the same class and category; ROG cells in the 50-55 dBZ category. At altitude, h, the peak reflectivities for the four cells are quite different ranging from around 37 dBZ to 63 dBZ. The 10 dB relative contour about the peaks at altitude h, therefore, are referenced to a different peak reflectivity value for each cell. If distributions of area were generated which are conditioned only by ZC and h (e.g., P(A/ZC,h)), then the effect of different peak reflectivities as the reference for the relative contour is ignored. Thus, the contour parameters are sorted by category, altitude and local peak reflectivity.

Figure 7.5 shows the statistical modeling flow diagram for describing the contour area. It is similar to that shown in Figure 7.3 for reflectivity but with the additional sorting by local peak reflectivity. The frequency distribution is labeled p(A/ZC,h,Z) indicating the probability that a cell has some area, given the cell is from a certain class and category, and has a given peak reflectivity at a specified altitude. Again in the case of ROG cells, the 'all' category indicates the probability that an area will be encountered at some given altitude with a given reflectivity regardless of the cell category. Such a probability is p(A/ZC,h,z) where ZC is for all ROG class of cells, more simply written p(A/h,Z).

The cumulative frequency distribution is interpreted, again, as the probability that the area encountered is less than or equal to some value for the given conditions.

Figure 7.6 shows the modeling diagram for the length-to-width ratio and orientation of the contour major axis. Note that the calculation of the mean and standard deviation are not included as for reflectivity and area. Both parameters are bounded and, as such, the mean value can be misleading. The orientation, for example, is restricted to 0 to 180 deg while the length-to-width ratio by definition will always be 1.0 or greater.

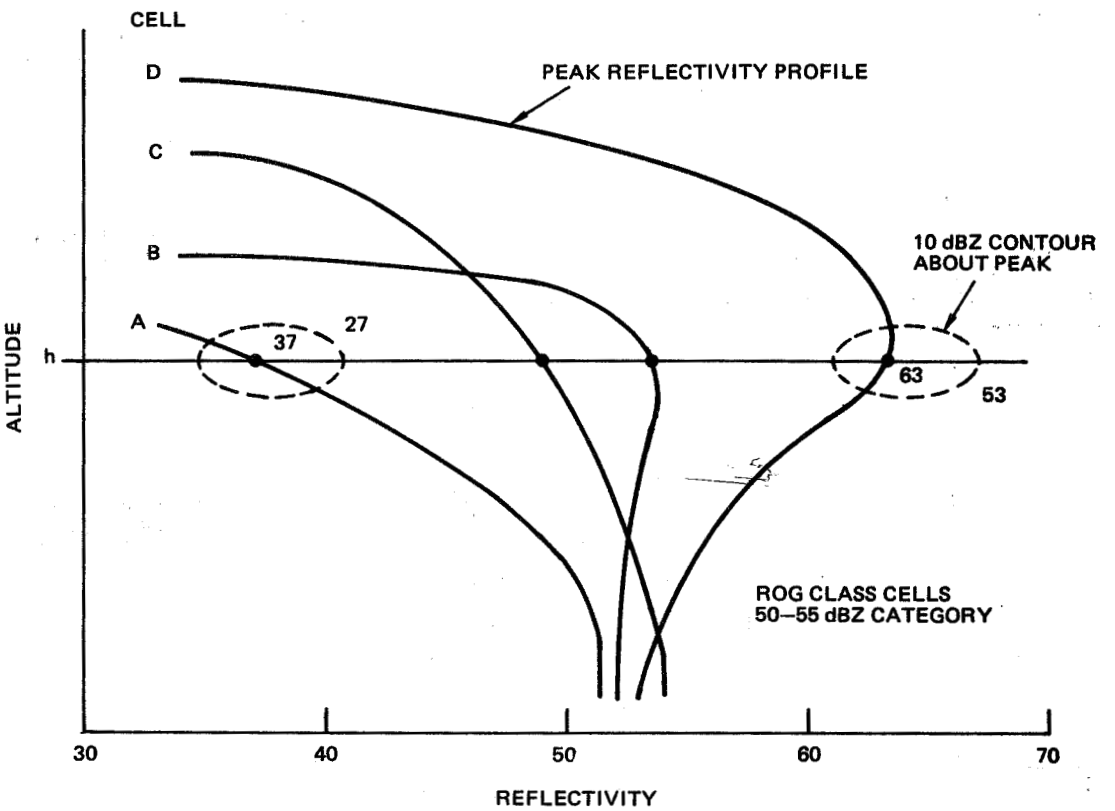

Figure 7.4. Sketch of Reflectivity Profile for Several Cells in Same Category

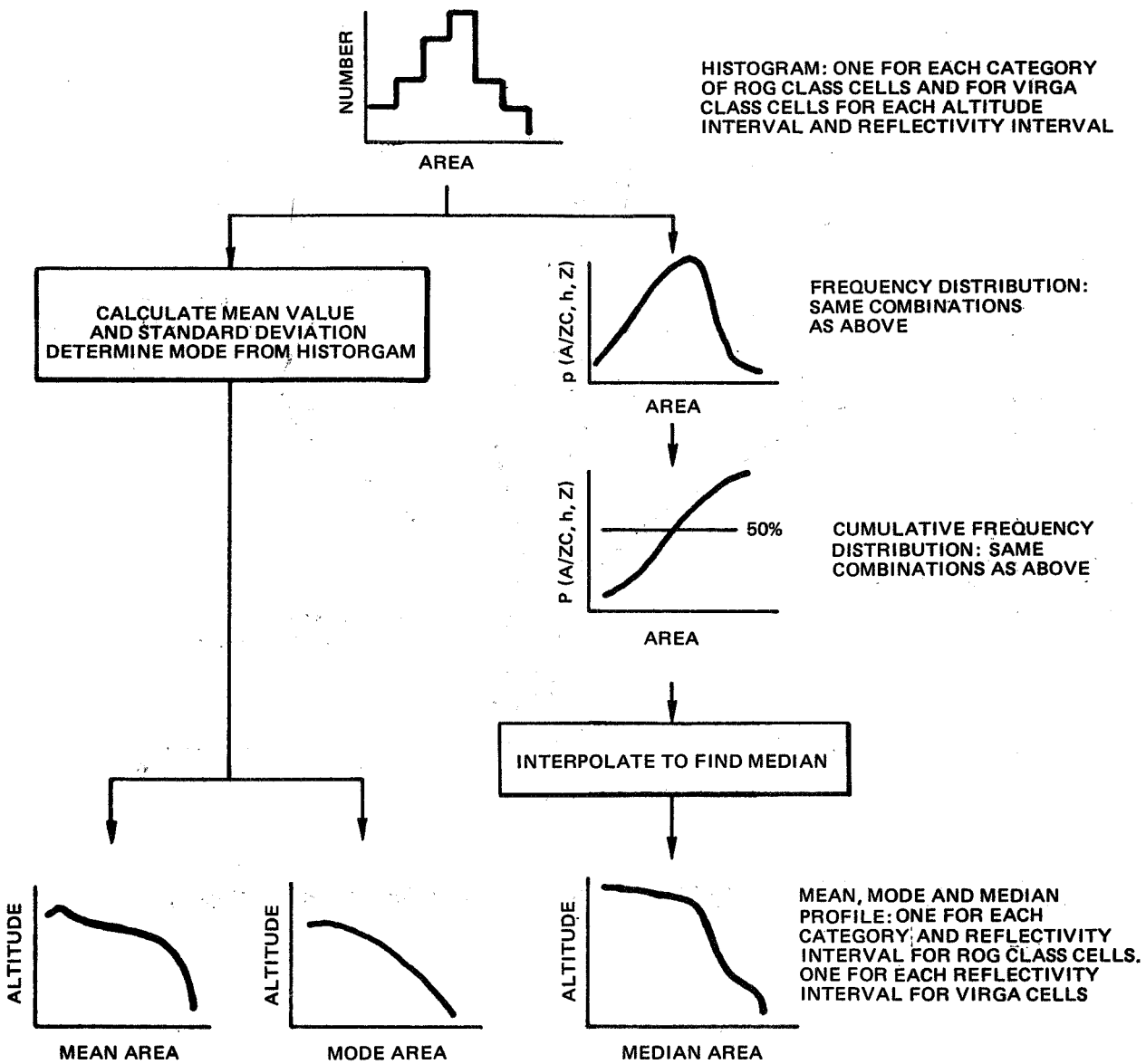

Figure 7.5. Statistical Modeling Flow Diagram for Contour Area

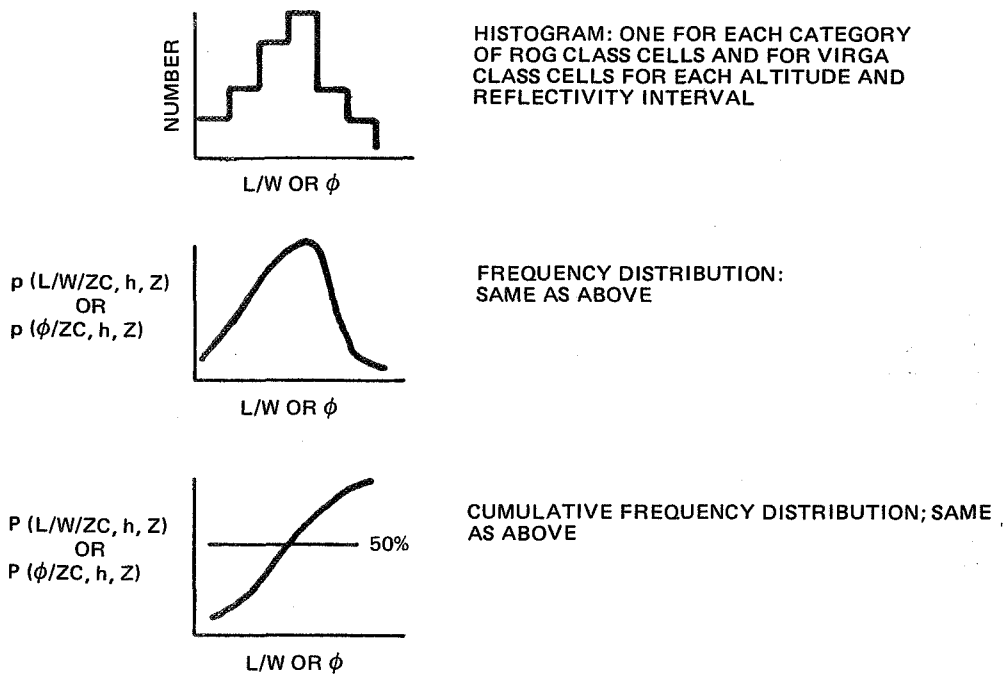

Figure 7.6. Statistical Modeling Flow Diagram for Length-to-Width Ratio (L/W) and Orientation (ϕ)

7.5.3 Distributions of Reflectivity Ratio and Altitude of the Maximum Reflectivity

Statistical descriptions of the reflectivity ratio and height of the maximum peak reflectivity for the ROG class cells are illustrated in Figure 7.7. The reflectivity ratio for the Virga cells was not calculated since the rain did not reach below 2 km and there was no common reference altitude for the ratio. Again, we interpret the frequency distribution and cumulative frequency distribution in terms of probability: p(ZR/ZC) being the conditional probability of a cell having a particular value of reflectivity ratio (ZR) given that the cell is of a particular category (ZC) of the ROG class; and P(ZR/ZC) being the probability that the value is less than the particular value.

7.5.4 Distribution of Number of Cells by Category for Given Altitude Interval

The distribution of the number of cells according to their class and category in a given altitude interval is illustrated in Figure 7.8. The formation of the frequency distribution and, in turn, cumulative frequency distribution from the basic histogram and the calculation of the statistical descriptors is similar to that discussed in the two previous sections. The distributions show the probability of encountering a cell of some category at any given altitude. Alternatively, it is the probability that a cell at a given altitude is from some class or category, i.e., raining on the ground with some intensity. Note that this is not the probability of a reflectivity at that altitude, p(Z/h), except at 0-2 km (discussed below), but only the probability that the cell is from some category. The cumulative distribution is the probability that the cell category will be less than some value. Statistical descriptions were calculated in two ways: (1) for all cells at each altitude, including both ROG and Virga class cells; and (2) for the ROG class cells only. The first case was computed in the third and fourth pass programs whereas the second was calculated by hand using the output data from the first case, i.e., the percentages were recalculated excluding the Virga class cells.

The distributions in the lowest altitude interval, 0-2 km, are of particular interest since these are the distributions or probabilities which may be compared directly with the ground-based rainfall rate data from other stations for extrapolation purposes. In the 0-2 km altitude interval the probability of encountering a cell of a particular category, p(ZC/h), is the same as the probability of a reflectivity of some value at the 0-2 km interval, p(Z/h), using the ROG class cells (discussed in Section 3.5), since the histogram is, by definition, a

NOTE: ZR AND H WERE NOT CALCULATED
FOR VIRGA CLASS CELLS

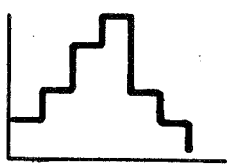

HISTOGRAM; ONE FOR
EACH CATEGORY OF
ROG CLASS CELLS

p (ZR/ZC)
OR
p (H/ZC)

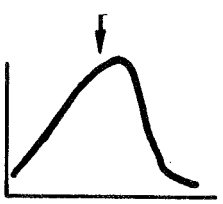

FREQUENCY DISTRIBUTION;
ONE FOR EACH CATEGORY
OF ROG CLASS CELLS

P (ZR/ZC)
OR
P (H/ZC)

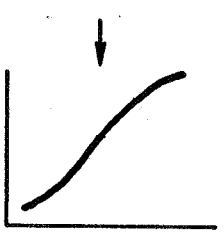

CUMULATIVE FREQUENCY
DISTRIBUTION; ONE FOR
EACH CATEGORY OF
ROG CLASS CELLS

Figure 7.7. Statistical Modeling Flow Diagram for Reflectivity Ratio (ZR) and Altitude of the Maximum Reflectivity (H)

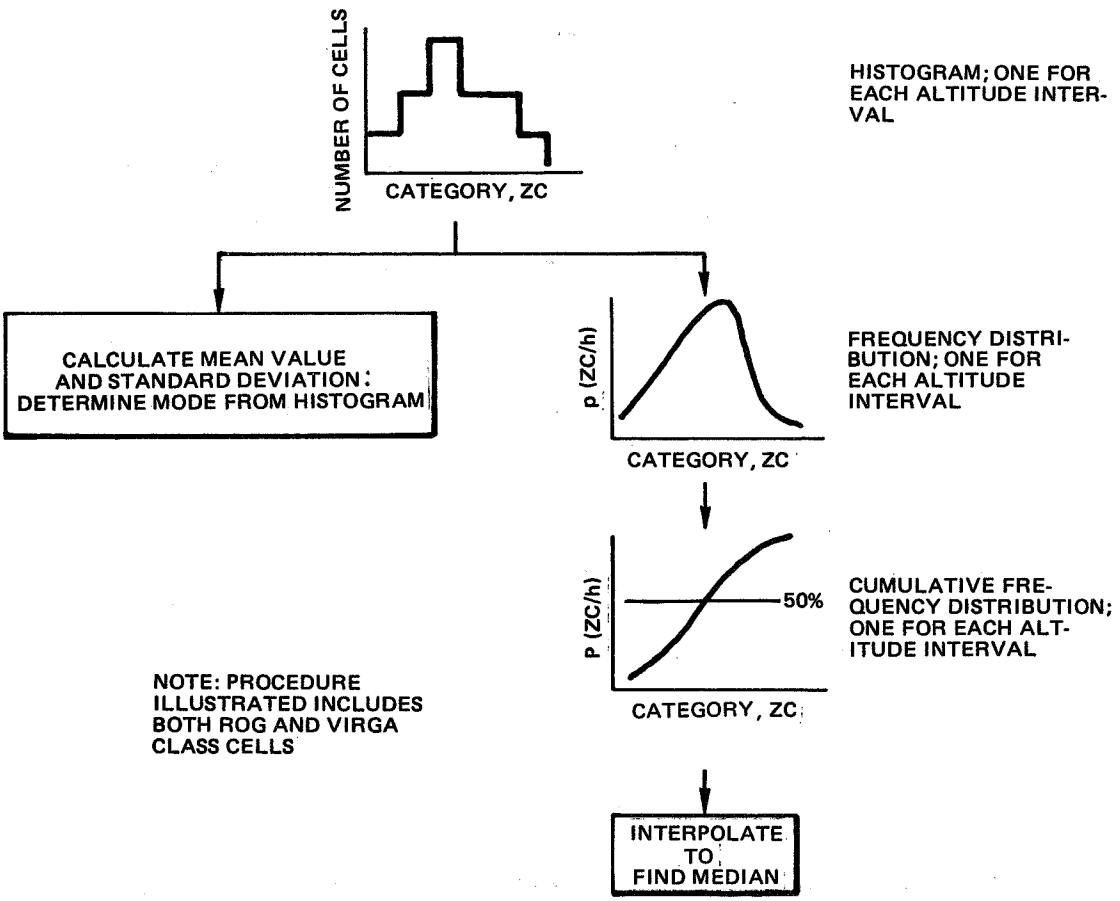

Figure 7.8. Statistical Flow Diagram — Number of Cells in Each Category and Class for Given Altitude Interval

single bar, i.e., the reflectivity at 0-2 km is the category. Essentially this distribution shows the probability of experiencing a rain cell of a given intensity on the ground somewhere within the area of observation.

7.5.5 Distribution of Cells with Altitude for Given Category

Figure 7.9 illustrates the curves compiled to show the distribution of cells with altitude for a given class and category. Note that histograms are formed for both the ROG and Virga class cells. The frequency distribution was formed by dividing the number of cells at an altitude (for given ROG class cell category) by the number of cells in the first altitude interval, i.e., by the number of cells in the population. (This is somewhat different than the usual method where the total number of counts in the histogram are used as the divisor.) The distributions may be interpreted as the probability of a cell of given category reaching some altitude. Phrased another way, given rain on the ground of a particular intensity (category) what is the probability that the cell reaches some altitude, i.e., that it is raining at some altitude? This distribution then, gives the distribution of maximum echo heights of ROG cells of various categories. The "all" category, of course, includes all ROG class cells and the distribution is interpreted as, "given that it is raining on the ground with any intensity, what is the probability that the rain cell extends to some altitude?"

The interpretation of the various frequency distributions, cumulatives and conditional distributions are meant as examples only; other interpretation and phrasing of the probabilities are possible. For example, other authors refer simply to the distribution of echo heights which amount to the same thing.

7.6 PROGRAM OUTPUT

The output of the third pass program consists of three basic parts: (1) listings of input override parameters, control parameters, and results; (2) printer plots of the frequency distributions, cumulative frequency distributions, profiles of the mean, mode, and median values; and (3) punch card output containing number counts in the various bins for further accumulation in the fourth pass program. Again, the output of third pass is on a daily basis only. Table 7.3 shows the order of the computer printout which contains the listings and printer plots.

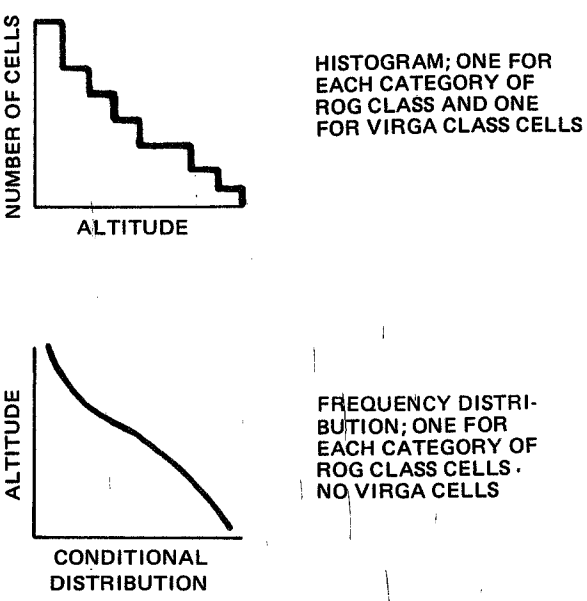

Figure 7.9. Statistical Flow Diagram – Number of Cells by Altitude for Given Category and Class

Table 7.3

Order of Printout of Third Pass Program

1. Listing of override preset values and complete listing of all parameters and their values.

2. Listing of control cards, i.e., cell identification in terms of day, scan, sweep, and peak. Also indication of whether the contour for each peak is to be used in statistical population, e.g., bad contour or no contour.

3. Listing and printer plots of histogram data and frequency distributions for the following combinations of cell class, category, and altitude interval for reflectivity.

Class	Category	Altitude Interval
ROG	All	0-2 km
ROG	30-35 thru 65-70 dBZ	
ROG	All	2-3
ROG	30-35 thru 65-70	
Virga	---	
ROG	All	3-4
ROG	30-35 thru 65-70	
Virga	---	
	etc.	etc.
ROG	All	19-20
ROG	30-35 thru 65-70	
Virga	---	

Table 7.3 (Continued)

4. Listing and printer plots for mean, mode, and median reflectivity as a function of altitude for each class and category in the following order.

Class	Category
ROG	All
ROG	30-35 thru 65-70 dBZ
Virga	--

5. Same as 3 except for area.

6. Same as 4 except for area.

7. Same as 3 except for length-to-width ratio.

8. Same as 4 except for length-to-width ratio.

9. Same as 3 except for direction.

10. Same as 4 except for direction.

11. Listing and plots of histogram data and probabilities for the reflectivity ratio by category, for ROG class cells in the following order (no Virga).

All

30-35 thru 65-70 dBZ

12. Listing and plots of mean, median, and mode reflectivity ratio as a function of category for ROG cells.

13. Same as 11 except for altitude of maximum reflectivity.

14. Same as 12 except for altitude of maximum reflectivity.

15. Listing and plots of histogram data and probabilities of the number of cells by category for given altitude for both ROG and Virga class cells in the following altitude.

Table 7.3 (Continued)

0-2 km

2-3

.

.

.

19-20

16. Listing and plots of histogram and probability of the number of cells by height for given class and category in the following order.

Class	Category
ROG	All
ROG	30-35 thru 60-75 dBZ
Virga	---

7.6.1 Listings and Printer Plots

The first listing of the third pass output (item 1 of Table 7.3) contains the input override preset values followed by a complete set of parameter values for the run. An example of this listing is shown in Figure 7.10. Note the identification by day number. The parameter identification is given in Table 7.2.

The second listing is of the control cards or cell identification card (item 2 of Table 7.3). This is included in the output both as a check and a record of the cells which made up the population for a particular run. An example of this listing is shown in Figure 7.11. Note that a cell is identified alphabetically whereas scan, sweep and peak are numeric. The sweep-peak pair for a given cell and scan are listed consecutively as indicated by under brackets. As described in Section 3.3.2, the contour data for certain peak-sweep combinations were bad or nonexistent. A message on the control card determined whether contour data were to be used. This message is also included in the control card listing. In Figure 7.11 the contour data for sweep 1 of peak 1, cell A of scan 11 are not used, indicated by the circled '1' in the 14th column from the right.

An example of the listing and printer plot for items 3, 5, 7, and 9 of Table 7.3 is shown in Figure 7.12. The data for reflectivity are shown, but the format is identical for area, length-to-width ratio and direction. The third column, labeled probability (percent) is the frequency distribution described in Section 3.5 whereas the column labeled cumulative (percent) is the cumulative frequency distribution. The printer plots repeat the information in columns 1-5. The Virga class cells are identified in the heading as category 0-30 dBZ in all listings and plots. Listings and plots of the profiles of mean, mode, and median values (items 4, 6, 8, and 10 of Table 7.3) are presented as shown in Figure 7.13. Note that the values of these parameters were also listed in Figure 7.12 and are repeated here. The standard deviation is not plotted. The scale of the abscissa is chosen by an algorithm in the computer program. Thus, it will change from one day to the next depending on the data.

Figure 7.14 shows an example of the listing and plot of the reflectivity ratio, and Figure 7.15 presents an example of the statistical descriptors, items 11 and 12 in Table 7.3.

Examples for the altitude at maximum reflectivity are shown in Figures 7.16 and 7.17, items 13 and 14 of Table 7.3.

```
 THE FOLLOWING PARAMETERS OVERRIDE PRESET VALUES
AHI=1000
EHI=100
DA=10
DZR=2
PUNCH='NO'
IDENTIFICATION='DAY 186 OF 1973'

 THE COMPLETE PARAMETER SET FOR THIS RUN IS -
HLO= 2.000000E+00      HHI= 2.000000E+01      ZCLO= 3.000000E+01      ZCHI= 7.000000E+01      ZLO= 3.000000E+01
ZHI= 7.000000E+01      ALO= 0.000000E+00      AHI= 1.000000E+03      ELO= 1.000000E+00      EHI= 1.000000E+02
PHILO= 0.000000E+00    PHIHI= 1.800000E+02    ZRLO= 1.000000E+00     ZRHI= 1.010000E+02     BHLO= 0.000000E+00
BHHI= 2.000000E+01     DZC= 5.000000E+00      DZ= 5.000000E+00       DH= 1.000000E+00       DBH= 1.000000E+00
DA= 1.000000E+01       DE= 1.000000E+00       DZR= 2.000000E+00      DPHI= 5.000000E+00     IDENTIFICATION='DAY 186 OF 1973'
PUNCH='NO'             CONTOUR=       10;
```

Figure 7.10. Listing of Override Parameters and Complete Parameter Set

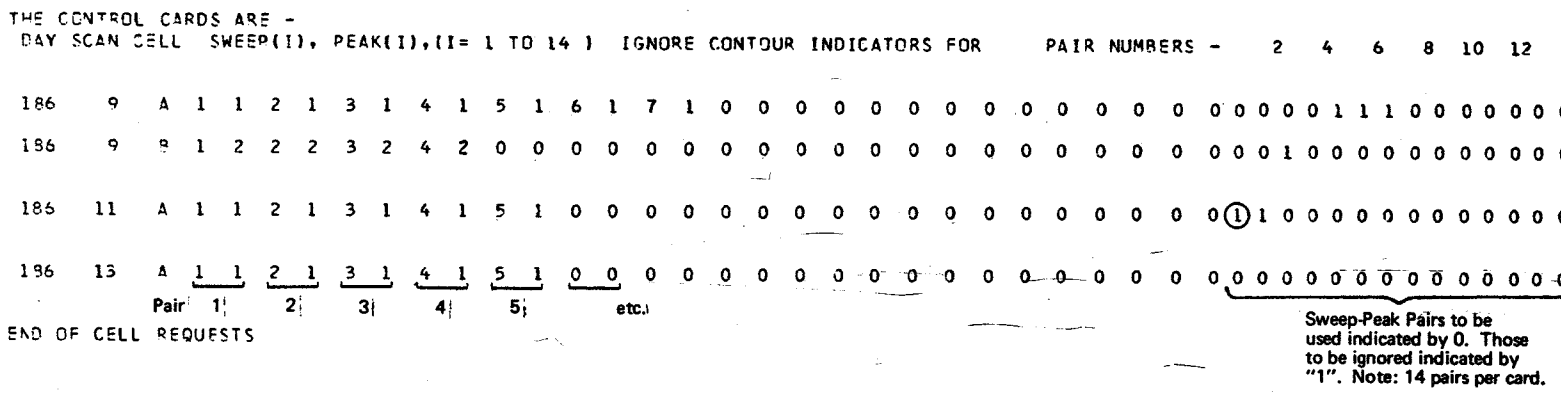

Figure 7.11. Listing of Control Cards Identifying Cells

DAY 186 CATEGORY ALL DBZ CONTOUR 10 DB ALTITUDE INTERVAL 2-3 KM

REFLECTIVITY (DBZ)	NUMBER IN HISTOGRAM	PROBABILITY (PERCENT)	CUMULATIVE (PERCENT)	TOTAL NO. OF CELLS	MEAN REFLECT.(DBZ)	MEDIAN REFLECT.(DBZ)	MODE REFLECT.(DBZ)	SIGMA (DBZ)
35-40	1	25.0	25.0	4	47.02	50.0	50-55	5.6
45-50	1	25.0	50.0					
50-55	2	50.0	100.0					

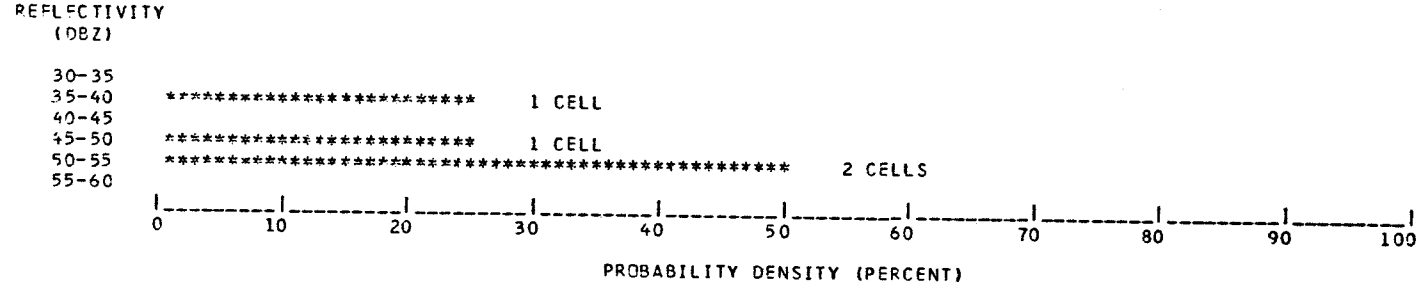

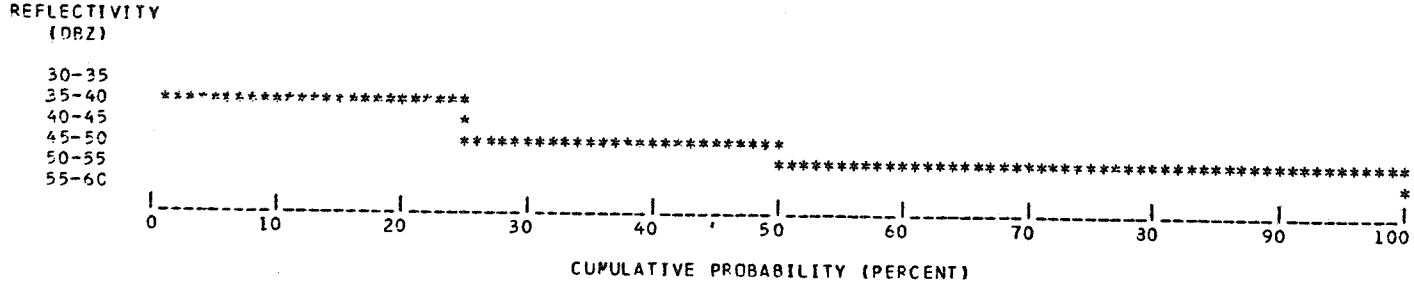

Figure 7.12. Listing and Printer Plot of Output from Third Pass for Reflectivity Factor. Format is Identical for Area, Length-to-Width Ratio and Direction

DAY 186 CATEGORY ALL DBZ CONTOUR 10 DB REFLECTIVITY

ALTITUDE INTERVAL (KM)	MEAN (DBZ)	MEDIAN (DBZ)	SIGMA (DBZ)	MODE (DBZ)	
0-2	45.20	45.0	6.2	50-55	
2-3	47.02	50.0	5.6	50-55	
3-4	49.12	50.8	6.3	50-55	
4-5	45.70	47.5	6.9	50-55	
5-6	46.10	45.0	1.7	40-45	45-50
6-7	40.10	42.5	0.0	40-45	
7-8					
8-9					
9-10					
10-11					
11-12					
12-13					
13-14					
14-15					
15-16					
16-17					
17-18					
18-19					
19-20					

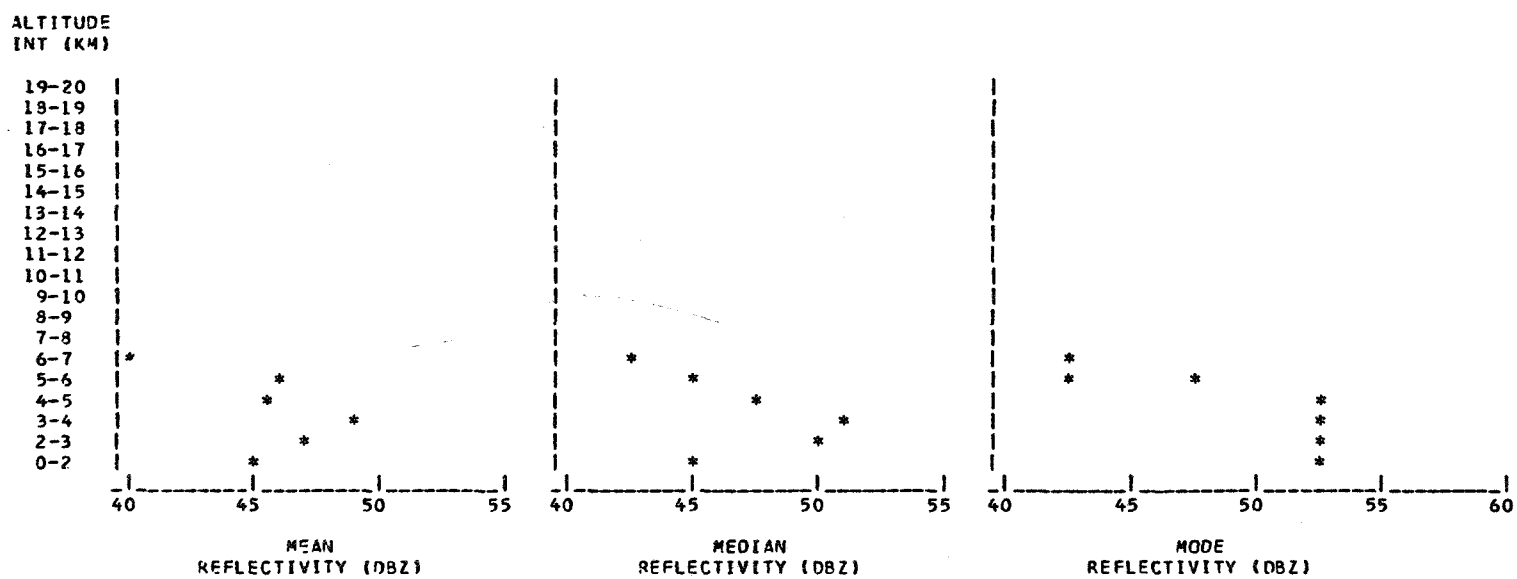

Figure 7.13. Listing and Printer Plots of Mean, Median and Mode Reflectivity Factor as a Function of Altitude. Format is Identical for Area, Length-to-Width Ratio and Direction

DAY 186 CATEGORY ALL DBZ CONTOUR 10 DB REFLECTIVITY RATIO

REFLECTIVITY RATIO	NUMBER IN HISTOGRAM	PROBABILITY (PERCENT)	CUMULATIVE (PERCENT)	TOTAL NO. OF CELLS	MEAN RATIO	MEDIAN RATIO	MODE RATIO	SIGMA RATIO
1-3	3	75.0	75.0	4	3.67	2.3	1-3	3.5
9-11	1	25.0	100.0					

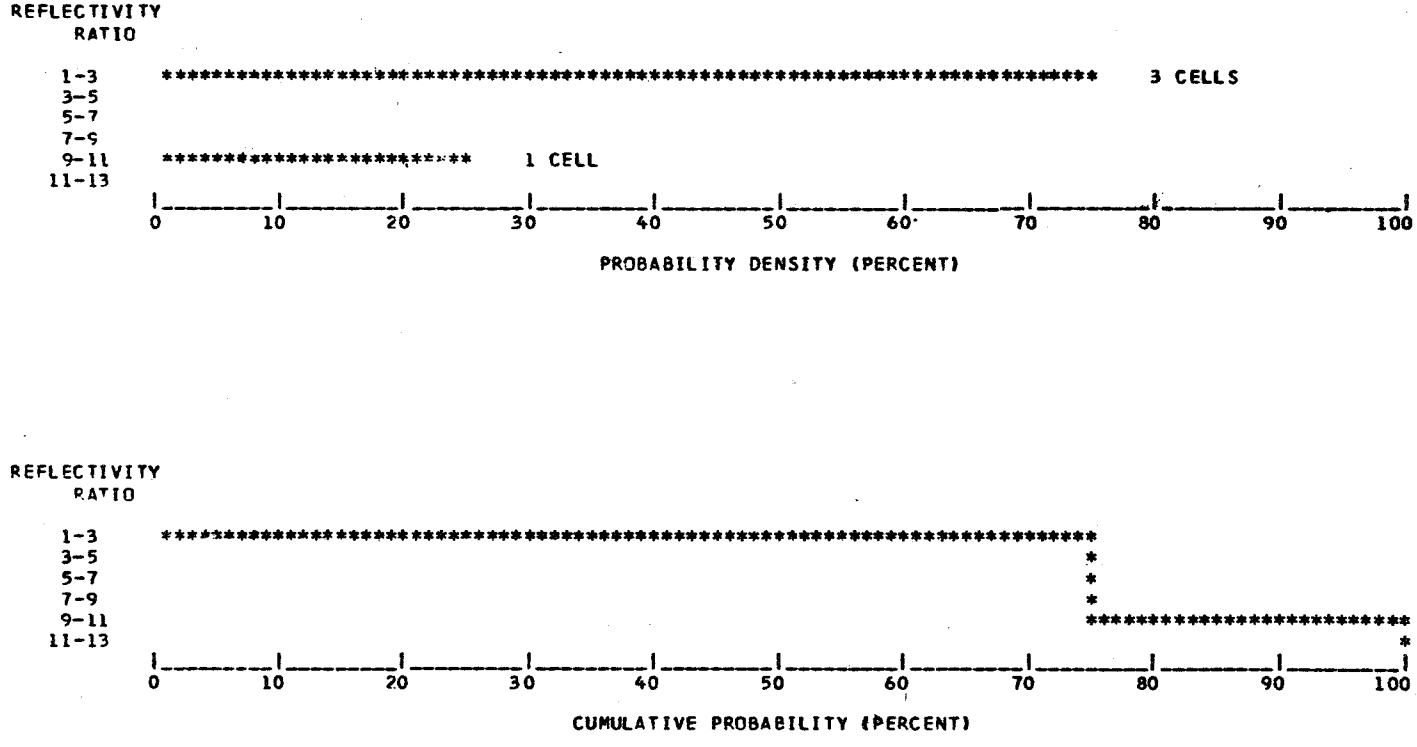

Figure 7.14. Listing and Printer Plot for Reflectivity Ratio

DAY 186 CONTOUR 10 DB REFLECTIVITY RATIO

CATEGORY (DBZ)	MEAN RATIO	MEDIAN RATIO	SIGMA RATIO	MODE RATIO
30-35				
35-40	1.58	2.0	0.0	1-3
40-45	9.77	10.0	0.0	9-11
45-50				
50-55	1.66	2.0	0.3	1-3
55-60				
60-65				
65-70				

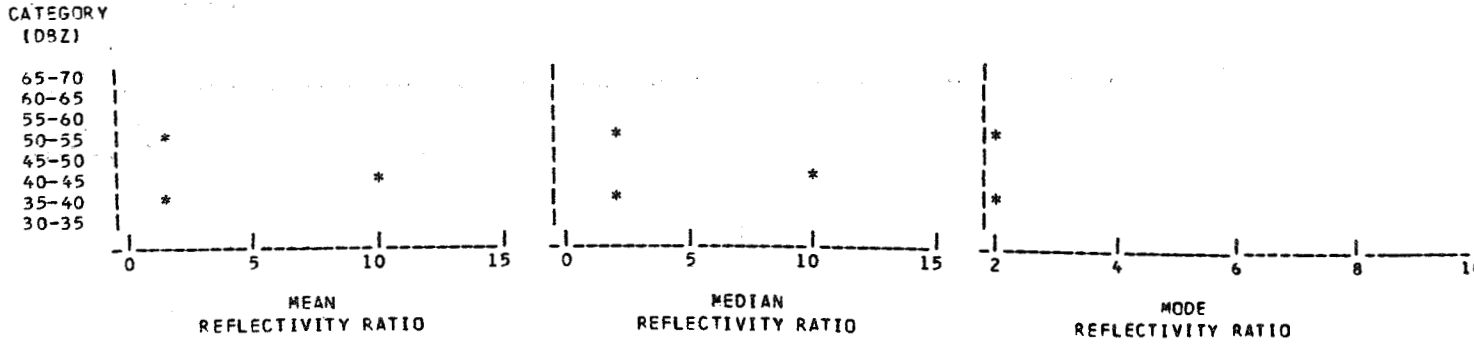

Figure 7.15. Listing and Printer Plot of Mean, Median and Mode Reflectivity Ratio as a Function of Altitude

DAY 186 CATEGORY ALL DBZ CONTOUR 10 DB ALTITUDE AT MAX REFLECTIVITY

ALT. AT MAX REFLECT. (KM)	NUMBER IN HISTOGRAM	PROBABILITY (PERCENT)	CUMULATIVE (PERCENT)	TOTAL NO. OF CELLS	MEAN ALT. (KM)	MEDIAN ALT. (KM)	MODE ALT. (KM)	SIGMA ALT. (KM)
2-3	2	50.0	50.0	4	2.90	3.0	2-3	0.7
3-4	2	50.0	100.0				3-4	

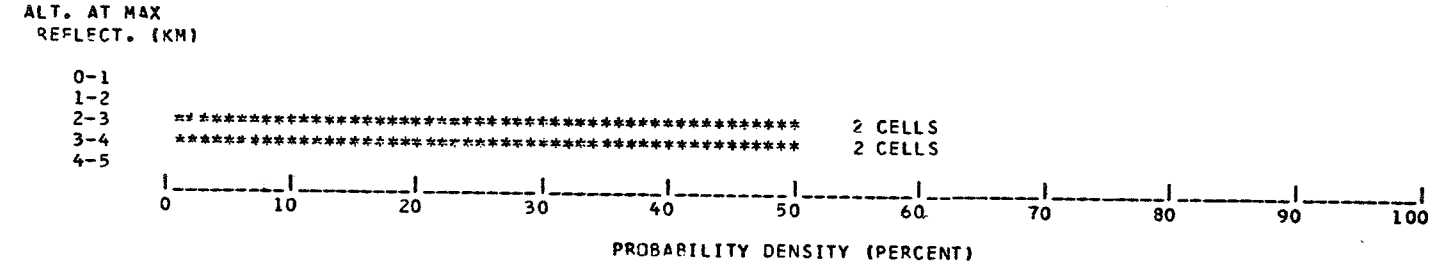

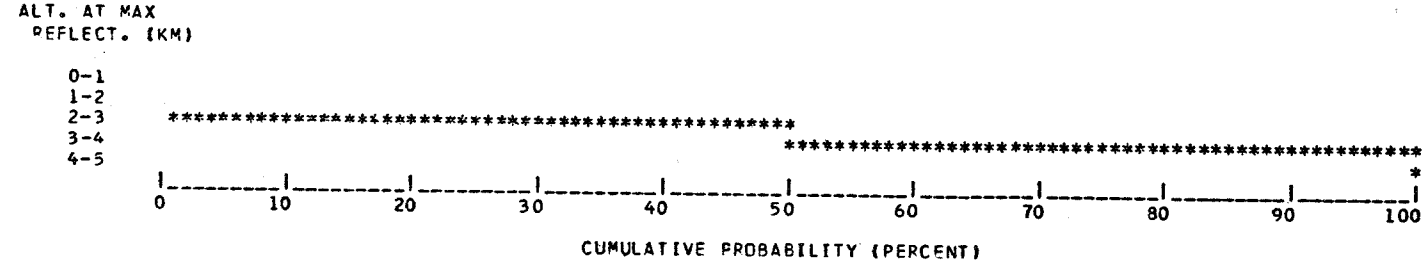

Figure 7.16. Listing and Printer Plot for the Altitude at Maximum Reflectivity

DAY 186 CONTOUR 10 DB ALTITUDE AT MAX REFLECTIVITY

CATEGORY (DBZ)	MEAN (KM)	MEDIAN (KM)	SIGMA (KM)	MODE (KM)	
30-35					
35-40	2.20	2.5	0.0	2-3	
40-45	3.20	3.5	0.0	3-4	
45-50					
50-55	3.10	3.0	0.8	2-3	3-4
55-60					
60-65					
65-70					

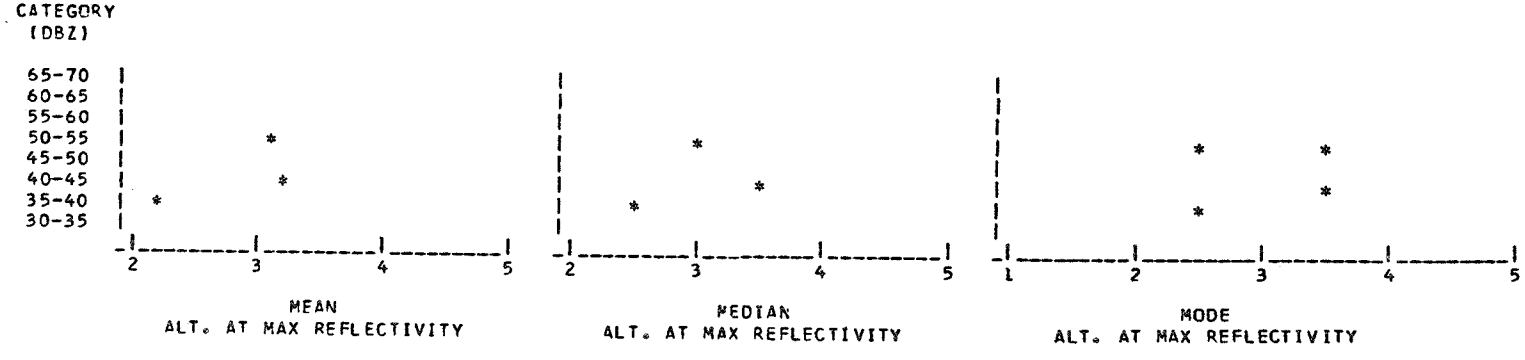

Figure 7.17. Listing and Printer Plot of Mean, Median and Mode Altitude at Maximum Reflectivity

The number of cells by category for a given altitude interval, item 15 of Table 7.3, is shown in Figure 7.18. Note that the Virga class cells are listed as category 0-30 dBZ and are included in the total number of cells as well as the frequency distributions.

Item 16 of Table 7.3, number of cells by height for a given category, is shown in Figure 7.19. As noted in Table 7.3 the frequency distributions are not included for the Virga (0-30 dBZ) cells.

7.6.2 Punch Card Output

The number counts in the various bins for all the histogram data are punched on cards for use in the fourth pass program. The format of these cards is as follows.

The first two cards contain descriptive information about the reflectivity contour data which is taken from the input override parameters and is punched in the last 49 columns on the card and also parameter information giving lower and upper bounds when inputting data.

The punched cards which contain the frequency counts and statistical data are in Edit-directed format as follows:

Column	Format	Description
1	CHAR	Card type, that is, R,E,D, or A for reflectivity data, eccentricity data, direction data, or area data, respectively
2-4	XXX	Day number. Note: In fourth pass, the day number is replaced by a run identification and the format would be a character string of length 3. See Section 8.3
5-6	XX	Altitude index
7-8	XX	Category index
9-10	XX	Sequence number to determine whether more than one card will be punched for a particular type

DAY 186 CONTOUR 10 DB ALTITUDE INTERVAL 2-3 KM

NUMBER OF CELLS BY CATEGORY FOR GIVEN ALTITUDE

CATEGORY (DBZ)	NUMBER OF CELLS	PROBABILITY (PERCENT)	CUMULATIVE (PERCENT)	TOTAL NO. OF CELLS	MEAN REFLECT.(DBZ)	MEDIAN CATEGORY	MODE CATEGORY
0-30	0	0.0	0.0	4	47.02	40-45	50-55
30-35	0	0.0	0.0				
35-40	1	25.0	25.0				
40-45	1	25.0	50.0				
45-50	0	0.0	50.0				
50-55	2	50.0	100.0				
55-60	0	0.0	100.0				
60-65	0	0.0	100.0				
65-70	0	0.0	100.0				

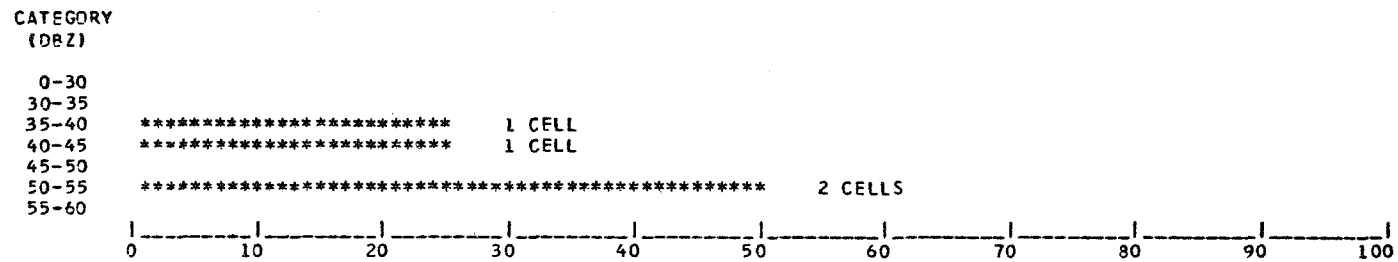

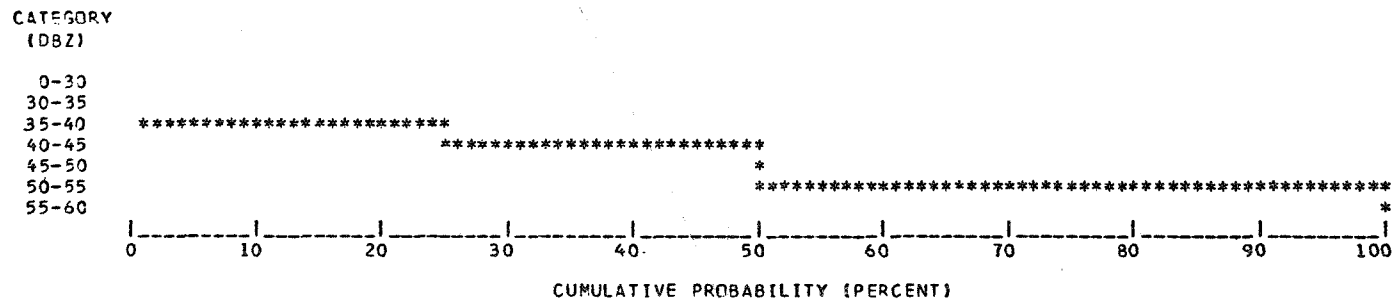

Figure 7.18. Listing and Printer Plot of the Number of Cells by Category for a Given Altitude Interval

DAY 186 CONTOUR 10 DB CATEGORY 35-40

NUMBER OF CELLS BY HEIGHT
FOR GIVEN CATEGORY

ALTITUDE INTERVAL (KM)	NUMBER OF CELLS	CONDITIONAL (PERCENT)
0-2	1	100.0
2-3	1	100.0
3-4	1	100.0
4-5	1	100.0
5-6	0	0.0
6-7	0	0.0
7-8	0	0.0
8-9	0	0.0
9-10	0	0.0
10-11	0	0.0
11-12	0	0.0
12-13	0	0.0
13-14	0	0.0
14-15	0	0.0
15-16	0	0.0
16-17	0	0.0
17-18	0	0.0
18-19	0	0.0
19-20	0	0.0

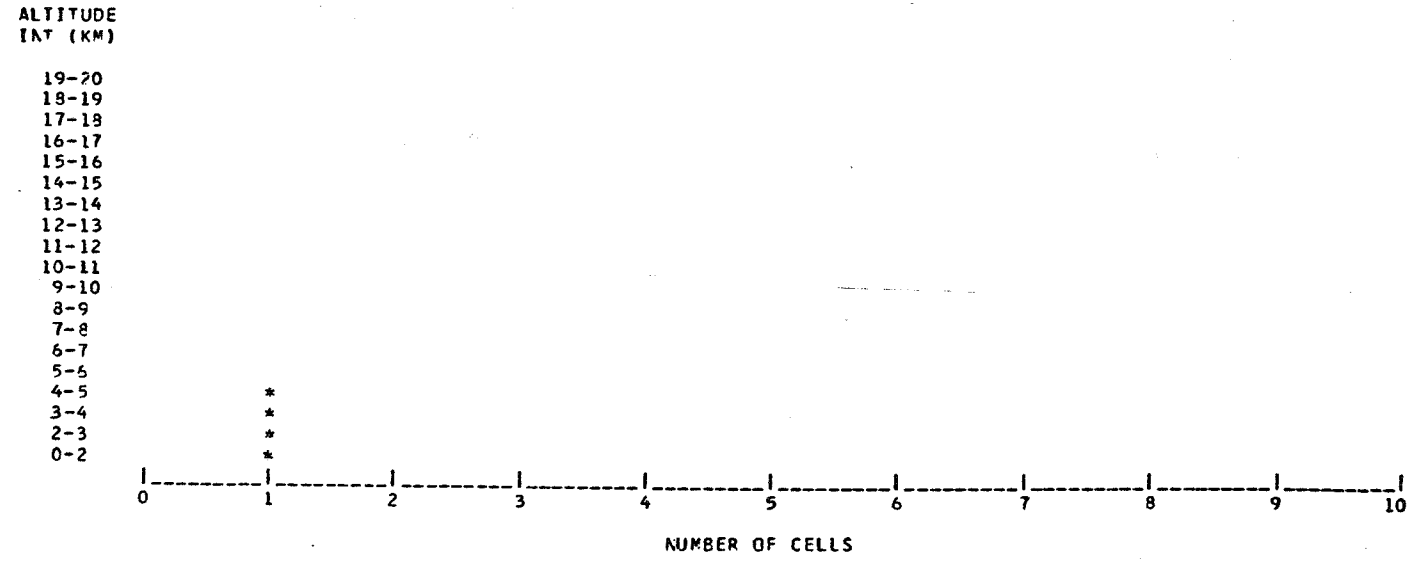

Figure 7.19. Listing and Printer Plot of the Number of Cells by Height for a Given Category

Column	Format	Description
11-19	XXXXXXX.X	Sum of data points
20-31	XXXXXXXXX.XX	Sum of the squares of data points
33-33	XX	Histogram index
34-38	XXXXX	Histogram count
39-45	Same description and format as 32-38	
.		
.		
.		
74-80	Same description and format as 32-38	

If this information exceeds one card, subsequent cards are used where columns 1-10 will be the same and the histogram index and count number will start in column 11; the sum of the data and the sum of the squares of the data will be omitted on these cards.

Cards for the reflectivity ratio and the maximum altitude will have the following format.

Column	Format	Description
1	CHAR	Card type, i.e., Z or H for reflectivity ratio, and the maximum altitude, respectively
2-4	XXX	Day number. Note: In the fourth pass program, the day number is placed by a run identification and the format would be a character string of length 3. See Section 8.3
5-6	XX	Category index
7-8	XX	Sequence number
9-15	XXXXX.X	Sum of data points

Column	Format	Description
16-24	XXXXXX.XX	Sum of the squares of data points
25-26	XX	Histogram index
27-31	XXXXX	Histogram count
.		
.		
.		
74-80	Same description and format as 25-31	

If this information exceeds one card, subsequent cards are used containing the same information except that the histogram index and count will start in column 11, and the sum of the data and the sum of the squares of the data will be omitted.

8. FOURTH PASS COMPUTER PROGRAM

8.1 GENERAL DESCRIPTION

The fourth pass computer program (Ref. 8) is written to accept the number counts for the various histograms generated on a daily basis in the third pass program and accumulate the data for a number of days. The program has no classification or categorization capability. All this is performed in the third pass. The fourth pass merely accumulates the data which is supplied to it via the output cards from the third pass program.

8.2 INPUT TO FOURTH PASS COMPUTER PROGRAM

The input to the fourth pass computer program consists of the output cards from the third pass program plus the input parameters, i.e., the override preset parameters. The override parameters must be the same, of course, for all the days supplied to the fourth pass. For example, all altitude intervals, the contour level, all upper and lower bounds, etc., must be the same for all days. Further, the input parameters to the fourth pass must be identical to those of the third pass output cards. The fourth pass program is an accumulation program only. It has no capability to modify the input data, e.g., make the reflectivity interval twice what is was in the third pass. The requirement

for identical input parameters for the third and fourth pass cannot be overemphasized.

8.3 OUTPUT

The output of the fourth pass program is identical to that of the third pass (discussed in Section 7.6) with one very slight exception. Listings, printer plots and card formats are the same as for the third pass. The exception is that the day number is replaced by a run identification number, but the character string is still three; see note in paragraph 7.6.2 for columns 2-4. This means that the outputs from the fourth pass program may also be used as input to the fourth pass program for further accumulation of data. For example, assume the data for a number of days for a given summer have been accumulated using the fourth pass program. Further, assume that similar data were available for a second summer. These data, in turn, could be combined by submitting the output cards for the two summers (output cards from the two fourth pass runs) to another fourth pass run. An alternate but far more tedious method would be to submit the output cards from the third pass for each day of the two summers. Fourth pass output was specifically designed to eliminate this procedure. Again, caution should be exercised to ensure that all input parameters are identical.

9. RAIN CELL POPULATION USED IN STATISTICAL DESCRIPTIONS

9.1 INDEPENDENT CELL CRITERIA

The data taken during the experiment and the portion of the raw data processed through the first and second pass computer programs on the NASA 360/95 computer were summarized in Table 4.1. These listings represent the data base from which the cell population for statistical analysis was taken. All the data reduced and all the cells identified were not used in the analysis, however. In many cases multiple scans through a group of cells were taken as quickly as possible for time history and cell development purposes. The use of cells from such scans in the statistical analysis would bias the data since the data were essentially from the same cells, i.e., the cell characteristics would be essentially the same from scan to scan. A criterion for selecting scans was established which limits the analysis to (essentially) independent cells. Only those scans which were separated by one half hour or more were included in the statistical analysis of cell characteristics. There is some evidence from work by other investigators that the typical lifetime of intense cells is on the order of a half hour. Even if a cell has a longer lifetime, however, the characteristics will have changed markedly. The assumption in this case is that although

the cell itself may be the same for scans separated by a half hour, the characteristics have changed to the extent that the two (or more) observations may be treated as independent rain cells.

9.2 TOTAL CELL POPULATION

Table 9.1 shows the total number of scans taken on each day with the total number of scans reduced and the total number of cells identified. These columns include all the data taken and reduced in the first and second pass computer programs regardless of time spacing. The final two columns show the number of independent scans, i.e., separated by a half hour and the number of cells included in the cell population for statistical modeling. Data control cards (Section 7.3.2) were made up for only those cells in the final column of Table 9.1.

10. STATISTICAL RESULTS

10.1 DAILY STATISTICS

Data from each of the 21 days were processed through the third pass program. Computer output (for each day) as described in Section 7.6 is contained in a set of separate volumes. Due to the voluminous quantity of output, these data are not included in this report, but are available from the author or from NASA/GSFC.

The statistics on a daily basis are not significant by themselves. As shown in Table 9.1, some days have very few cells. The statistical descriptions generated in the third pass, therefore, are not representative for classes or categories of cells. Examples of computer output on a daily basis were presented in Section 7.6.1 and as such will not be repeated.

10.2 ALL SUMMER STATISTICS

The rain cell statistics for the entire summer were obtained by combining the data from the 21 days of data in Table 9.1 using the fourth pass program. The computer output, i.e., the listings and printer plots, are contained in a separate volume. Again, because of the voluminous nature of the computer output data, they are not contained in this report. They are also available from the author or from NASA/GSFC. The cumulative frequency distributions of the various physical parameters and statistical descriptors have been extracted, replotted, and examples are shown in this section.

Table 9.1

Cell Population Used in Statistical Model

Day	Number of Scans Taken	Number of Scans Reduced	Number of Cells Identified	Number of Scans Used in Model	Number of Cells Used in Model
May 9	5	0			
14	5	0			
15	4	0			
17	7	0			
23	8	5	23	2	16
24	13	6	53	6	53
29	13	12	59	10	50
Jun 13	13	10	26	10	26
18	13	12	136	10	115
20	2	0			
21	17	11	72	11	72
22	27	18	131	13	100
26	2	0			
27	7	0			
28	4	0			
29	31	26	135	17	95
Jul 3	15	12	73	11	70
5	6	5	6	3	4
10	21	18	125	13	95
11	17	0			
18	4	0			
20	4	0			
27	15	13	25	10	22
31	12	10	61	6	43
Aug 1	16	11	77	8	57
2	13	6	89	3	36
3	19	0			
13	27	18	69	12	55
14	11	6	40	4	30
15	16	14	118	10	88
16	16	15	33	10	22
20	10	9	58	9	58
21	9	9	37	8	34
Total	402	246	1446	185	1141

10.2.1 Peak Reflectivity

Cumulative frequency distributions of peak or core reflectivities as a function of altitude for the categories of ROG class cells are shown in Figures 10.1 through 10.8. These curves may be interpreted as follows: Given an ROG cell of some intensity, what is the probability that the reflectivity will be equal to or less than some value at an altitude? The probability of experiencing a reflectivity equal to the category at 0-2 km is, of course, always 100 percent since the category was established using the reflectivity in this altitude and the histogram is a single bar.

It is interesting to note the change in the character of the altitude distributions with category. Consider the 35-40 categories. A good portion of the altitude curves lie to the right of the category value. This indicates that the probability of experiencing a reflectivity at an altitude which is higher than that on the ground is quite significant. For example, given a very low reflectivity at the ground, say 35-40 dBZ, the probability that the reflectivity at 5-6 km is 40 dBZ or less is around 60 percent. Alternatively, the probability that the reflectivity at 5-6 km is greater than 40 dBZ is 40 percent.

As the reflectivity category increases the location of the altitude curves moves to the left of the reflectivity category value until finally, for the highest category, 65-70 dBZ, they are entirely to the left. At this point, the probability of the reflectivity being less than the category value at all altitudes is 100 percent. As the altitude increases, the probability that a reflectivity is less than some value also increases, again indicating that the core reflectivities typically fall off as a function of altitude for the high category cells. A good example of this characteristic is shown by the 55-60 dBZ category cells.

One may ask the question: Given a cell of a given category (ROG of given intensity) what is the maximum value of reflectivity which is never exceeded as a function of altitude? The answer to this question is simply the cross plot of the 100 percent values of each category.

An alternate question is: Given an ROG of some intensity, what is the probability that this value is exceeded at each altitude? Again this may be answered by using a cross plot of the data in Figures 10.1 through 10.8. The probability that the surface value is exceeded is one minus the probability value at each altitude for a reflectivity equal to that on the ground, i.e., the category value. For example, in Figure 10.2, given a surface reflectivity of 35-40 dBZ, the probability that the reflectivity at 3-4 km is greater than 35-40 dBZ is 30 percent (100 minus the value at 37.5 dBZ for 3-4 km; 100 - 70 = 30).

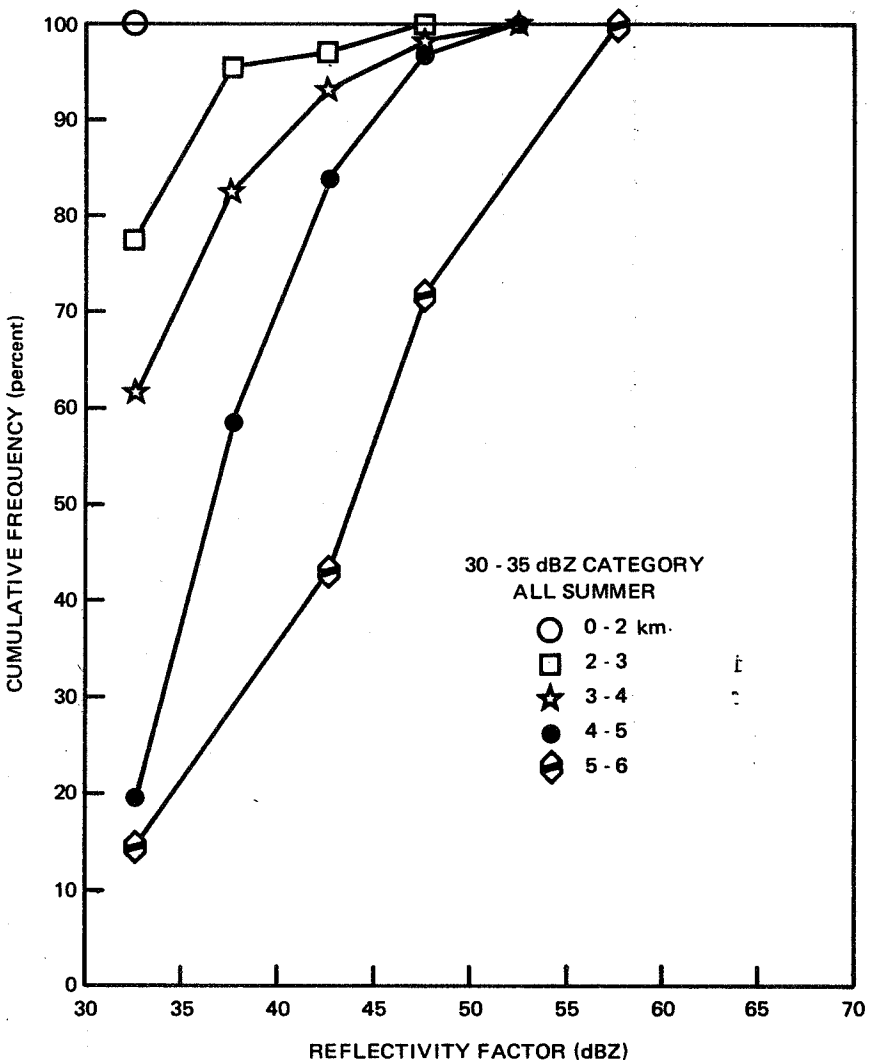

Figure 10.1. All Summer Cumulative Frequency Distribution of Peak Reflectivity Factor According to Altitude for ROG 30 - 35 dBZ

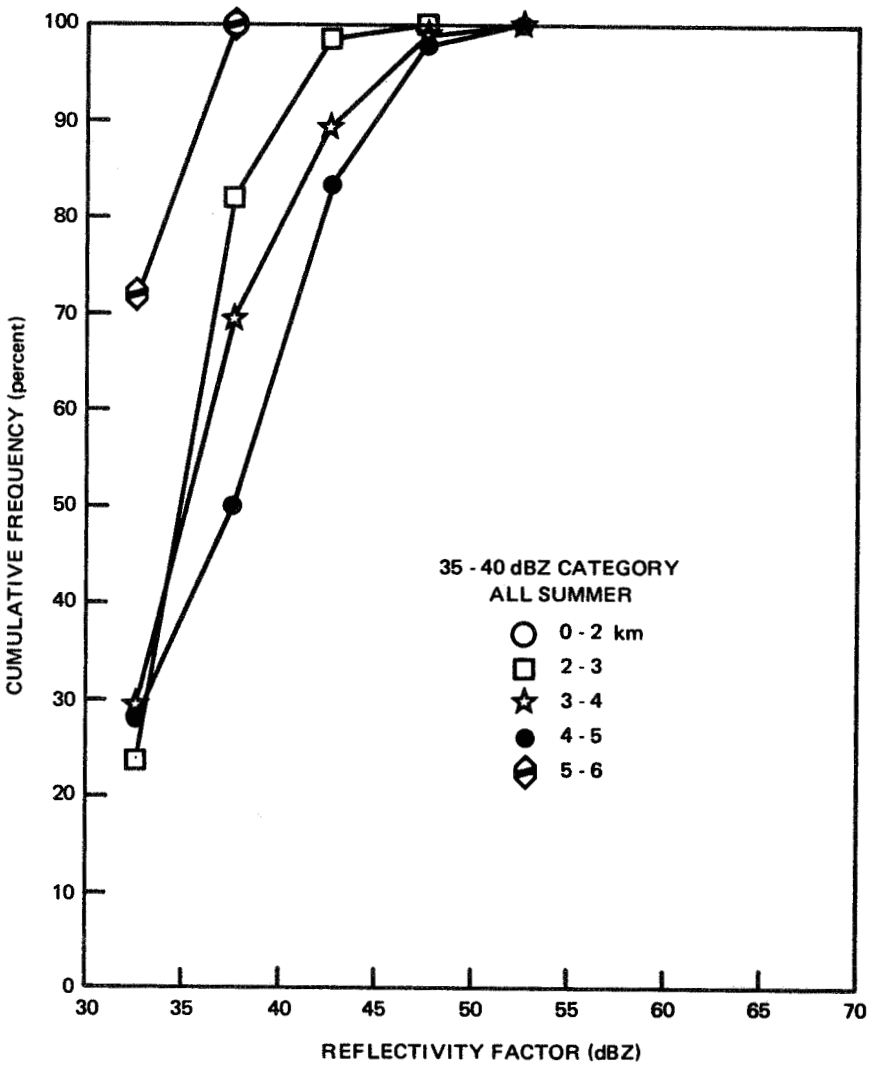

Figure 10.2. All Summer Cumulative Frequency Distribution of Peak Reflectivity Factor According to Altitude for ROG 35 - 40 dBZ

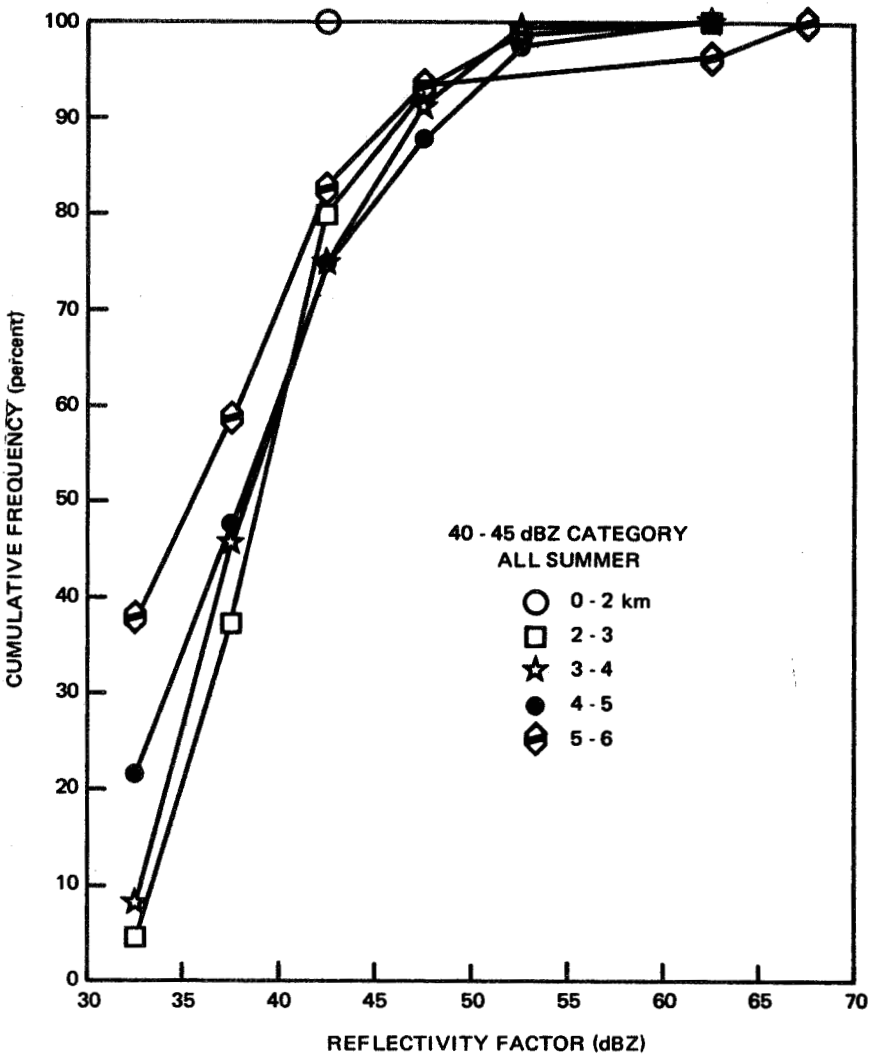

Figure 10.3. All Summer Cumulative Frequency Distribution of Peak Reflectivity Factor According to Altitude for ROG 40 - 45 dBZ

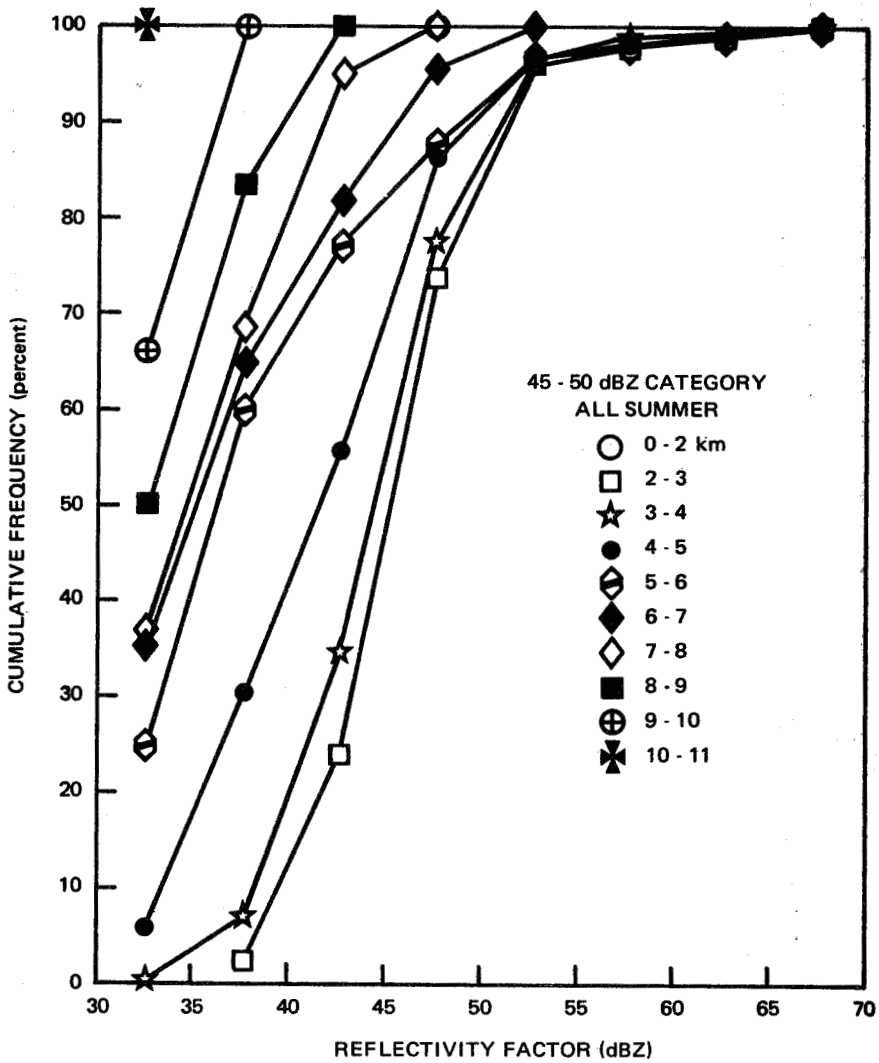

Figure 10.4. All Summer Cumulative Frequency Distribution of Peak Reflectivity Factor According to Altitude for ROG 45 - 50 dBZ

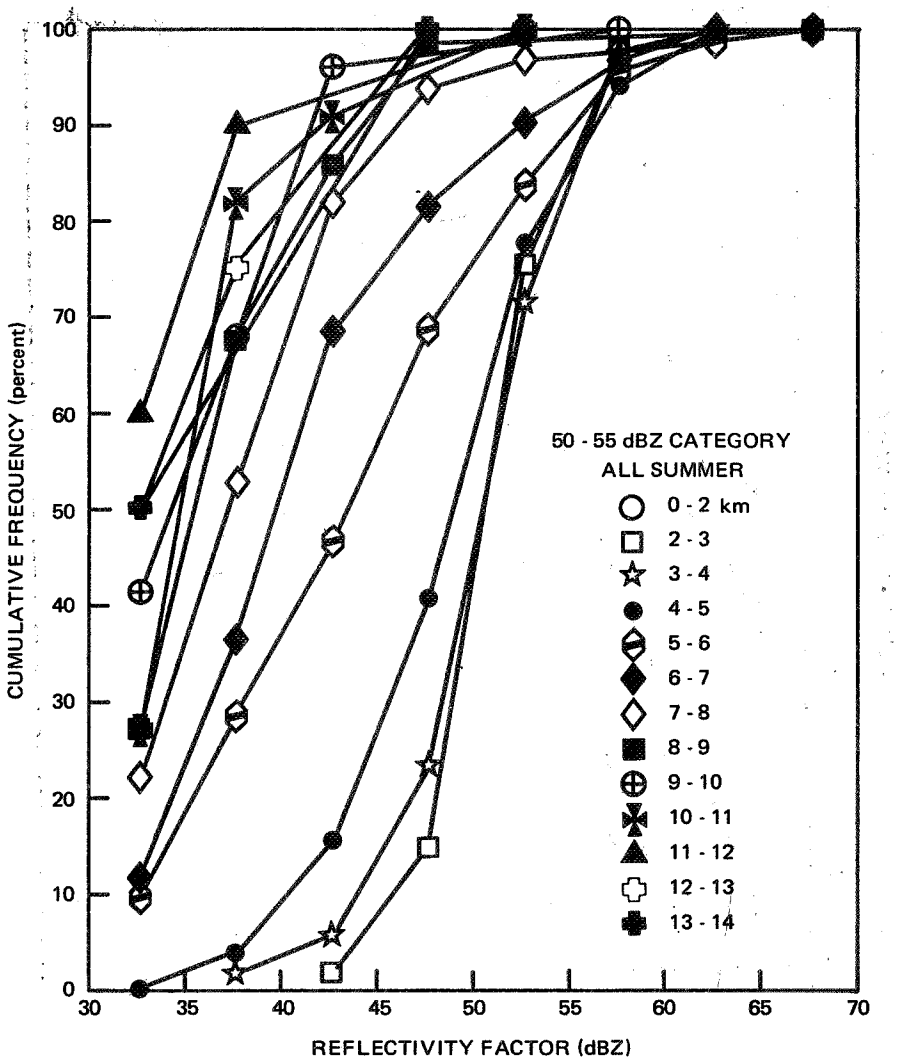

Figure 10.5. All Summer Cumulative Frequency Distribution of Peak Reflectivity Factor According to Altitude for ROG 50 - 55 dBZ

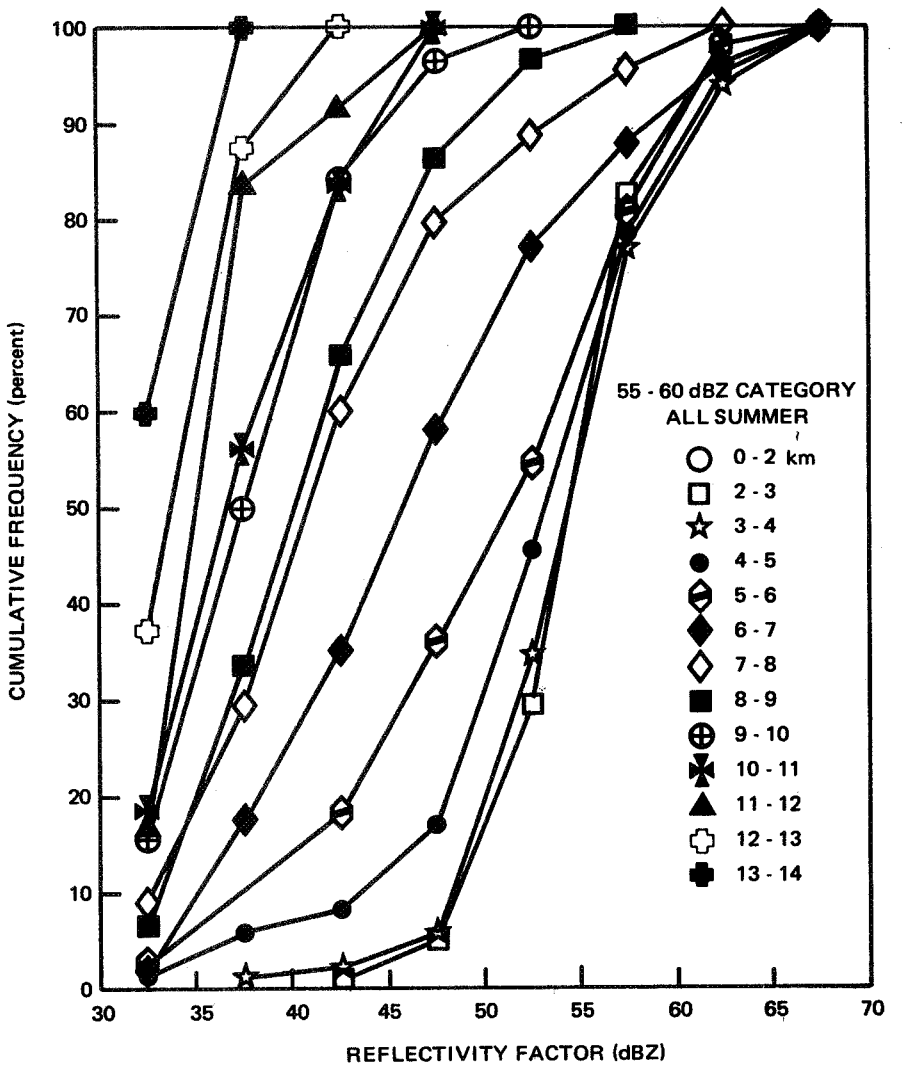

Figure 10.6. All Summer Cumulative Frequency Distribution of Peak Reflectivity Factor According to Altitude for ROG 55 - 60 dBZ

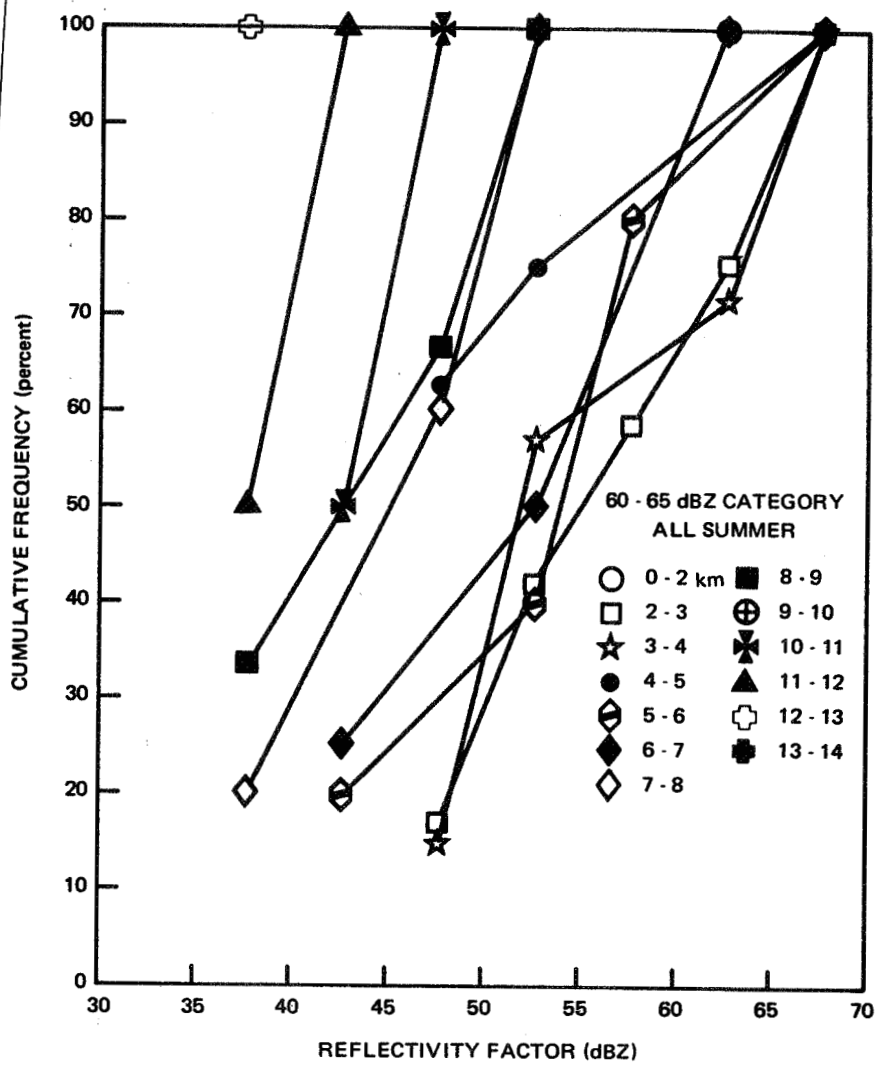

Figure 10.7. All Summer Cumulative Frequency Distribution of Peak Reflectivity Factor According to Altitude for ROG 60 - 65 dBZ

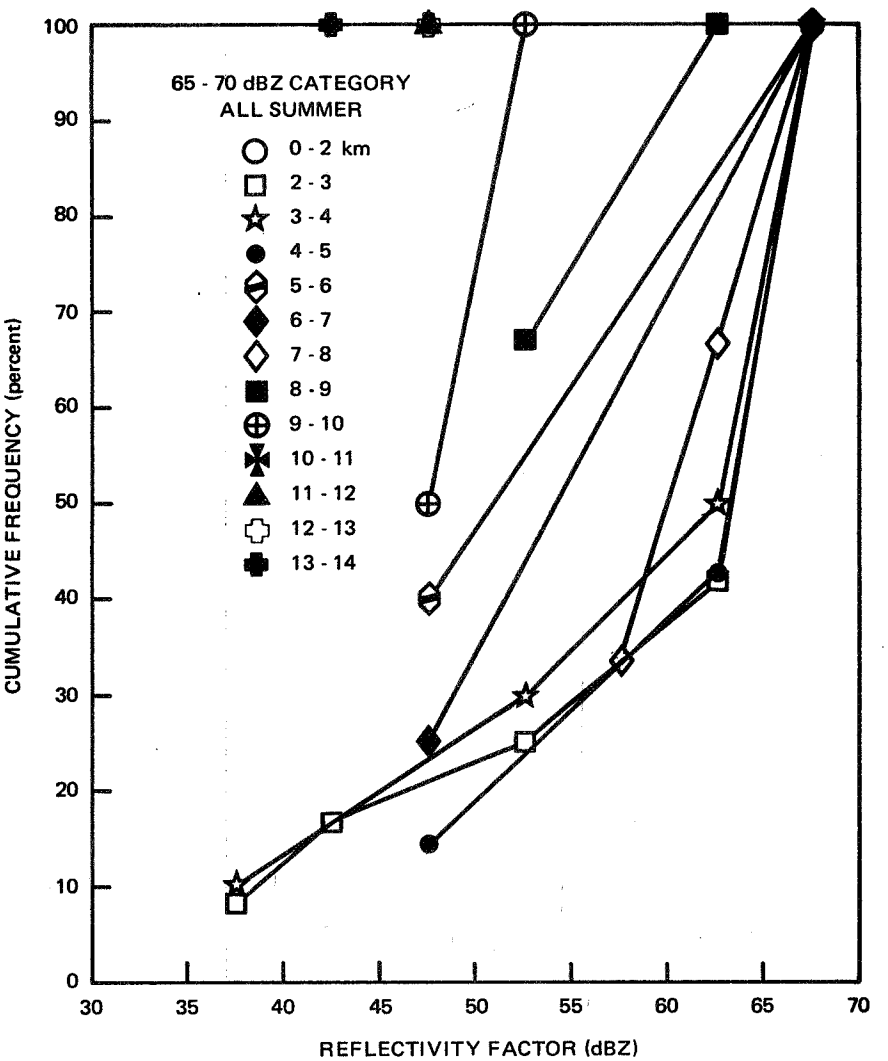

Figure 10.8. All Summer Cumulative Frequency Distribution of Peak Reflectivity Factor According to Altitude for ROG 65 - 70 dBZ

Profiles of the mean and median reflectivity for the ROG class cells according to category are shown in Figures 10.9 and 10.10, respectively. Note that the mean and median profiles for the high category cells fall off with altitude whereas those for the low category cells initially increase slightly with altitude and finally fall back toward lower values.

An indication of the validity or meaningfulness of the mean and median profiles of peak reflectivity may be gleaned from the standard deviation profiles for each category. These are shown in Figure 10.11. In the 0-2 km altitude interval, the standard deviation is small, around 1 to 2 dBZ. This is to be expected since the increment in peak reflectivity used in categorization was 5 dBZ, e.g., categories 30-35 dBZ, 35-40 dBZ, etc. As the altitude increases, however, the variation in the peak reflectivity for a given altitude also increases, reaching a maximum generally around 6 km and then falls off toward zero at the highest altitudes. The low standard deviation at the highest altitude for each category simply reflects the fact that there are very few data points at that altitude and for that category. In the extreme case, the standard deviation will be zero at an altitude where there is only one cell for a particular category. The number of cells for a given category which survive to some altitude is discussed in Section 10.2.8. Variation in the standard deviation is also indicated in Figures 10.1 through 10.8 by the changing slope of the individual distributions with altitude. In simplest terms, Figure 10.11 says that there is a wide variation in the peak reflectivity at a given altitude for any given category of ROG class cells. That is, although the cells have the same peak reflectivity on the ground, they vary considerably in their reflectivity structure with altitude.

In Figure 10.12, the cumulative frequency distribution of reflectivity as a function of altitude regardless of category is shown for the ROG class cells, i.e., the "all" category in Section 7.4. This probability was discussed in Section 7.5.1 as P(Z/h), or the probability of some reflectivity value or less given an altitude interval, or more simply, the distribution of reflectivity at altitude. Again, a cross plot at 100 percent represents the maximum reflectivity which will be encountered at a given altitude for the ROG class cells, i.e., given only that it is raining on the ground.

The Virga class cells are shown in Figure 10.13. The distributions are similar to those for the ROG class cells but somewhat less well behaved.

Profiles of the mean and median peak reflectivities for the ROG class cells and for the Virga class cells are shown in Figures 10.14

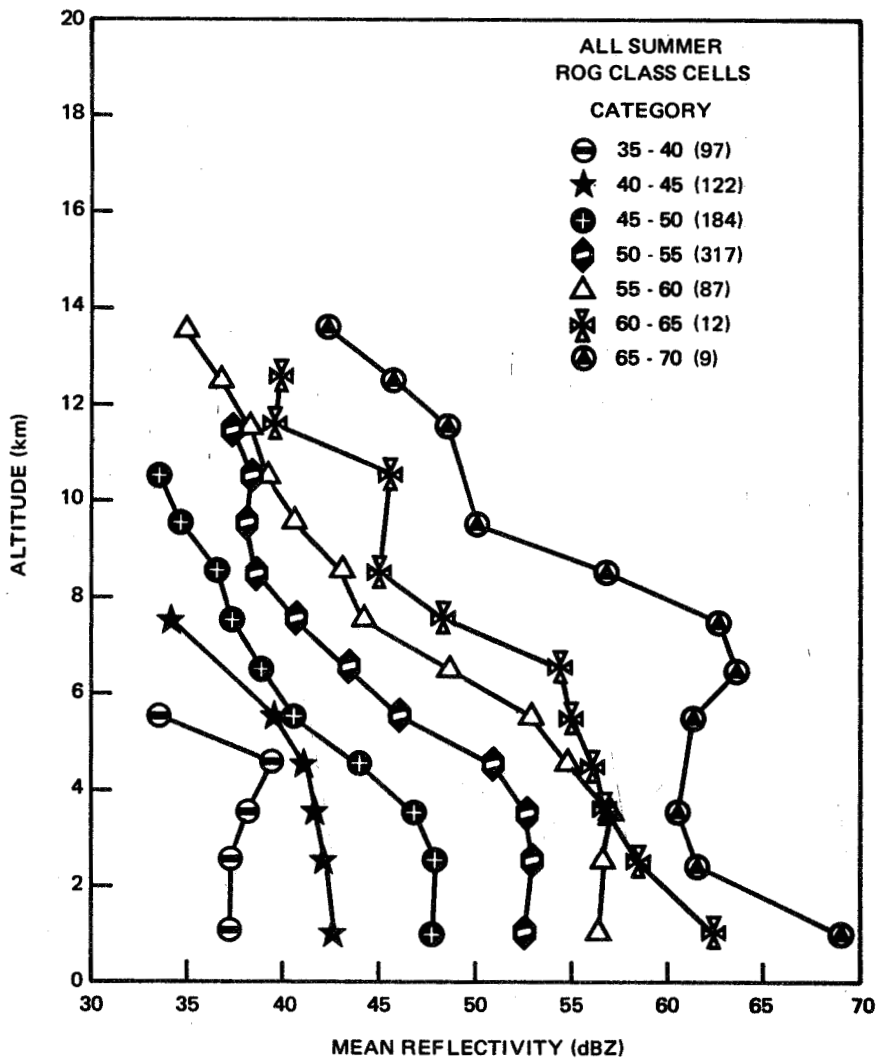

Figure 10.9. Profile of Mean Core Reflectivity. Number of Cases in Each Category Given in Parenthesis

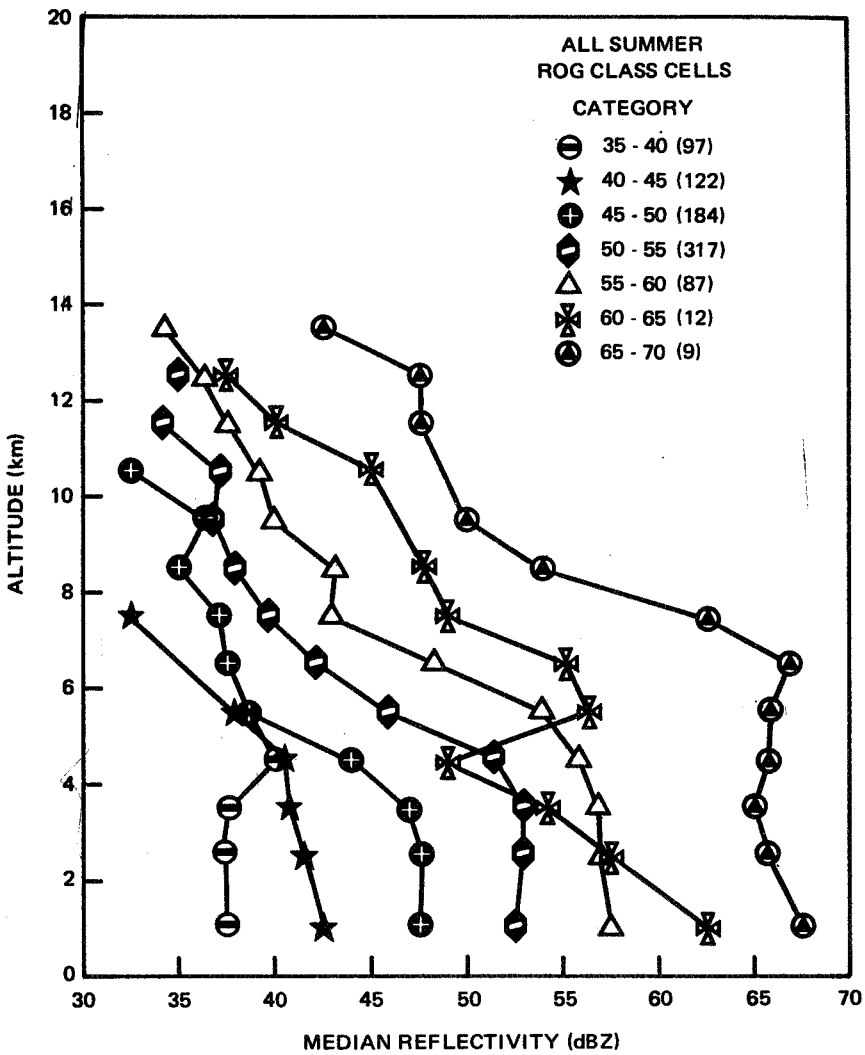

Figure 10.10. Profile of Median Core Reflectivity. Number of Cases in Each Category Shown in Parenthesis.

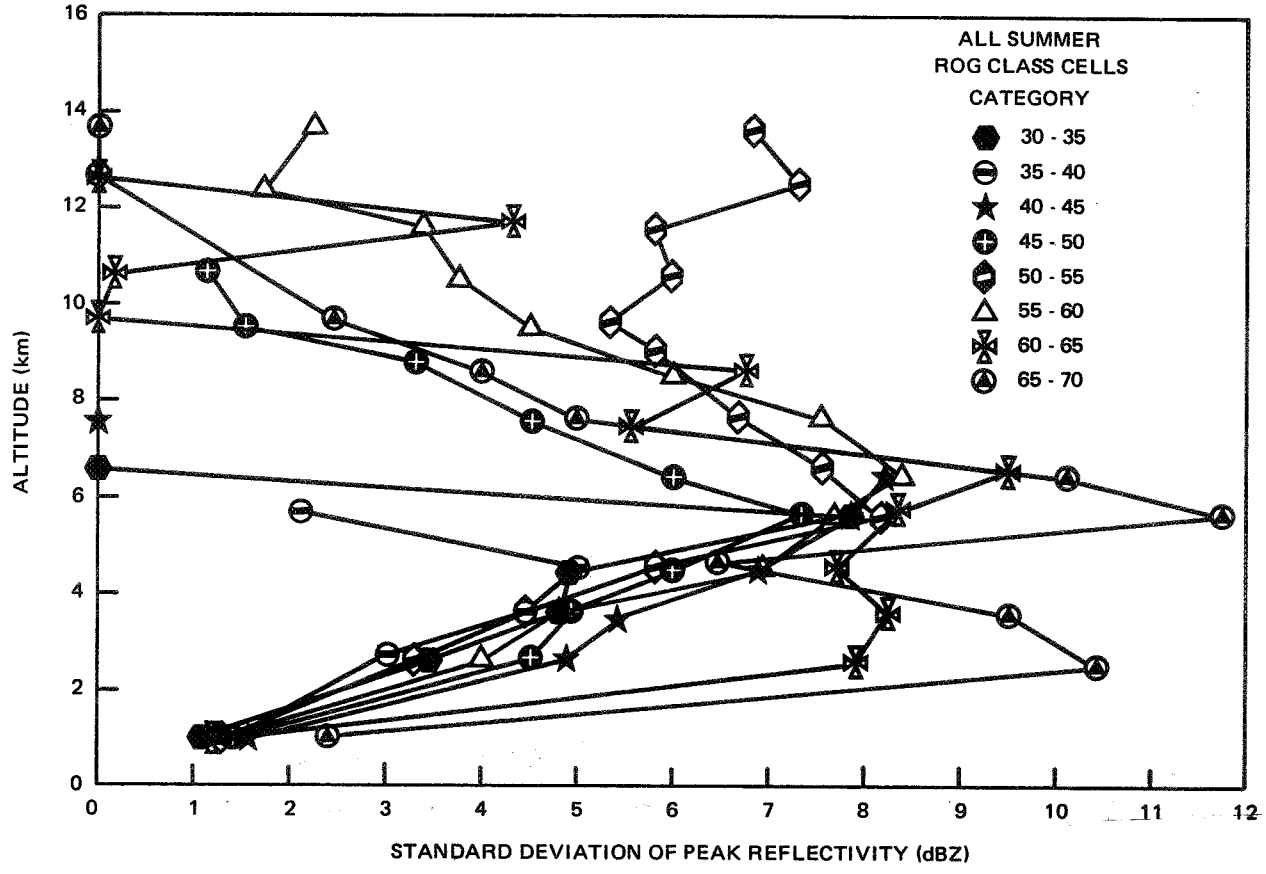

Figure 10.11. Standard Deviation of Peak Reflectivity for Each Category According to Altitude

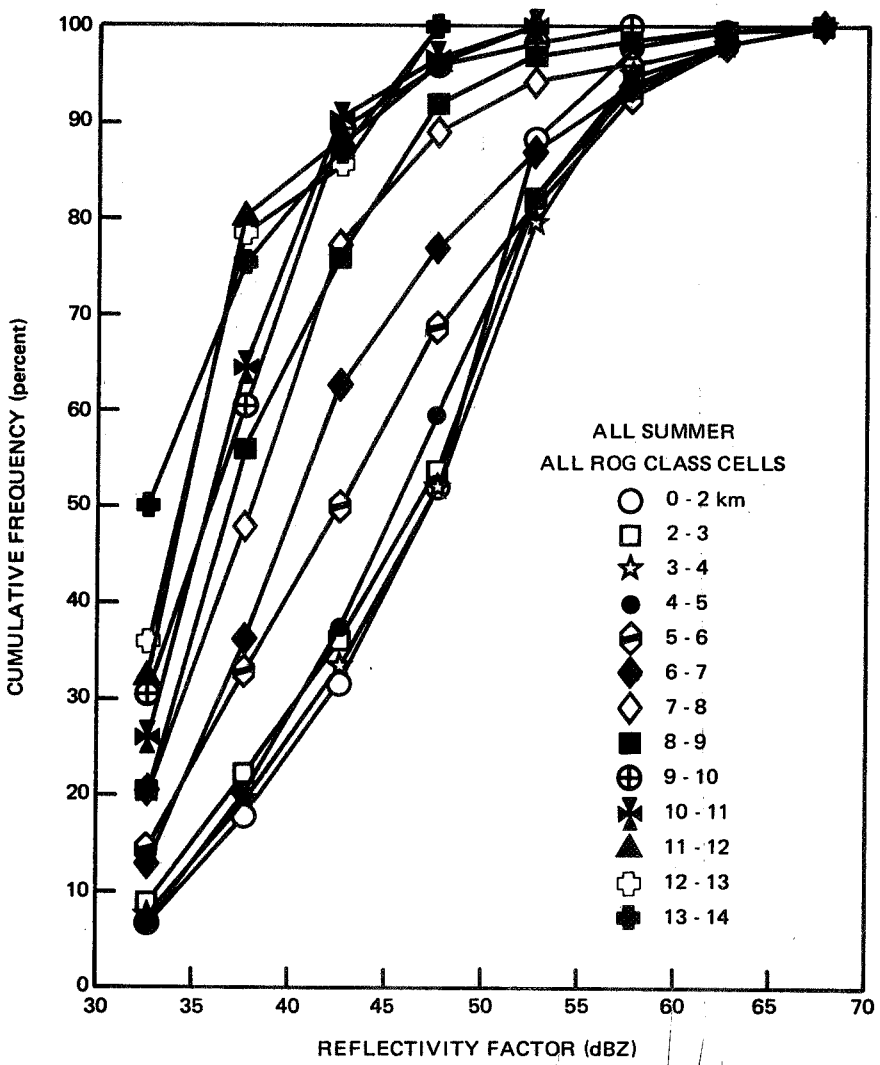

Figure 10.12. All Summer Cumulative Frequency Distribution of Peak Reflectivity Factor According to Altitude for All ROG Class Cells

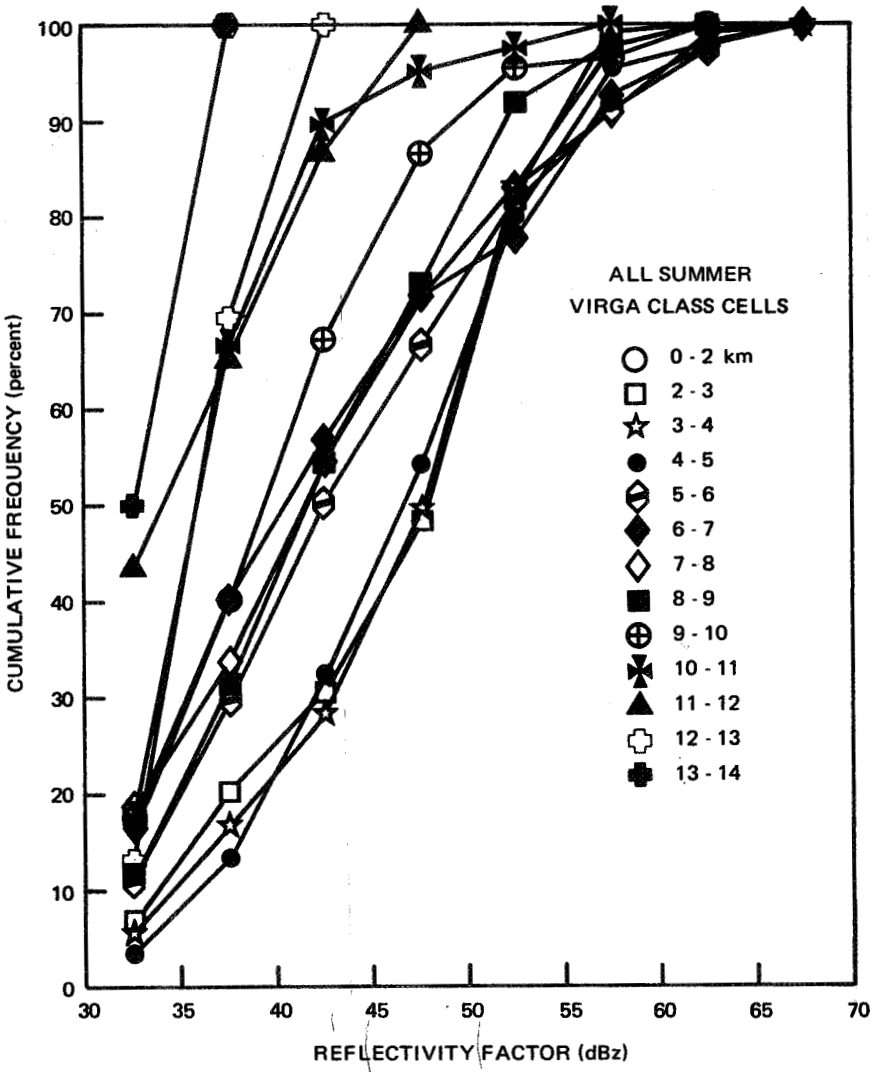

Figure 10.13. All Summer Cumulative Frequency Distribution of Peak Reflectivity Factor According to Altitude for Virga Class Cells

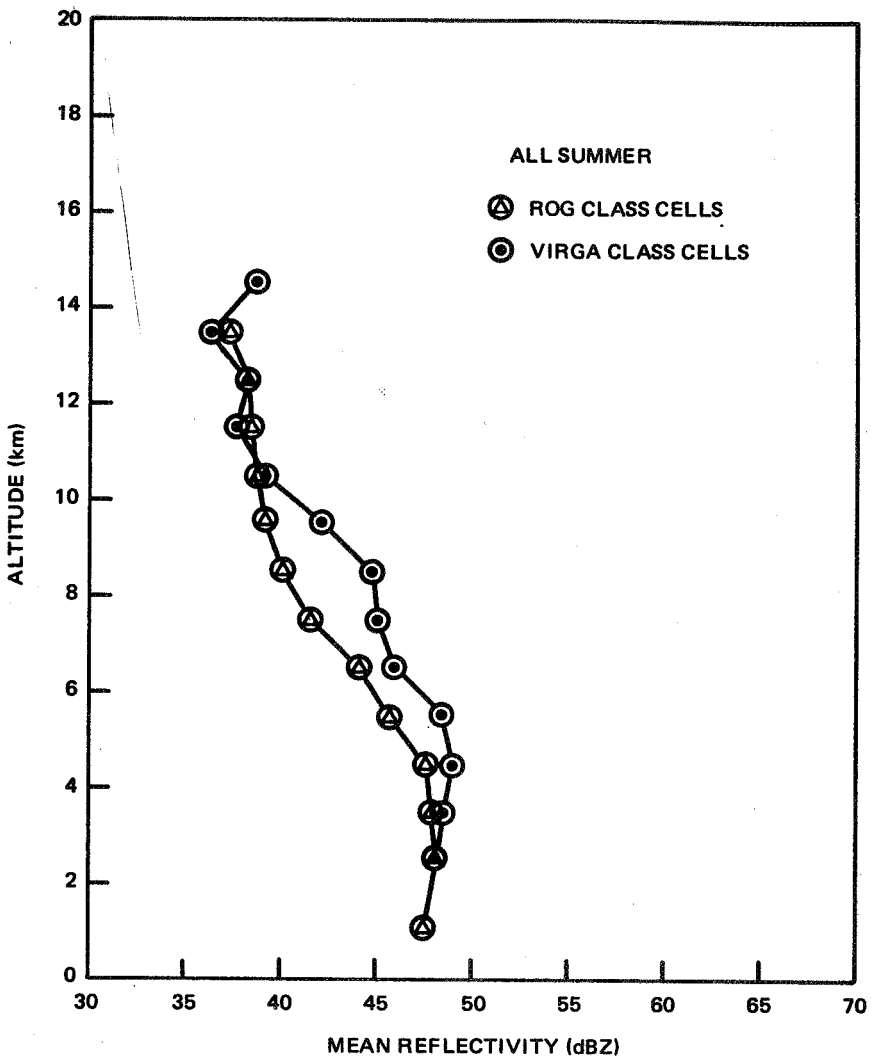

Figure 10.14. Profile of Mean Core Reflectivity for All ROG Class Cells and for Virga Class Cells

and 10.15, respectively. In these figures, of course, there is no distinction according to category but only according to the general class of cells. The standard deviation in the peak reflectivity for these two classes of cells is shown in Figure 10.16. Again, note the large variation with altitude followed by a fall-off to zero.

A word of caution concerning the validity of the data at the low reflectivities. As discussed in earlier sections, peaks with reflectivity values less than 30 dBZ were not included. As the peak reflectivity of a given cell falls off with increasing altitude, the 30 dBZ lower limit tends to bias the data remaining in the population toward larger values. Thus, the mean and median reflectivity at the higher altitudes for any given category tends to be high by some unknown amount. The reflectivity profile, in other words, falls off faster with altitude than is shown.

10.2.2 Reflectivity Ratio

The reflectivity ratio for the various categories of the ROG class cells is shown in Figure 10.17. As noted above, the reflectivity for the low category cells, 30-35 dBZ and 35-40 dBZ, typically increases with altitude and as such they show much higher reflectivity ratios (or lower cumulative frequency values) than the more intense cells. When all the cells are combined, the single curve shown in Figure 10.18 results. The increment in reflectivity ratio is a factor of 2, and the points are plotted in the center of the interval.

Since no interpolation or curve fitting of the reflectivities with altitude was performed to find the absolute maximum, the values of the reflectivity ratio shown will be lower than the actual value. The procedure in the third pass program used was simply to save the largest value of reflectivity in a cell, i.e., in the sweeps of a scan. The maximum reflectivity thus obtained will always be less than the actual maximum unless the PPI sweep should intercept the cell exactly at the real maximum value. Such a coincidence is most unlikely. The curves shown, then, may be considered as a conservative estimate of the ratio, i.e., the probability that the ratio is equal to or less than some value will be lower. Alternatively, the probability that the value is exceeded will be greater.

Although the mean, median, and mode of the reflectivity ratio were calculated by the computer, they are not presented here since none of these parameters have a meaningful interpretation. In the case of the median, over half of the values fall in the first reflectivity ratio interval, i.e., see Figure 10.17. The computer algorithm used to find

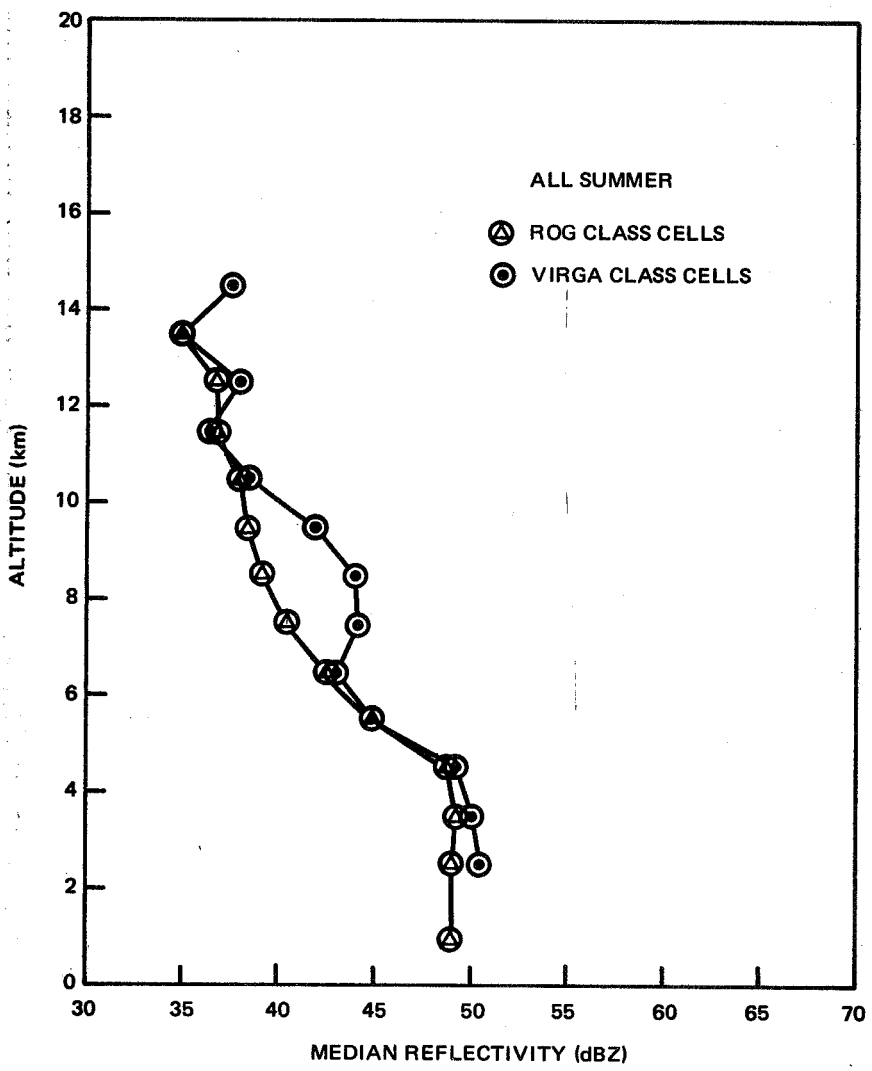

Figure 10.15. Profile of Median Reflectivity for All ROG Class Cells and for Virga Class Cells

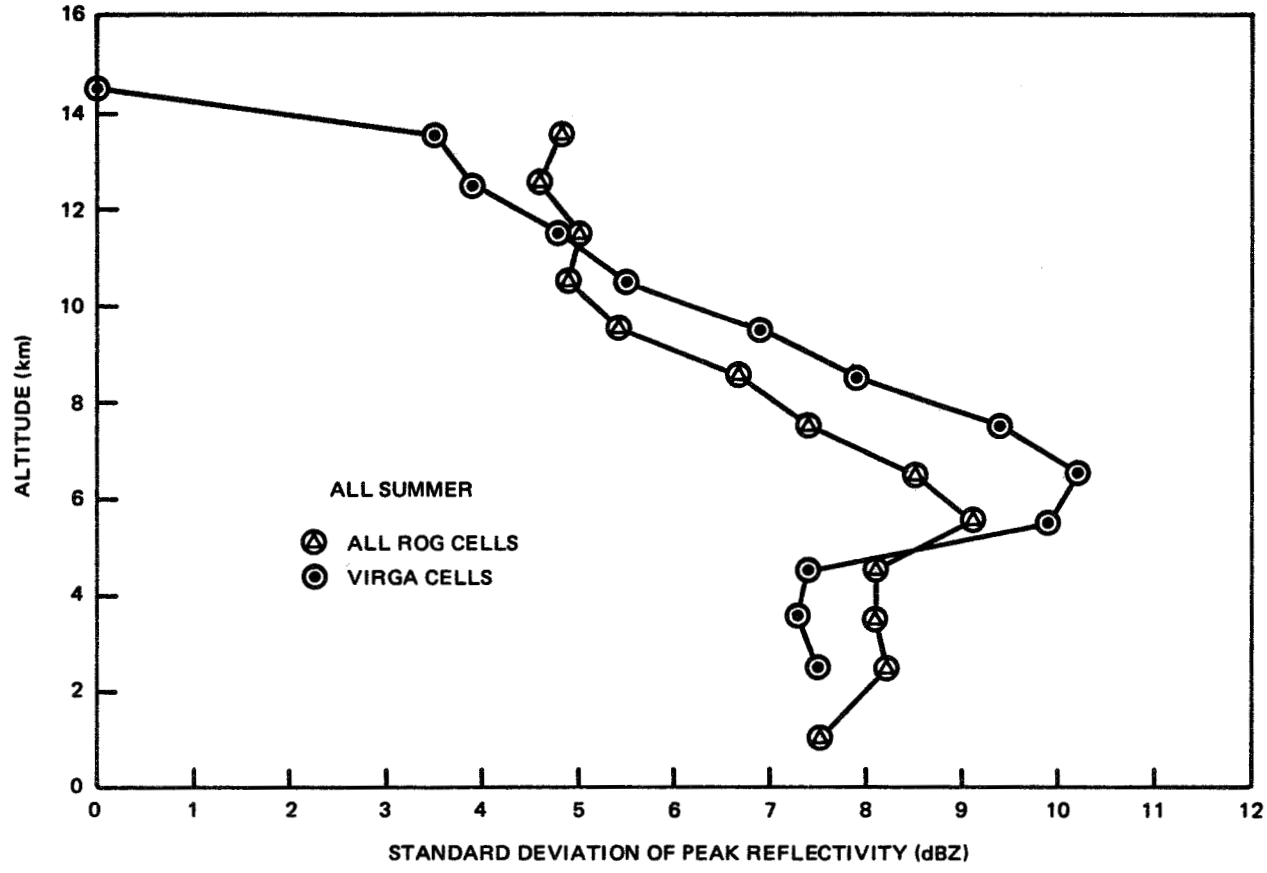

Figure 10.16. Standard Deviation of Peak Reflectivity for All ROG Class Cells and Virga

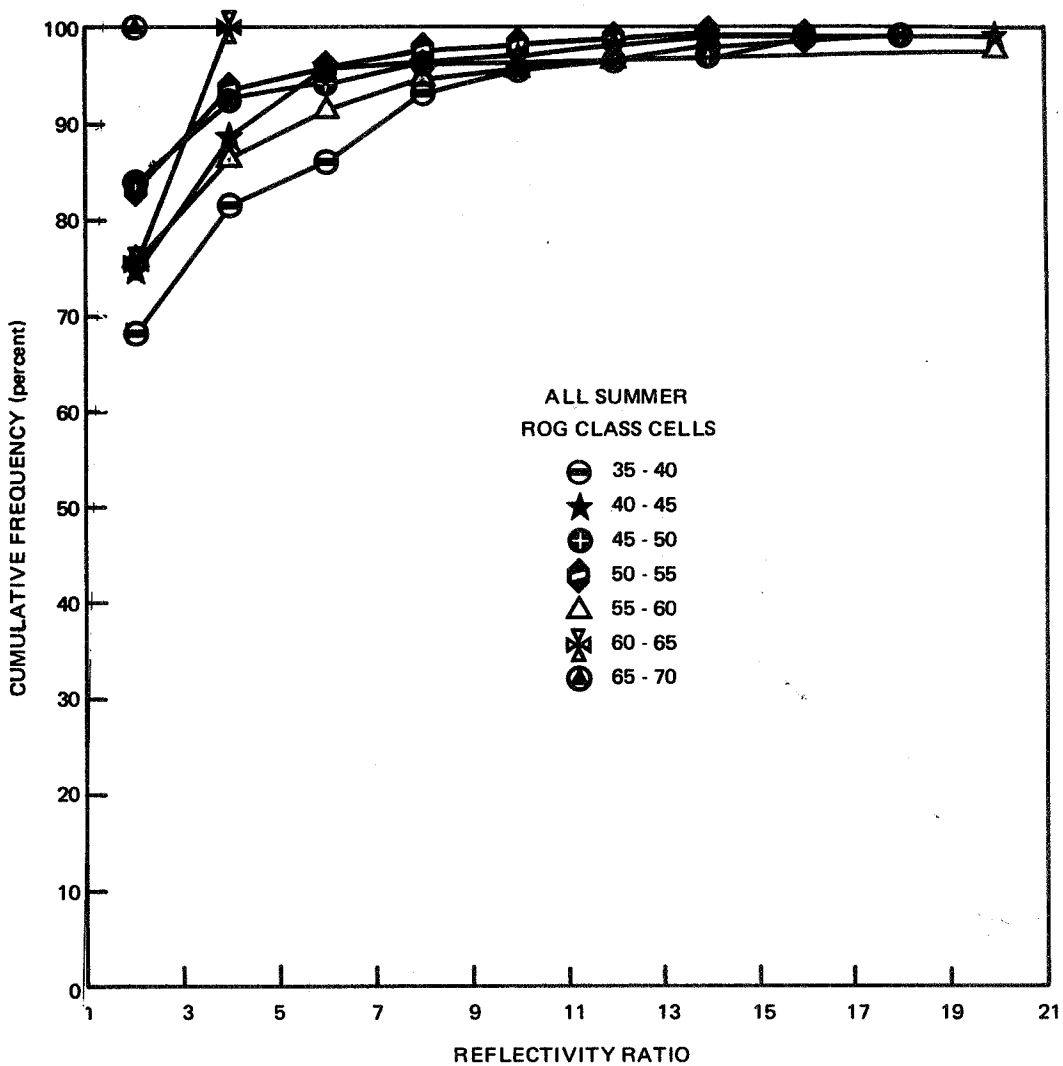

Figure 10.17. Cumulative Frequency Distribution of the Reflectivity Ratio for Various Categories of ROG Class Cells

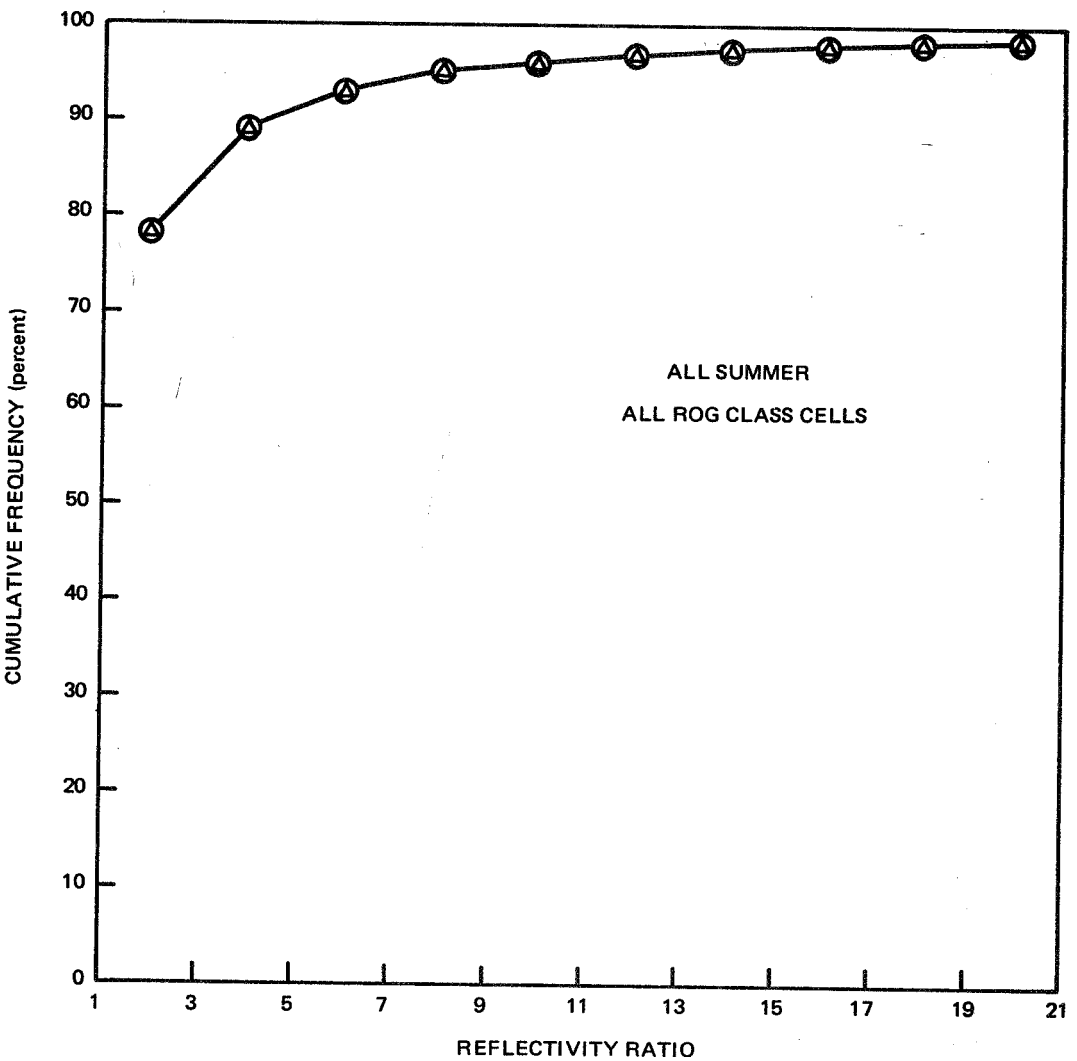

Figure 10.18. Cumulative Frequency Distribution of the Reflectivity Ratio for All ROG Class Cells

the median, namely, linear interpolation between two points, results in a nonmeaningful value. The algorithm is not applicable in a situation such as this.

The mean ratio is also questionable, if not meaningless, because the ratio is bounded by a minimum value of 1.0. Thus, the mean value of the ratio for any given category will always be greater than one, regardless of what the mean reflectivity profile does. For example, assume that a category has 10 cells where the reflectivity falls off with altitude continuously from the lowest altitude for 9 of the 10 cells. The reflectivity profile of the 10th cell increases with altitude before falling off, i.e., it has a Z_{max} at some altitude H. The reflectivity ratio for the 9 cells is 1.0 whereas for the 10th cell it is some value greater than 1.0. Thus, the mean reflectivity ratio is greater than 1.0 despite the fact that the mean peak reflectivity may show a continuous fall off with altitude; an obvious contradiction!

10.2.3 Height of Maximum Reflectivity

Figure 10.19 shows the height of the maximum reflectivity as a function of ROG class cells and Figure 10.20 shows the height for all ROG class cells observed during the summer observations. The mean and median values are presented in Figure 10.21. It is interesting to note that the maximum reflectivity occurs in a rather narrow height range, roughly 1.5 to 3 km for both the mean and median. Roughly 90 percent of the cases are below 4 km as shown in Figure 10.20. The mean height of the zero isotherm for the 21 days of observation was 4.8 km. Thus, the maximum reflectivity occurred considerably below the melting layer (bright band).

10.2.4 Area of 10 dBZ Contour About the Peak

The area used in the statistical analysis was the area of the reflectivity contour 10 dB down from the peak or core value. As discussed in Section 7.5.2 the areas were sorted according to the cell class and category, the altitude interval and the value of the local peak reflectivity, i.e., the peak reflectivity at altitude. The distributions, therefore, represent the probability of an area given a cell class and category, an altitude interval and a reflectivity level at that altitude. With three conditions for sorting the area, a large number of distributions results, i.e., 9 categories (including the "all" category), 9 altitude intervals and 8 peak reflectivity intervals for a total of roughly 650 possible combinations. All combinations were not observed, however, and many combinations which were observed had so few cells that there is no statistical significance to the distribution.

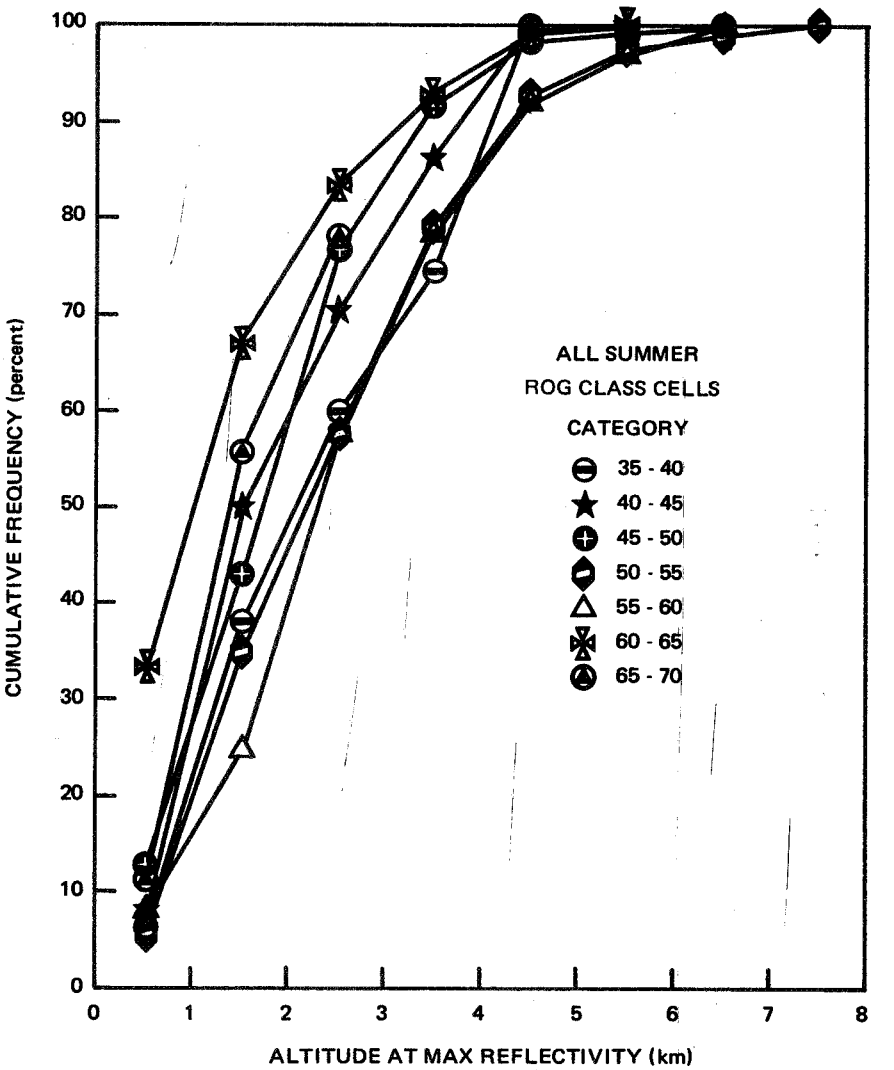

Figure 10.19. Cumulative Frequency Distribution of the Altitude at Maximum Peak Reflectivity for Various Categories of ROG Class Cells

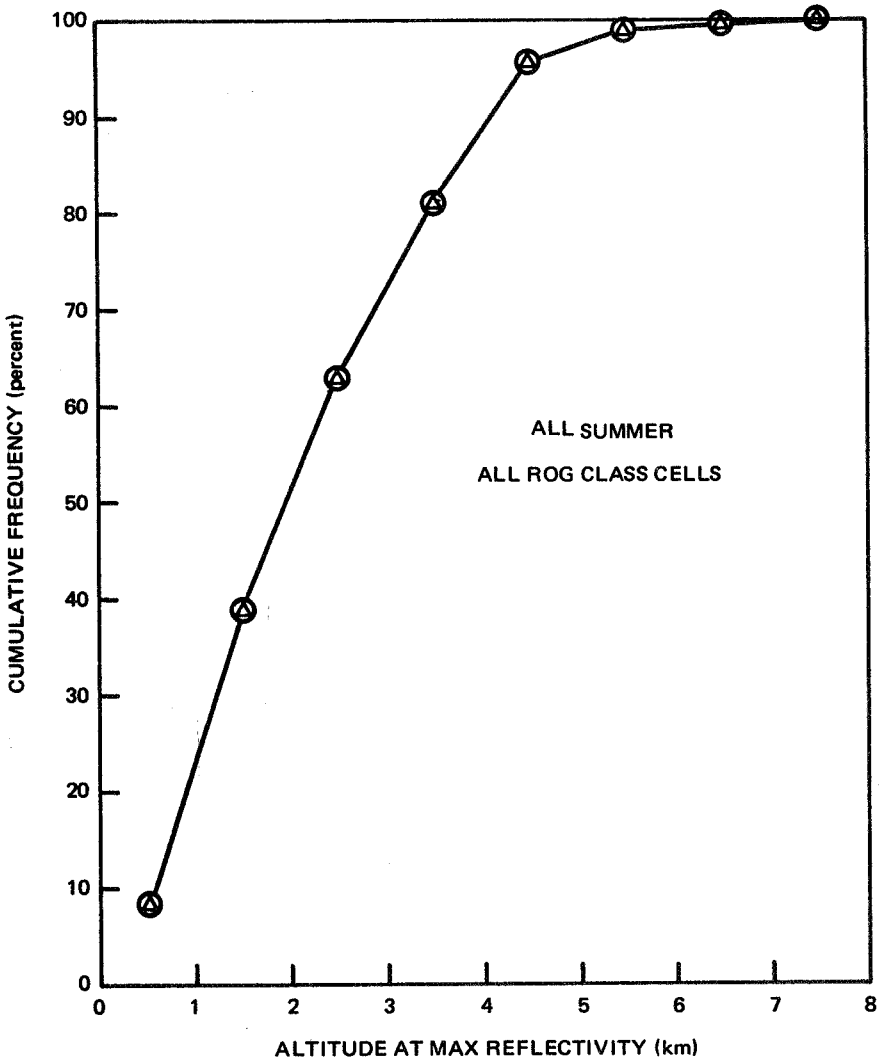

Figure 10.20. Frequency Distribution of the Altitude of Maximum Peak Reflectivity for All ROG Class Cells

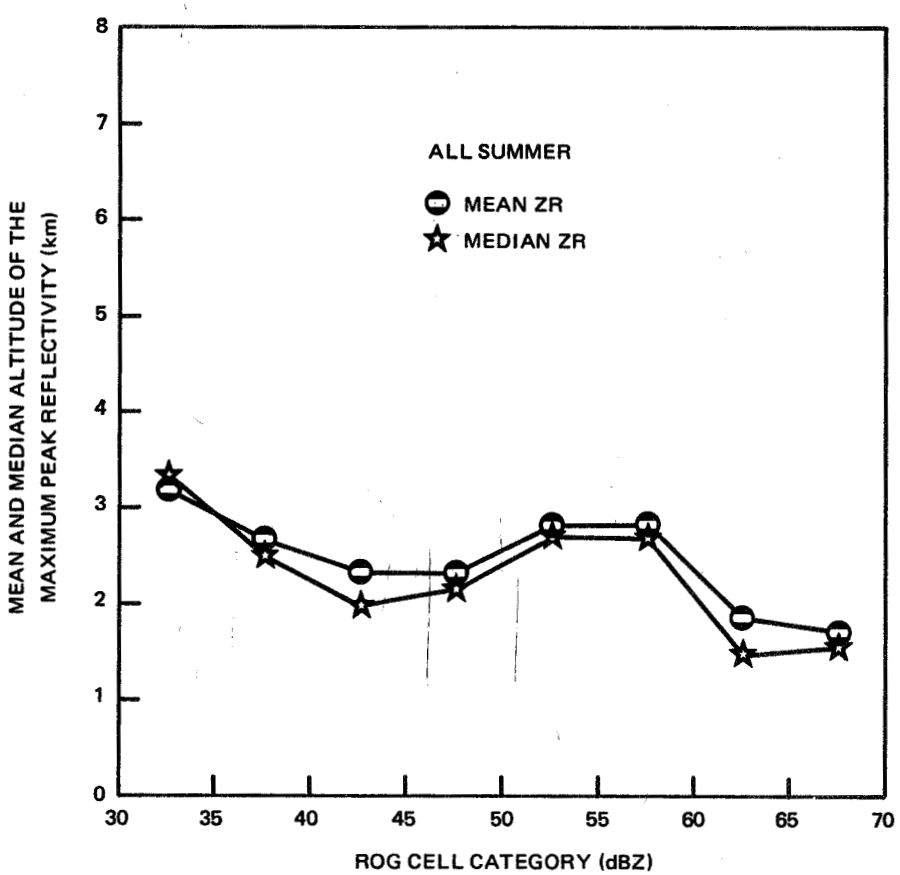

Figure 10.21. Mean and Median Height of Maximum Peak Reflectivity According to ROG Cell Category

Because of the large number of graphs, only examples of the distributions for ROG class cells ("all" category) and the Virga class cells are presented here. All combinations have been plotted, however, and are available from the authors.

Figure 10.22 shows an example of the cumulative frequency distribution of area for all the ROG cells observed in the peak reflectivity interval from 40-45 dBZ and altitude. Note that the value of the contour itself is 30-35, i.e., 10 dBZ less than the peak. The number of cells in each distribution is shown on the figure in parenthesis. The mean and median areas at each altitude and reflectivity interval are shown in Figures 10.23 and 10.24. Note that the areas for a given reflectivity interval are not constant with altitude for the lower reflectivity values. This would indicate that there is no single, functional relationship between the area and the reflectivity. In general, however, there is a definite inverse relationship, i.e., large areas for small reflectivities and vice versa. The median values are generally smaller than the mean values indicating that a few large areas are dominating causing the mean to be greater than the median.

An example of the frequency distribution of area for the Virga class cells is presented in Figure 10.25 for the 40-45 dBZ reflectivity interval. Very little order to these distributions for the Virga class cell is evident. This may be characteristic of this class of cells. The mean and median profiles of area are presented in Figures 10.26 and 10.27. Again note the fact that the medians are, in general, smaller than the mean values for comparable reflectivity and altitude intervals.

Using all the cells, both ROG and Virga class cells below the average zero degree isotherm for the observation period, the mean contour area as a function of liquid water content was constructed. The equation used to relate the reflectivity factor of the contour to liquid water content was:

$$Z = 2.4 \times 10^4 M^{1.82}$$

where Z is in $mm^6\ m^{-3}$ and M is in $gm\ m^{-3}$. Only those altitudes below the freezing level were used to ensure that the reflectivities were all for liquid water and not snow or ice crystals. The results of these calculations are shown in Figure 10.28. Although the data scatter, there is a pronounced trend. Note that one ordinate is the reflectivity factor of the contour and not the peak value.

In general, the distributions and mean and median profiles for the 10 dB contour area are not as well behaved as those for core reflectivity. This may well indicate that the contour area is not a statistical function of the cell category or altitude but dependent on other

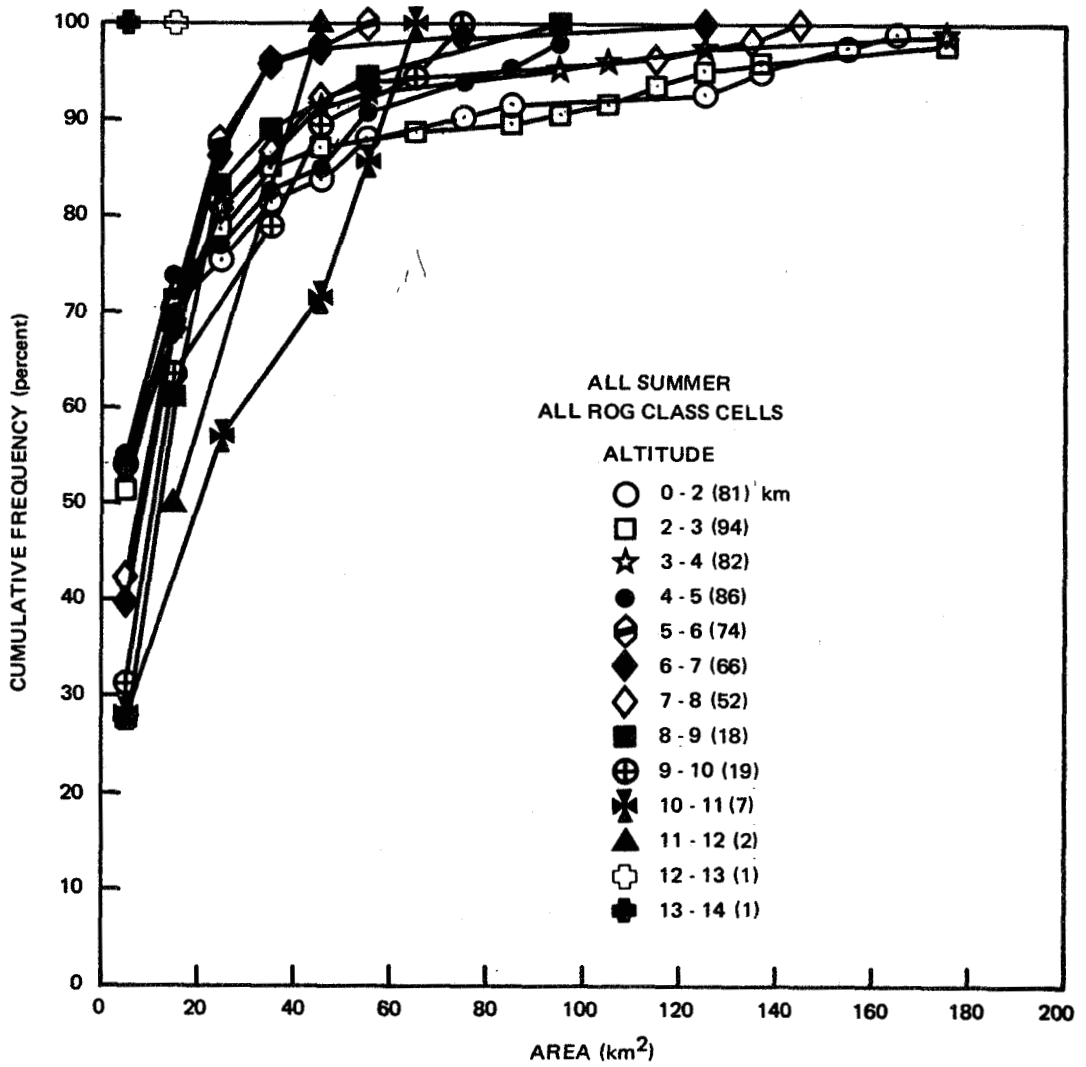

Figure 10.22. Frequency Distribution of Area of 10 dB Contour for All ROG Cells in Reflectivity Interval 40 - 45 dBZ

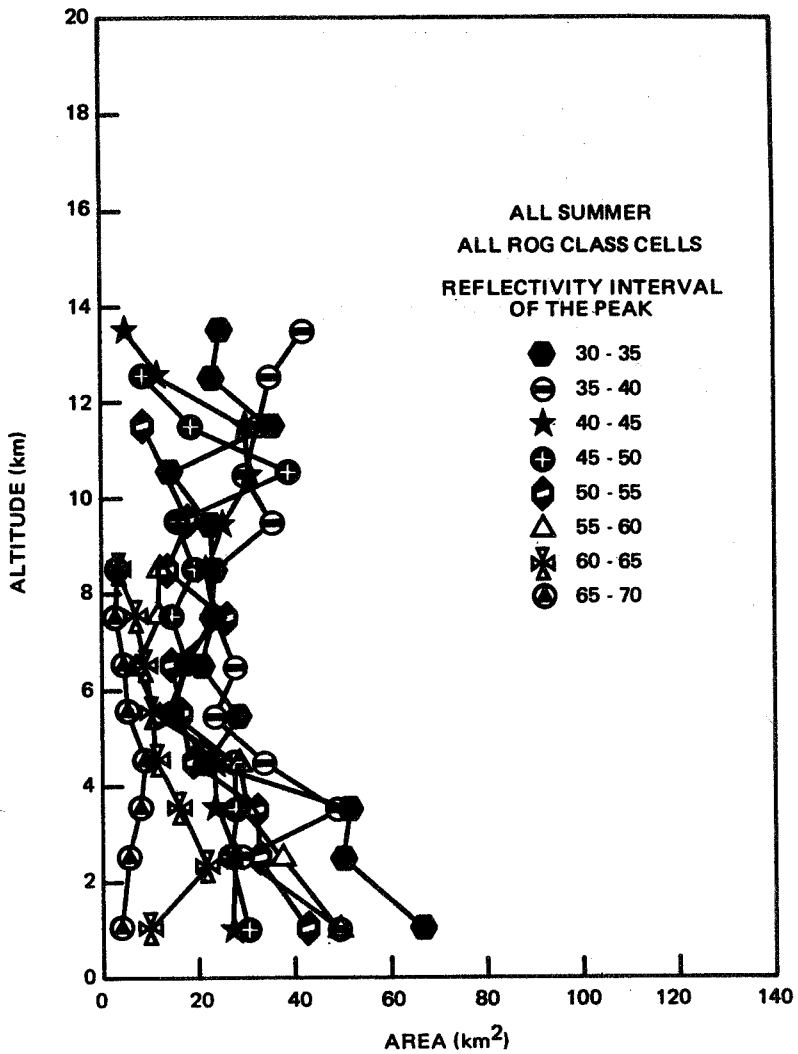

Figure 10.23. Mean Contour Area for All ROG Class Cells According to Reflectivity Interval of the Peak and Altitude

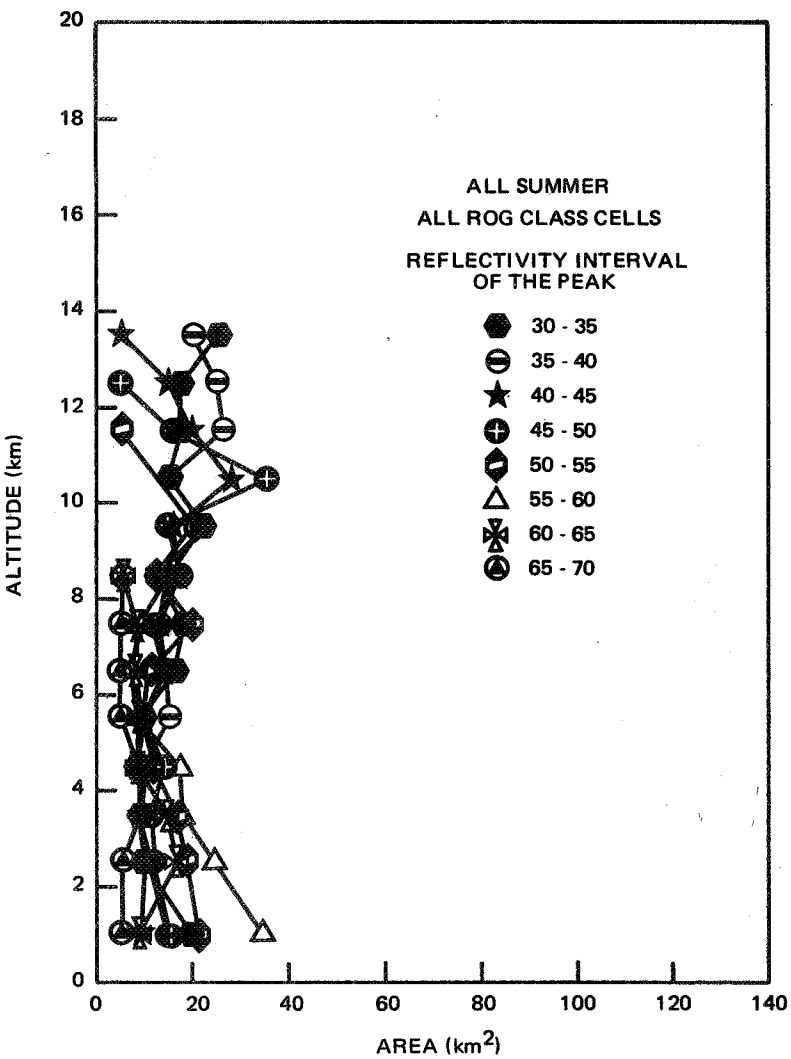

Figure 10.24. Median Area for All ROG Class Cells According to Reflectivity Interval of the Peak and Altitude

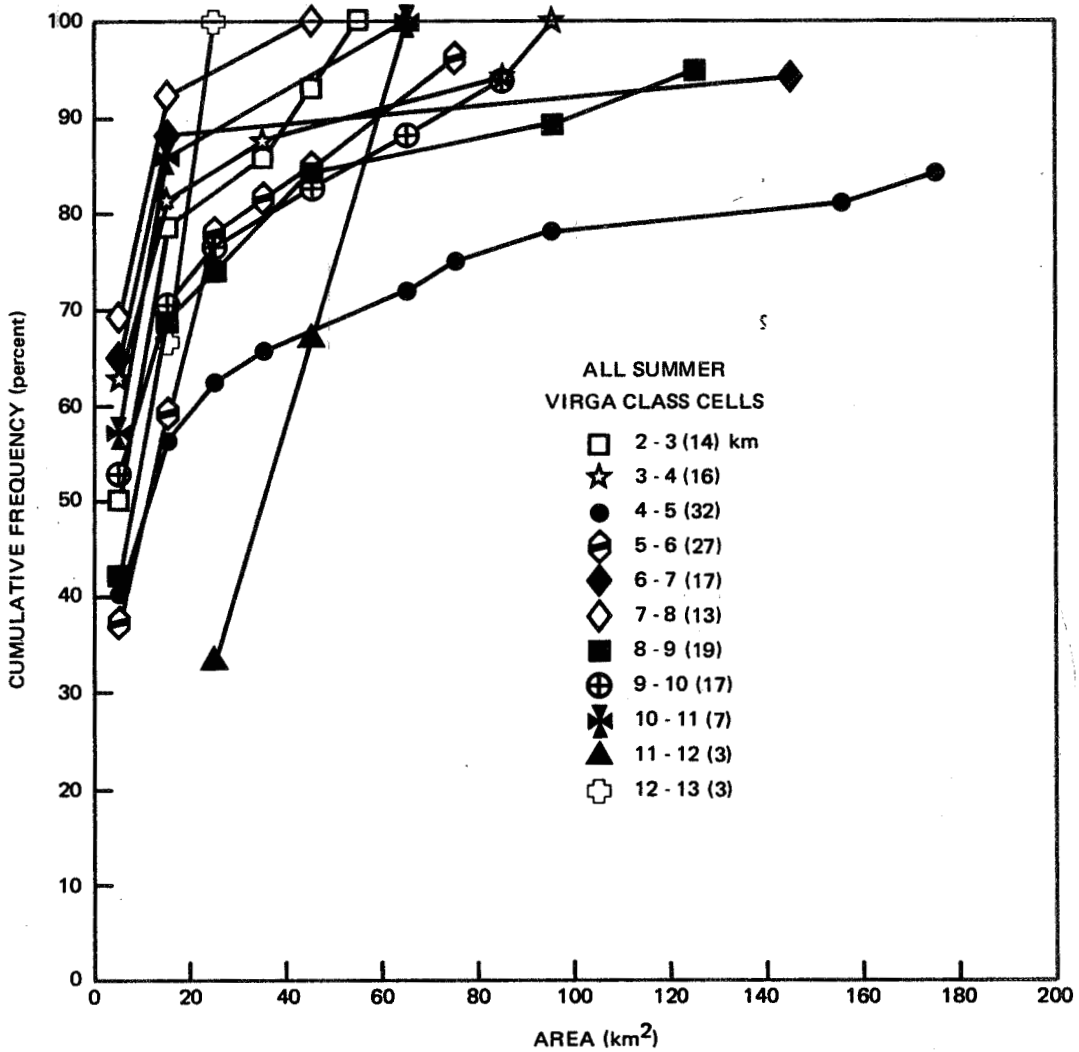

Figure 10.25. Cumulative Frequency Distribution of Area for the 40 - 45 dBZ Reflectivity Interval for Virga Class Cells According to Altitude

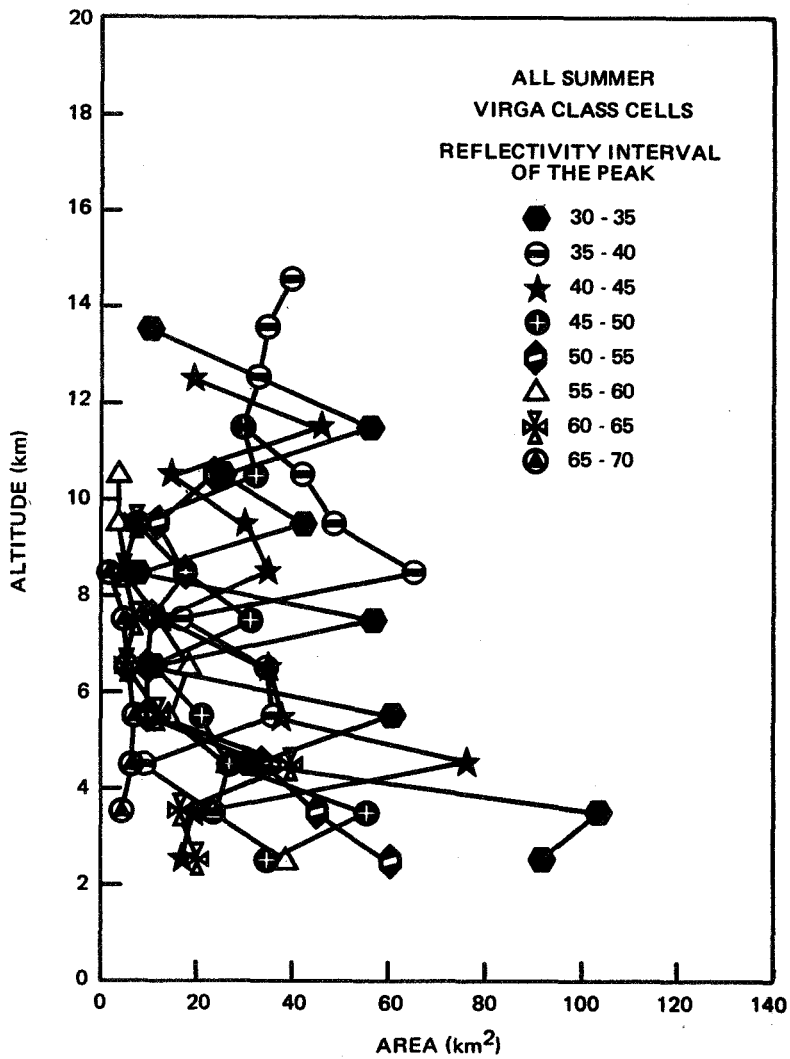

Figure 10.26. Mean Contour Area for Virga Class Cells According to Reflectivity Interval of the Peak and Altitude

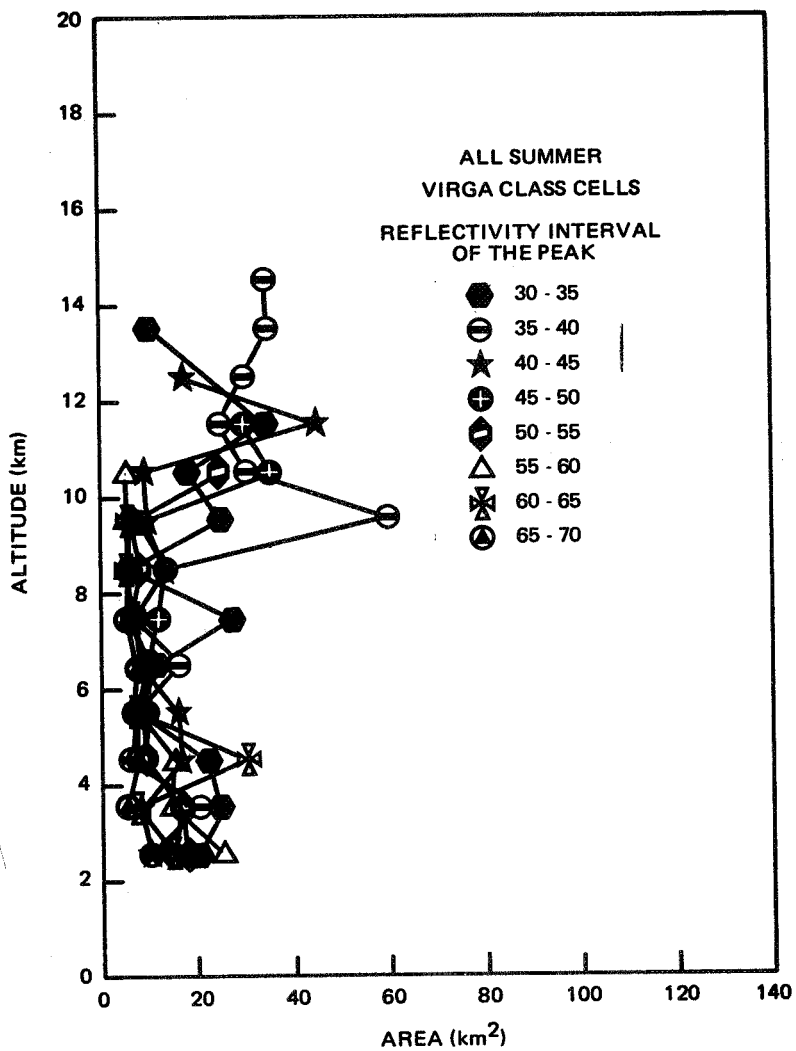

Figure 10.27. Median Area for Virga Class Cells According to Reflectivity Interval of the Peak and Altitude

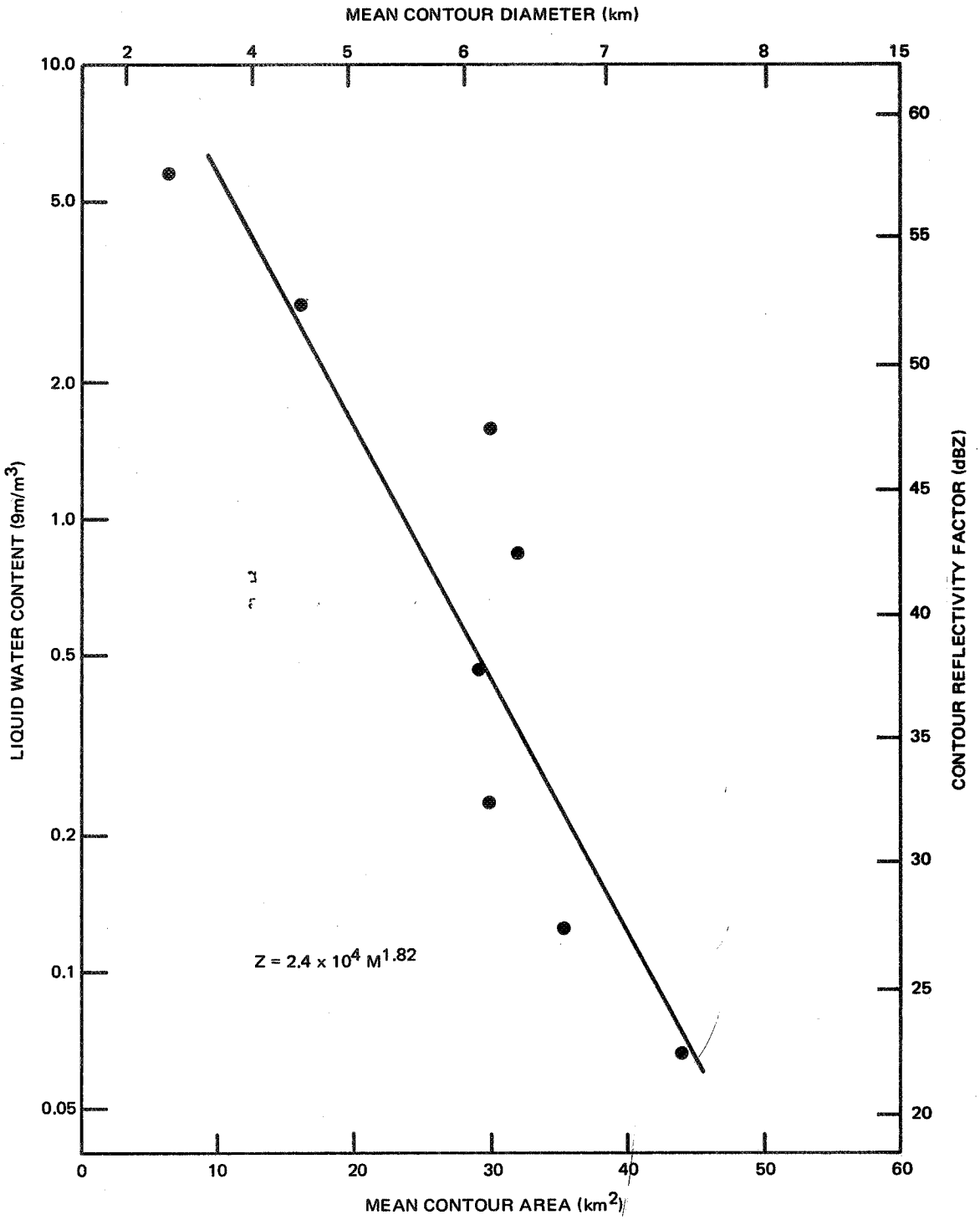

Figure 10.28. Mean Contour Area as a Function of the Contour Reflectivity Factor and Liquid Water Content

factors not yet identified. Further, one would strongly suspect that the area is related to the reflectivity level but, again, there may well be other physical parameters which bear on the relationship which were not considered or documented in this study. If one considers only "well shaped," isolated cells, the chances of extracting some orderly statistical feature is enhanced. In this study, all the cells were used, many of which are embedded in larger meso-scale systems. It is well known from surface rain gage records that the harder it rains the shorter the time period of that rain. This demonstrated fact indicates that some general or gross relationship similar to that shown in Figure 10.28 does exist. Whether it is a clear-cut statistical or functional relationship is not known. More detailed effort in this area is warranted. This is discussed further in the recommendations.

10.2.5 Length-to-Width Ratio of Contour

An example of the results of sorting the contour length-to-width ratio as described in Section 7.5.2 is presented in Figure 10.29. Again, only an example of the cumulative frequency distribution for all the ROG class cells ("all" category) according to reflectivity interval of the local peak reflectivity and altitude is shown. The total number of cells in each distribution for each altitude interval is shown in parenthesis. An example for the Virga class cells is shown in Figure 10.30.

The distributions exhibit no significant variation with the local peak reflectivity. That is, there is no consistent, marked difference in the form or character of the distributions with reflectivity. Nor does there appear to be any variation with altitude. All the curves have the same general shape with the majority of cells having low values of the length-to-width ratio. Note that the first interval is 1-2. Approximately 70 percent of the cells have a length-to-width ratio less than 4 regardless of the reflectivity interval and 90 percent have ratios less than 10. The median for all reflectivity intervals at all altitudes is less than 3. Note that the length-to-width ratio calculated as discussed in Section 3.2.3 is not a true eccentricity as in the case of ellipses. No attempt was made to fit the contours with an ellipse such as in Altman (Ref. 9). The ratio calculated is intended only as a gross indicator of the contour shape.

10.2.6 Orientation of Contour Major Axis

The orientation of the contour major axis as described in Section 3.2.3 was calculated and sorted according to the cell category, the altitude interval and the value of the local peak reflectivity as

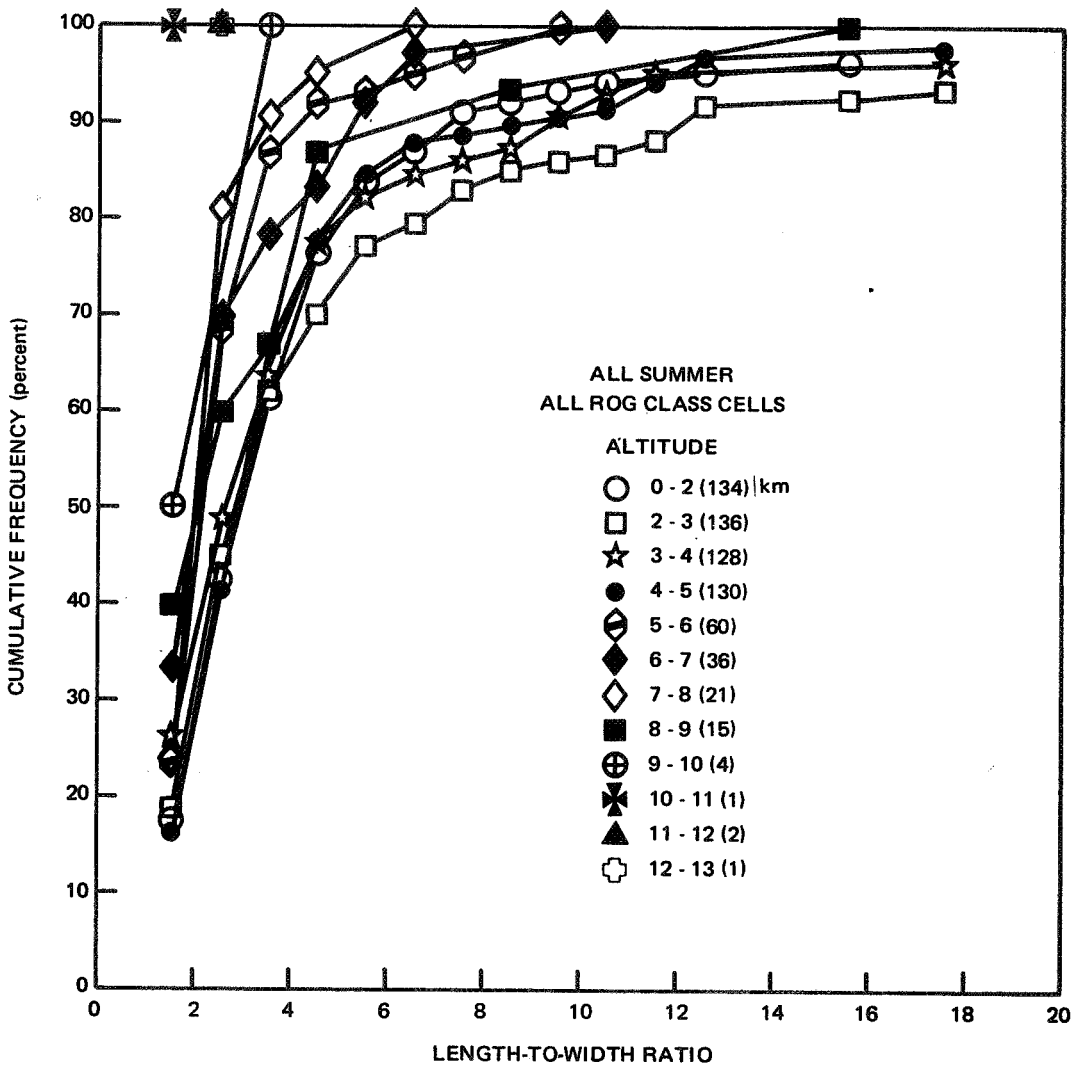

Figure 10.29. Frequency Distribution of the Contour Length-to-Width Ratio for All ROG Class Cells in the 45 - 50 dBZ Peak Reflectivity Interval

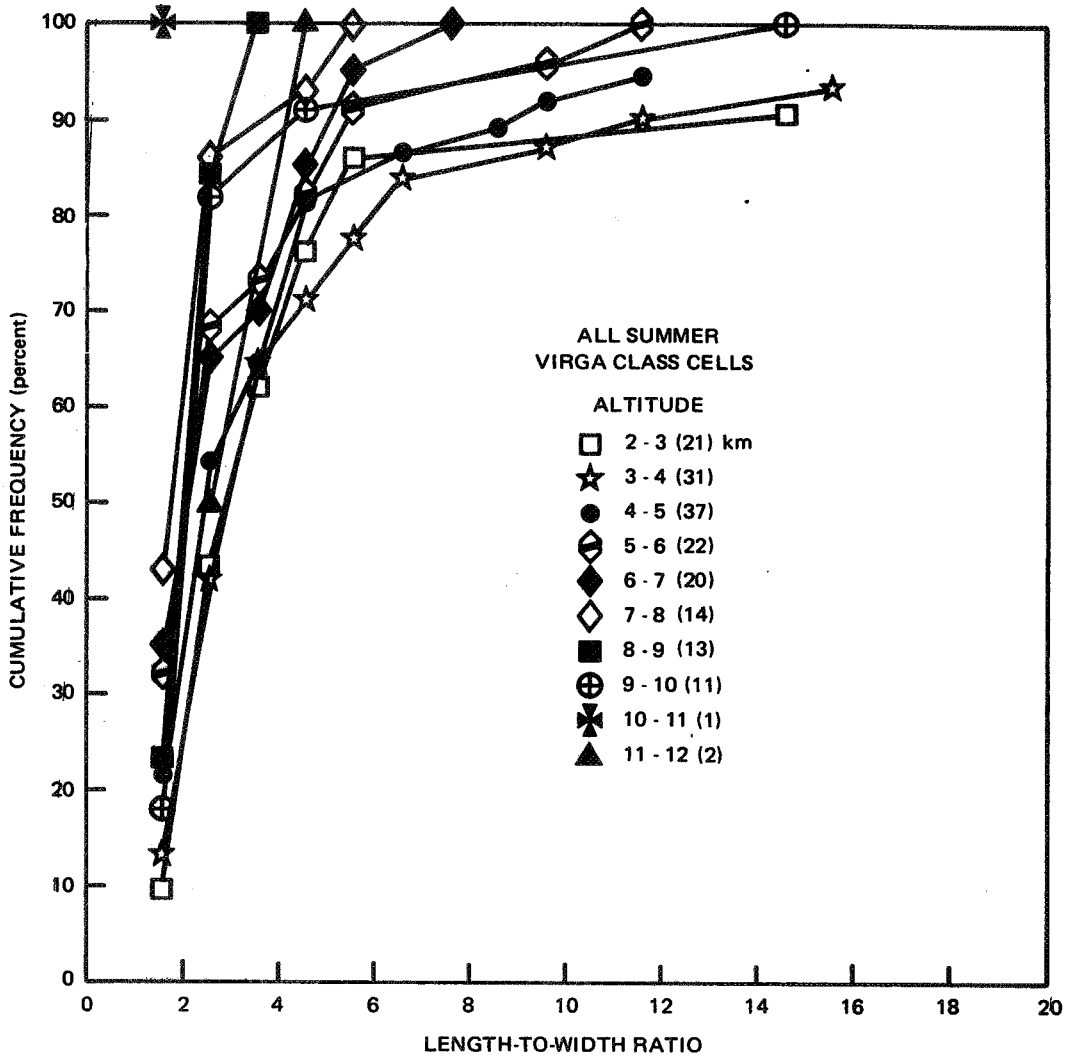

Figure 10.30. Frequency Distribution of the Contour Length-to-Width Ratio for Virga Class Cells in the 45 - 50 dBZ Reflectivity Interval According to Altitude

discussed in Section 7.5.2. Again, only the distributions for the "all" category of ROG class cells and the Virga class cells are presented, for the reasons discussed in Section 10.2.4.

Figure 10.31 presents an example of the cumulative frequency distribution of cell orientation for all the ROG class cells observed in the local peak reflectivity interval 40-45 dBZ, as a function of altitude. The total number of cells in each distribution at each altitude is shown in each figure in parenthesis. As noted in Section 7.5.2, the statistical descriptors of mean, median, and mode, although calculated by the computer, are not meaningful and, as such, are not presented.

The distributions in Figure 10.31 and those for other reflectivity intervals show no consistent, identifiable variation in the shape of the distribution with altitude. Further, the distributions show no preferred direction or orientation of the cell contour. When each angle is equally probable, the cumulative frequency distribution will be a straight line distribution from 0 to 180 deg and from 0 to 100 percent, respectively. With few exceptions, this appears to be the case. Where deviations occur such as in Figure 10.31 for an altitude of 8-9 km, the number of cases is small and the distribution has little statistical significance. The largest scatter in the curves, as a function of altitude, is for the case of the local peak reflectivity between 30 and 35 dBZ. This is not too surprising since these curves are for the very weak cells where the contour being examinned is 20-25 dBZ or around one mm hr^{-1} rain rate.

The data shown are for all the ROG class cells observed during the entire summer, i.e., the four-month observation period. During this time, the rain on a number of occasions was associated with frontal activity. It may be that the cell orientations are related to the direction of the front or to the wind direction along the front. The data presented here contains no such breakdown or comparison.

In Figure 10.32 an example of the distribution of cell orientation for the Virga class cells is presented. The same general conclusions may be drawn as above in the case of ROG class cells. The scatter in the Virga distributions is mainly attributed to the small number of cases in each distribution.

10.2.7 Distribution of Cells by Class and Category for Given Altitude Interval

The distribution of the number of cells by class and category with altitude is shown in Figures 10.33 and 10.34. Note that the distribution of cells is presented in two ways (as described in Section 7.5.4). Figure 10.33 includes both ROG and Virga class cells. The

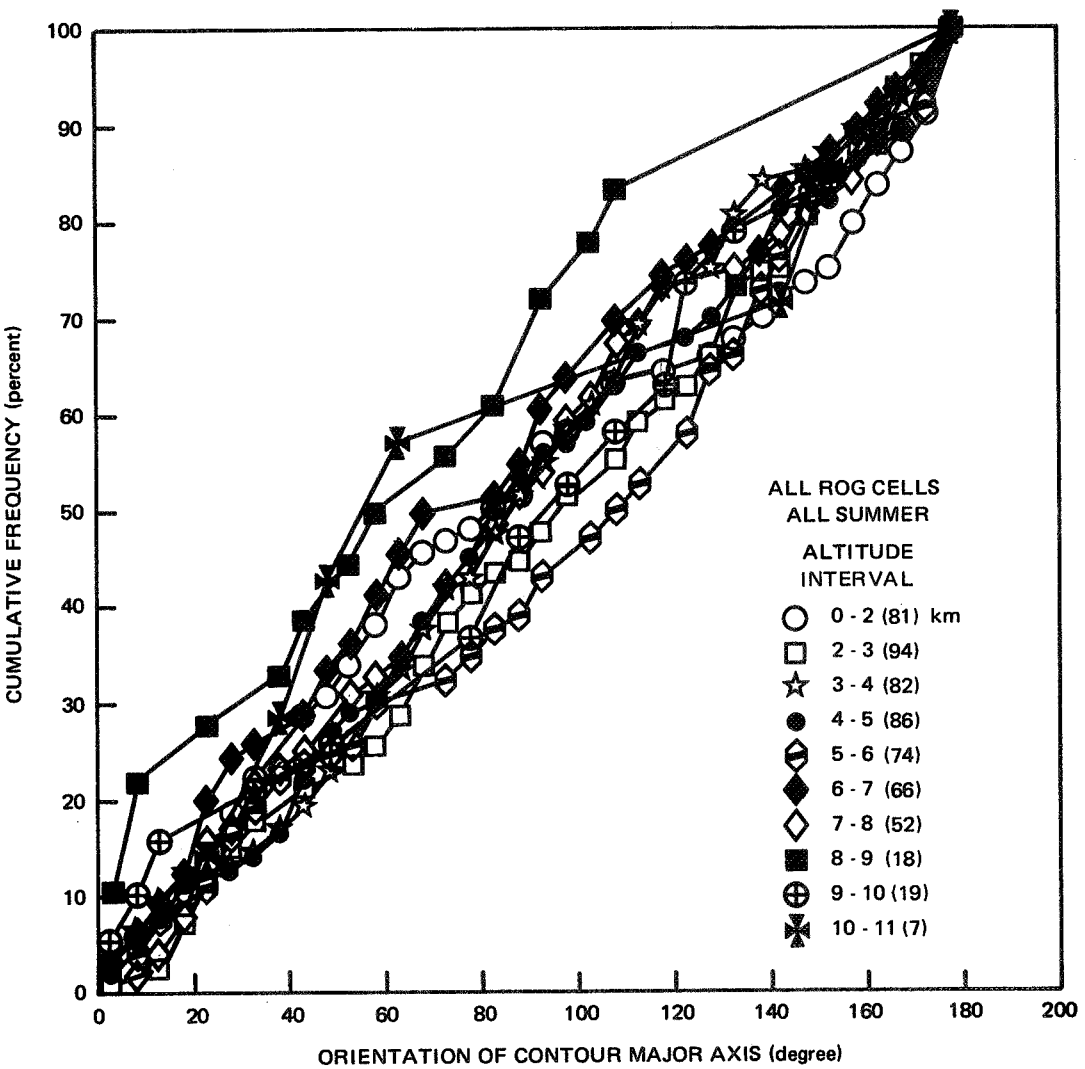

Figure 10.31. Frequency Distribution of the Orientation of the Contour Major Axis for All ROG Cells in the Reflectivity Interval 40 - 45 dBZ with Altitude

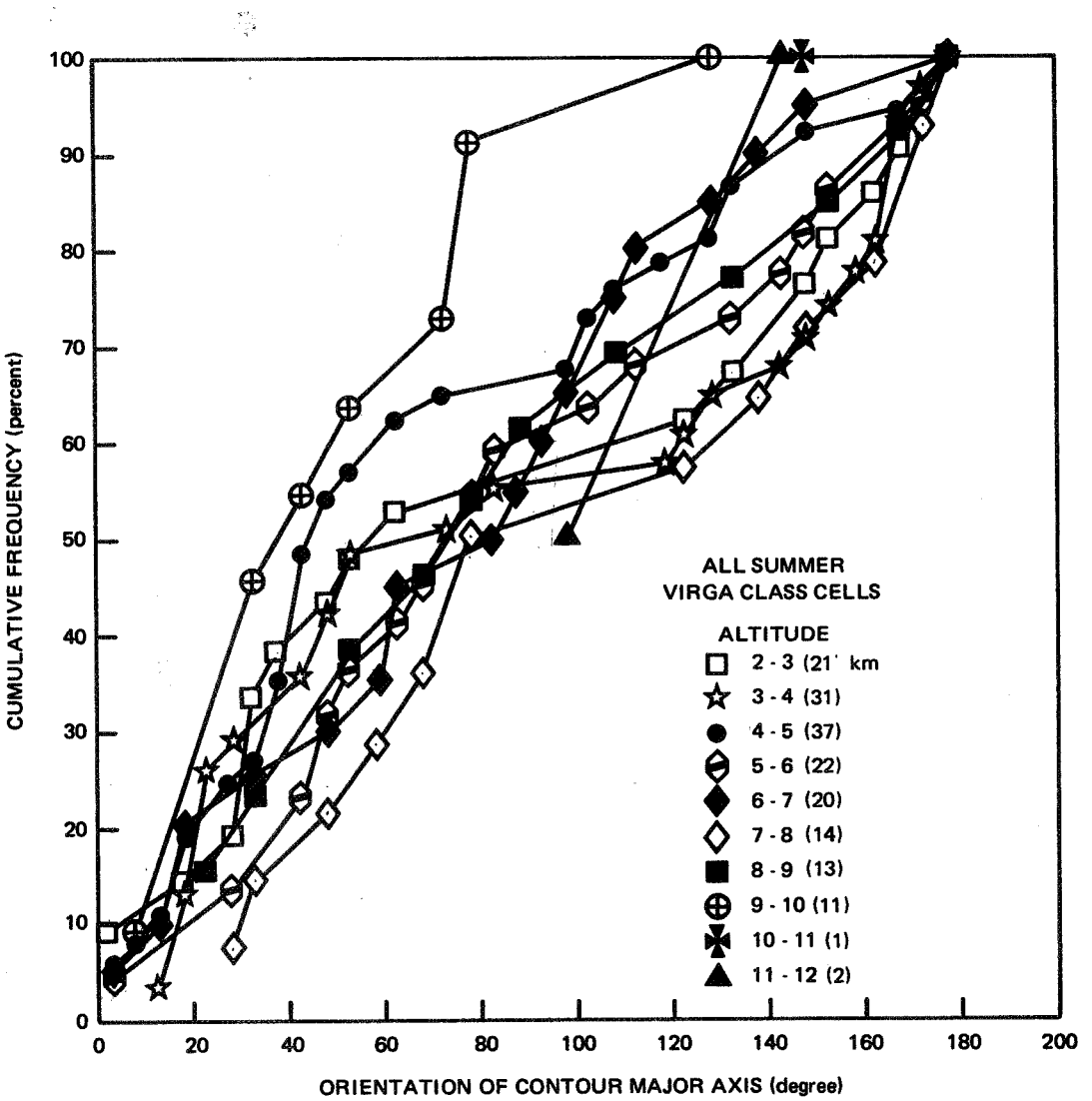

Figure 10.32. Frequency Distribution of the Orientation of the Contour Major Axis for Virga Class Cells in the Reflectivity Interval 45 - 50 dBZ for Various Altitudes

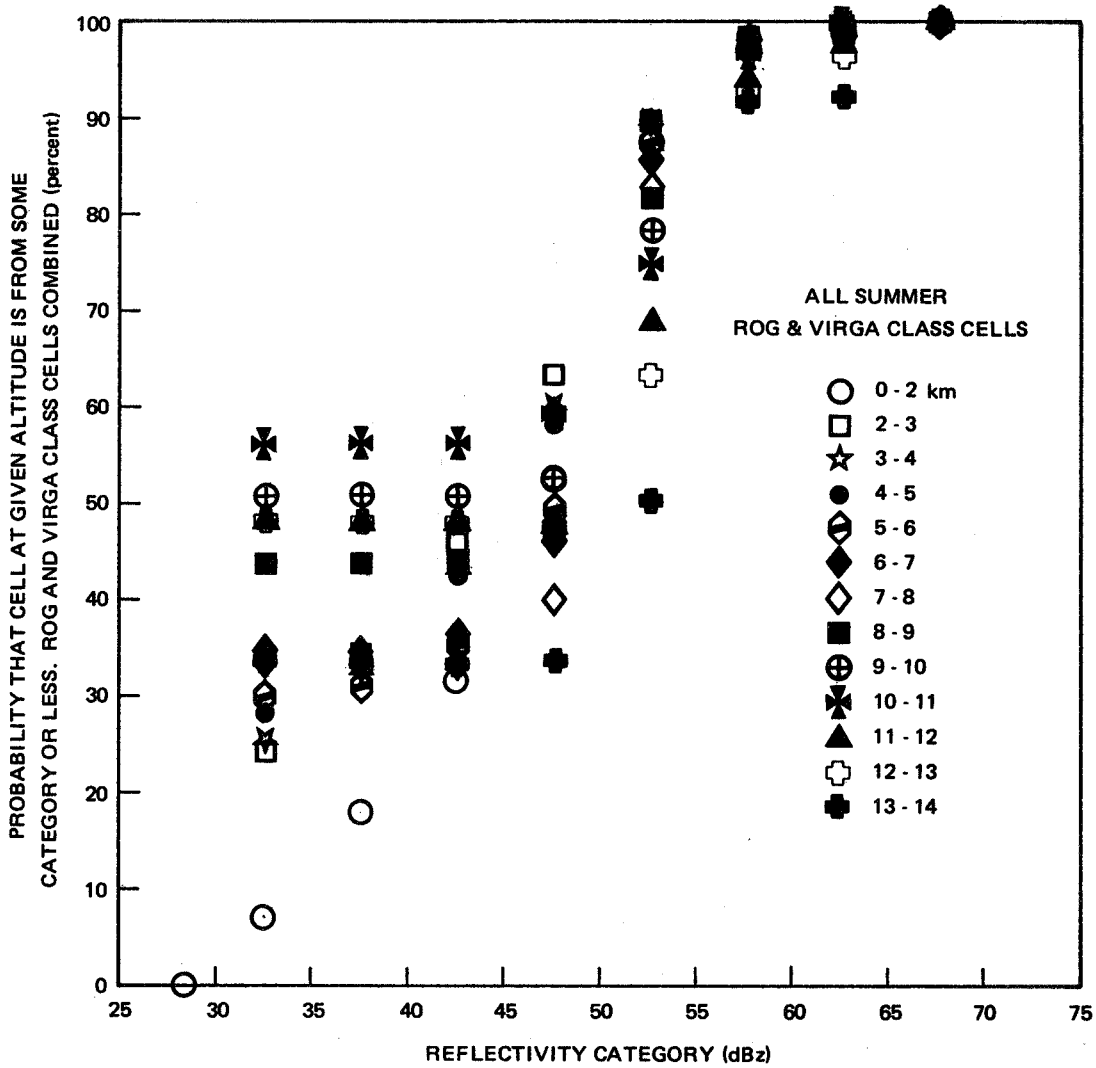

Figure 10.33. Distribution of Cells by Category for Given Altitude Interval for Both ROG and Virga Class Cells

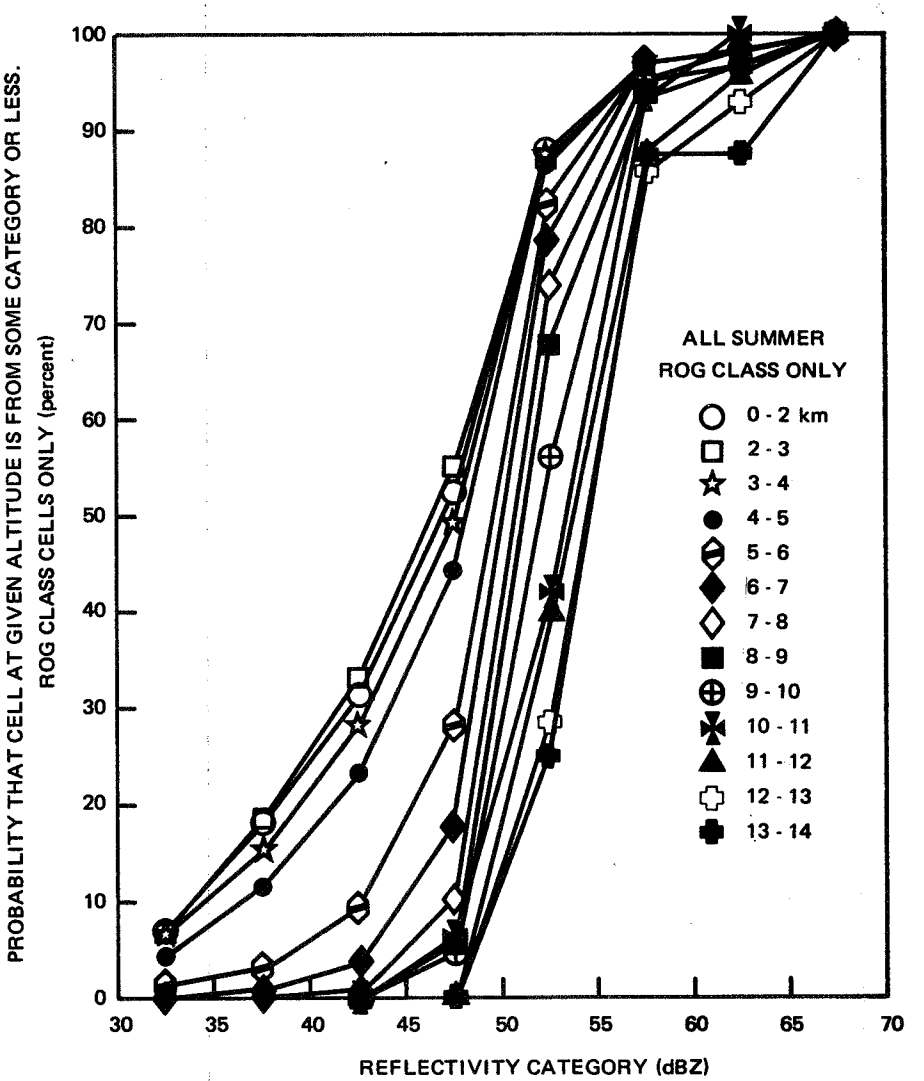

Figure 10.34. Distribution of Cells by Category for ROG Class Cells Only for Given Altitude Intervals

probabilities shown are those calculated in the fourth pass computer program. The distributions are dominated at the higher altitudes by the Virga class cells and cause the curves to flatten out at the low reflectivity category values (remembering that the curves show the probability that the cell at an altitude is of some category or less). Figure 10.34 presents the distribution for the ROG class cells only. These curves were calculated by hand using the data from Figure 10.33 and subtracting out the Virga class cells. The curves are well ordered and the probabilities for a given category fall off with increasing altitude. One may be tempted to cross plot these curves for a constant cell category to find the number of cells of a given category which survive to some altitude. Such a procedure is incorrect and should not be attempted. The question of cell heights or probability of occurrence with altitude for a given ROG class cell category is a separate question and is discussed in Section 10.2.8.

As noted in Section 7.5.4, the distribution of ROG class cells by category for the 0-2 km altitude interval is of particular interest since it may be interpreted as the probability of occurrence of rain cells of given peak or core intensity on the ground. This distribution is shown in Figure 10.35. In comparing this distribution with ground measurements of rain rate from rain gages, distrometers, etc., some caution should be exercised. The data used in the present analysis are areal data, i.e., the reflectivity (or rain rate) was measured over an area (the 75 nmi radius radar coverage) as opposed to a point, as with rain gages. The distribution determined here is the probability that a cell of some peak intensity on the ground will occur anywhere within the area of observation. An areal distribution similar to that derived from the radar data herein could conceivably be calculated using data from a large network of rain gages with small spacing.

The percentage of rain cells at each altitude which are ROG class cells was calculated by hand using the computer printout listings which show the number of Virga class cells (i.e., $Z < 30$ dBZ at $h < 2$ km) and the total number of cells at each altitude. The percentage thus calculated may be interpreted as follows: Given that it is raining with any intensity at some altitude, what is the probability that it is raining on the ground? Stated another way: For a given altitude, what is the distribution of cells between ROG and Virga class cells? Phrased still another way: What percentage of rain cells of any intensity observed at a given altitude actually reach the ground? One must keep in mind the basic definitions, i.e., ROG is defined as rain > 30 dBZ at $h < 2$ km.

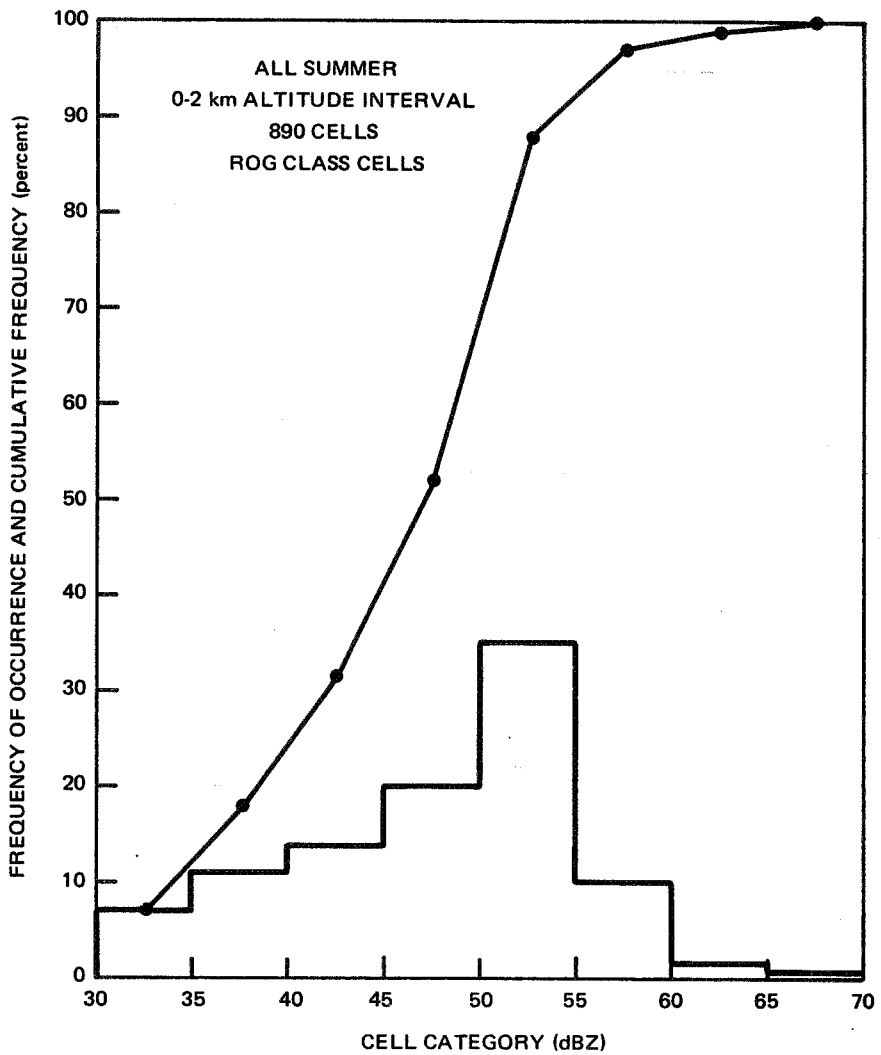

Figure 10.35. Distribution of ROG Class Cells by Category for the 0-2 km Altitude Interval

The percentage of ROG class cells at each altitude is shown in Figure 10.36. Note the essentially linear fall-off with increasing altitude to a value around 50 percent.

10.2.8 Distribution of Cells by Height for a Given Class and Category

The distribution of the number of cells by height for the various categories of the ROG class cells is shown in Figure 10.37. The percentages were calculated for each category by dividing the number of cells at each altitude by the number of cells in that category on the ground, i.e., in the 0-2 km interval. They may be interpreted as the probability that a ROG cell of a given category will extend to some altitude. For example, a rain cell which has a reflectivity (or rain intensity) on the ground (<2 km) of 40-45 dBZ has a 24 percent chance of extending to the 5-6 km interval; or alternately, 24 percent of the 40-45 dBZ category; ROG class cells extend to 5-6 km.

The curves are well ordered up to the 55-60 dBZ category, i.e., as the category increases, the height of the cell increases for the same probability. However, this trend is reversed for the two highest categories, 60-65 and 65-70 dBz. These two curves fall below those for lesser categories. This seems to say that when it is raining very hard on the ground, the probability of the cell extending to some altitude (e.g., 6 km) is less than that for a less intense rain. An alternate presentation is shown in Figure 10.38. This figure is simply a cross plot of the data in Figure 10.37 for these percentages, 10, 50 and 90 percent.

The distribution of cells with altitude for the two classes, ROG and Virga, is shown in Figure 10.39. In this case the ROG curve contains all cells regardless of category. As mentioned above, the percentages for the ROG class cells were calculated by dividing the number of cells at altitude by the number in the lowest altitude interval, 0-2 km. In the case of the Virga class cells there are no cells in this altitude interval by definition. In this case, the number of cells at each altitude was divided by the total number of Virga cells in the population. The interpretation of this curve is slightly different than for the ROG class. The curve simply shows the percentage of Virga cells at each altitude. There is no one altitude at which all the Virga class cells occur as with the ROG class cells.

10.3 RAIN TYPE STATISTICS

A first order attempt to separate the rain occurrences according to the type of rain was made by separating the 21 days for which data were reduced into (1) days where the cells were generally embedded

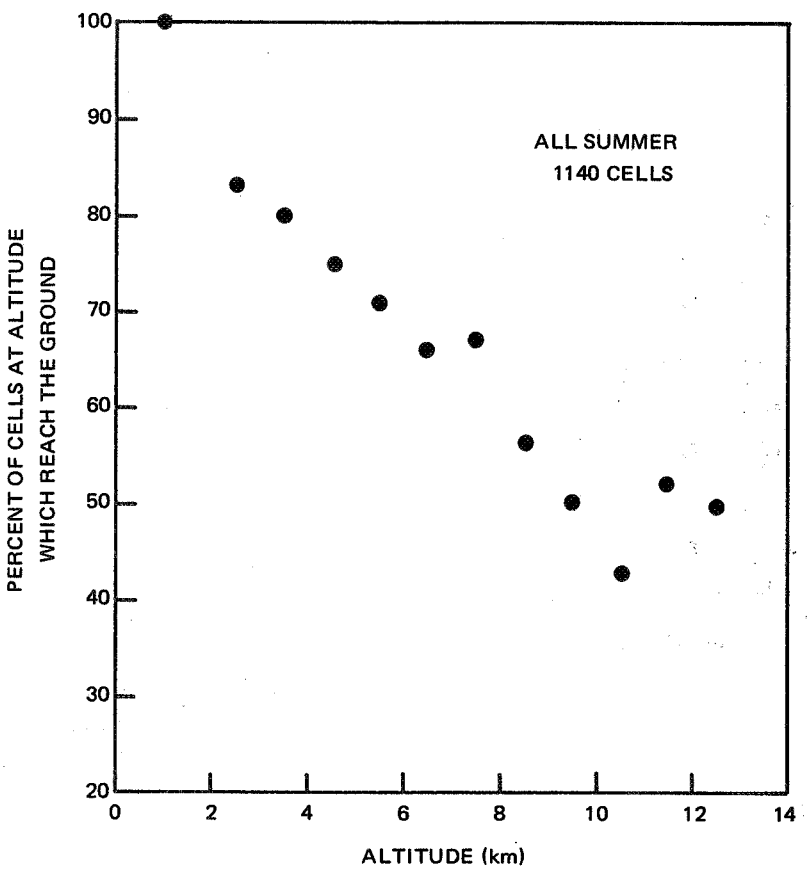

Figure 10.36. Percent of Cells at Altitude Which Reach the Ground

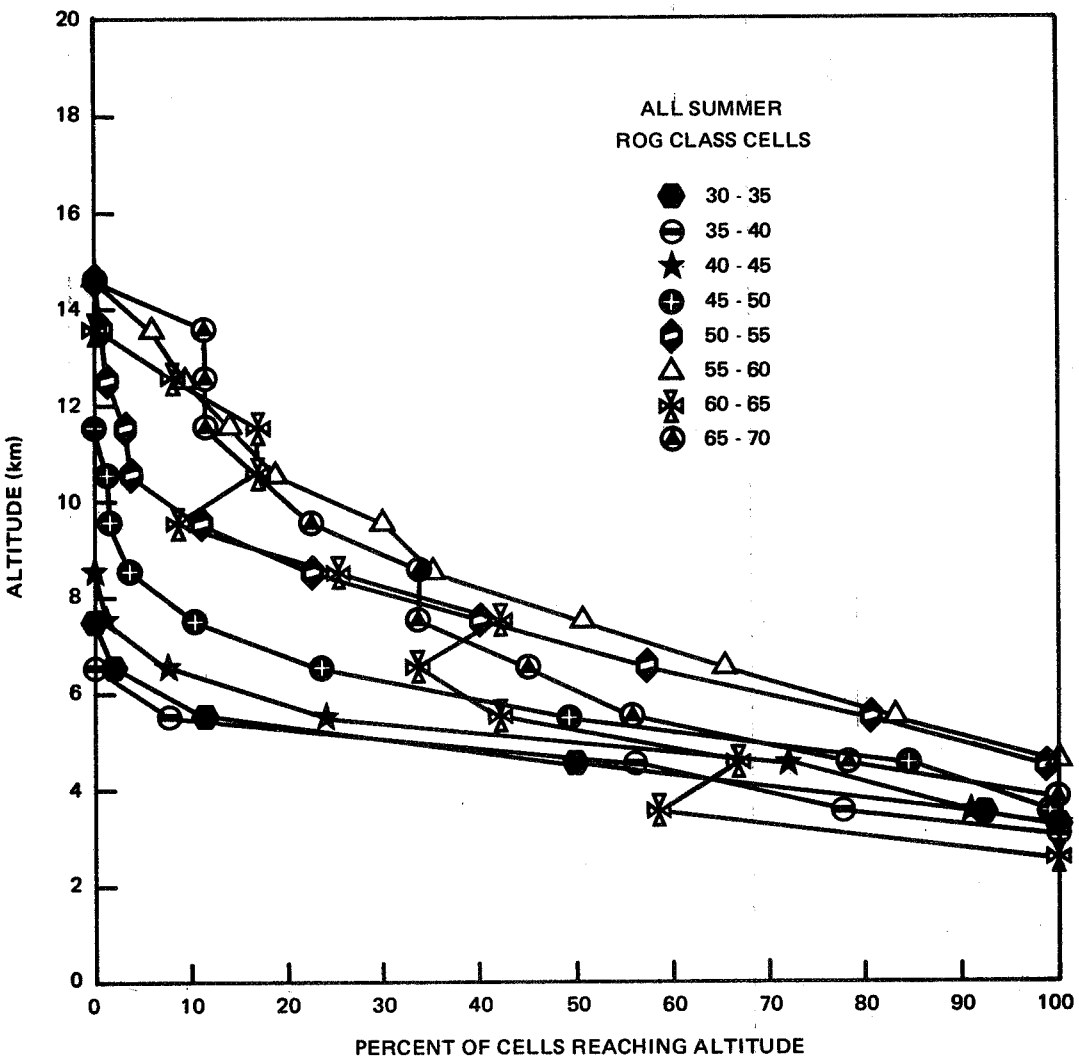

Figure 10.37. Percent of Cells in Given Category Which Reach Same Altitude

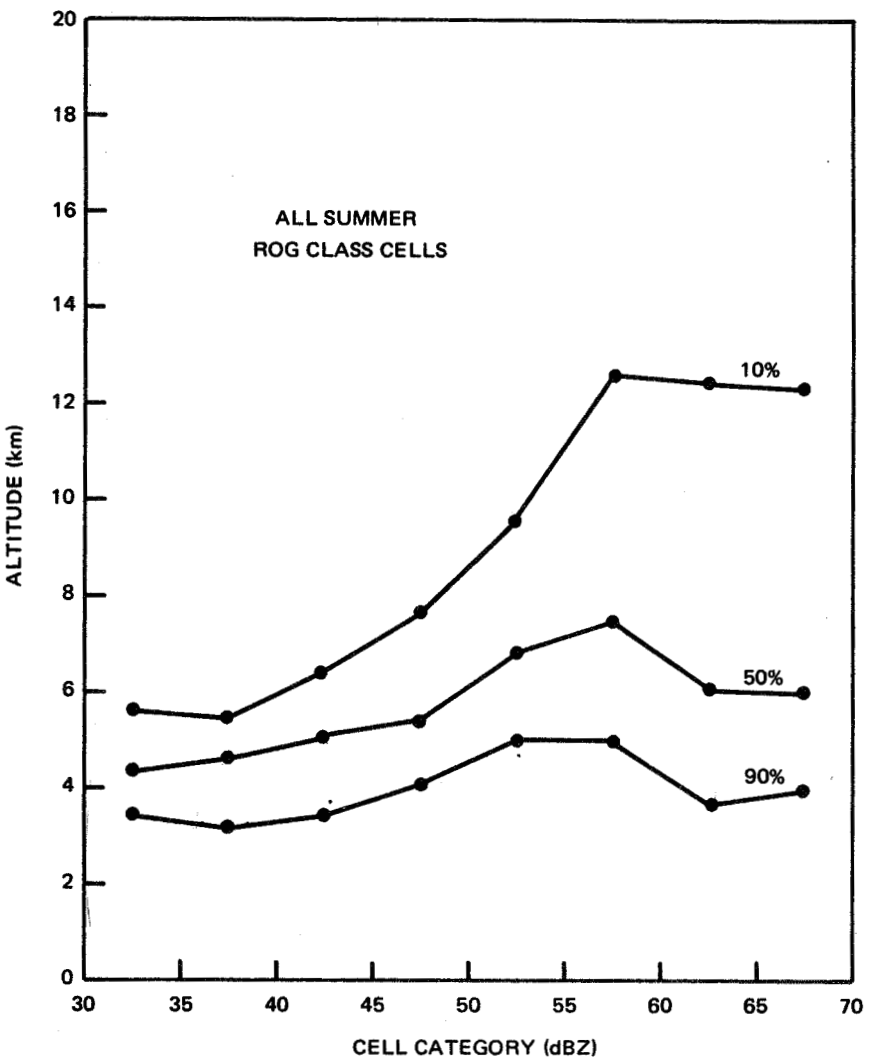

Figure 10.38. Probability of Cell of Given Category Extending to an Altitude

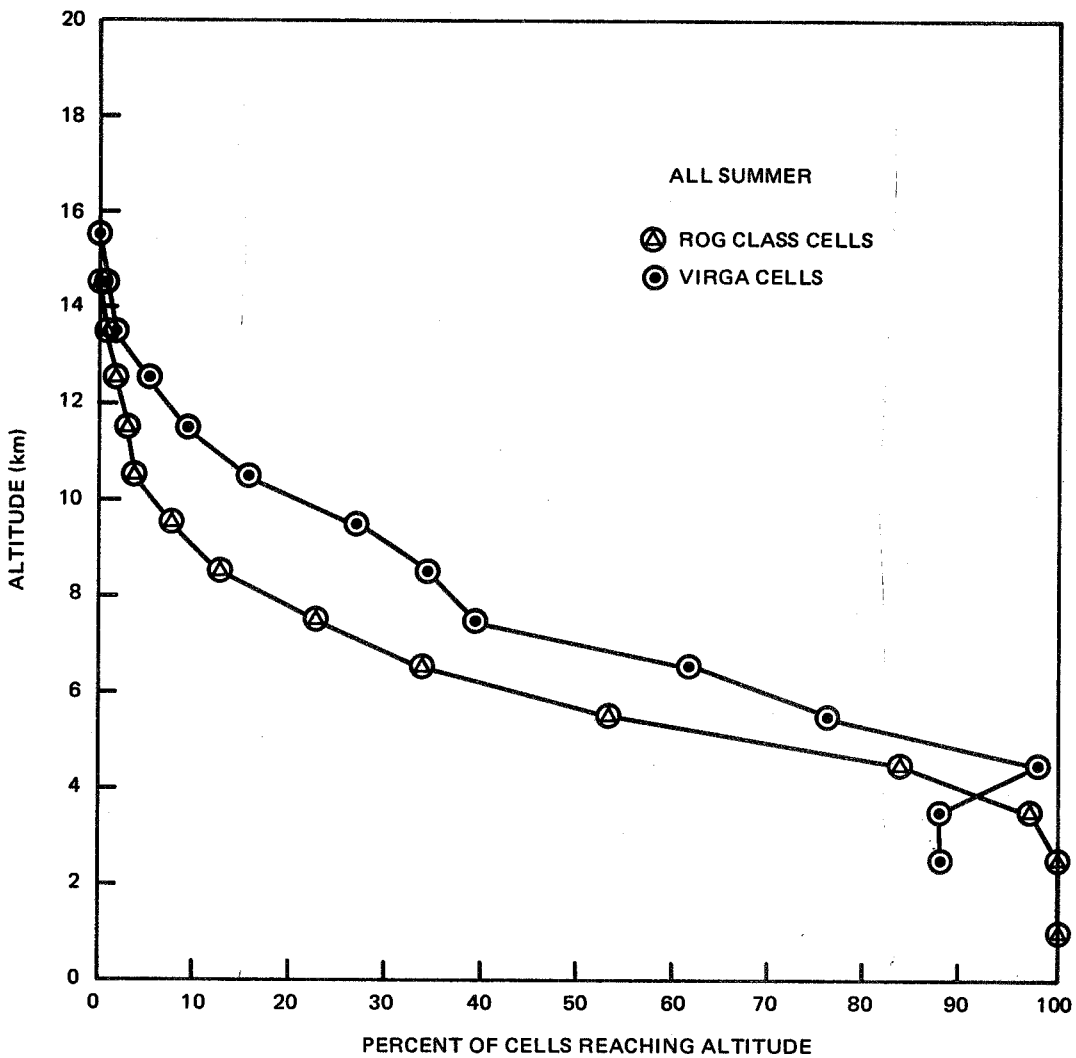

Figure 10.39. Percent of Cells Reaching Altitude for All ROG Class Cells and Virga

in a larger rain system such as a cold front, and (2) days where the cells were, in general, isolated. Identification of a day as an "isolated cell" day or an "embedded cell" day was subjective and based on the analyst's judgment of the patterns as displayed on the 2 deg elevation PPI pictures. Such a procedure is admittedly gross since characterizing the rain cell patterns does not characterize all the individual cells. For example, on a day where the rain was due to frontal activity, there are some cells in advance of the front or to the rear which are, in fact, isolated and not embedded within the frontal rain system itself. Conversely, on a day identified as an isolated cell day, there may be a cluster of cells which make up a larger entity. Such an entity is still smaller than that for the frontal activity however. Table 10.1 lists the days which were reduced and their identification as embedded or isolated cell days. For comparison, in a separate column, is the meteorological characterization based on the meteorological data described in Volume I and contained in Volume III, the Appendices. As noted above, the classification in terms of isolated or embedded was done solely on the basis of cell patterns on the PPI scope photographs. It is interesting to note, however, the general correspondence between the classification and meteorological description, i.e., embedded cell days are associated with fronts and isolated cells with air mass as might be expected.

In the following sections examples of the results of the fourth pass computer runs for reflectivity only are presented. Comparison of these results with the all summer results of Section 10.2 and with each other is discussed in Section 10.3.3.

10.3.1 Isolated Cell Days

10.3.1.1 Peak Reflectivity. An example of the distributions of the peak reflectivity for a given category of the ROG class cells on the isolated cell days at given altitude intervals is shown in Figure 10.40. The mean and median reflectivities for each category are presented in Figures 10.41 and 10.42. Distributions and profiles of the mean and median reflectivities for all ROG class cells (regardless of category) and for the Virga class cells are shown in Figures 10.43 through 10.46.

10.3.1.2 Reflectivity Ratio. The distribution of reflectivity ratio for the various categories is shown in Figure 10.47 and the curve for all ROG class cells is shown in Figure 10.48.

The mean, median and mode reflectivity ratios are not shown for the reasons discussed in Section 10.2.2. Again, over 50 percent of the values fall within the first reflectivity ratio interval.

Table 10.1

Clarification of Rain Days

Date	Meteorological Description	Classification
May 23	Frontal and Squall Line	Isolated
24	Frontal	Embedded
29	Pre-frontal and Frontal	Embedded
Jun 13	Trough Induced	Isolated
18	Frontal	Embedded
21	Squall Line and Pre-frontal	Isolated
22	Frontal	Embedded
29	Pre-frontal	Isolated
Jul 3	Squall Line and Showers	Isolated
5	Frontal	Embedded
10	Trough Induced	Isolated
27	Trough Induced	Isolated
31	Pre-frontal	Isolated
Aug 1	Pre-frontal	Embedded
2	Squall Line and Pre-frontal	Isolated
13	Pre-frontal	Isolated
14	Frontal and Pre-frontal	Embedded
15	Frontal	Embedded
16	Post-frontal	Isolated
20	Trough Induced	Isolated
21	Frontal	Embedded

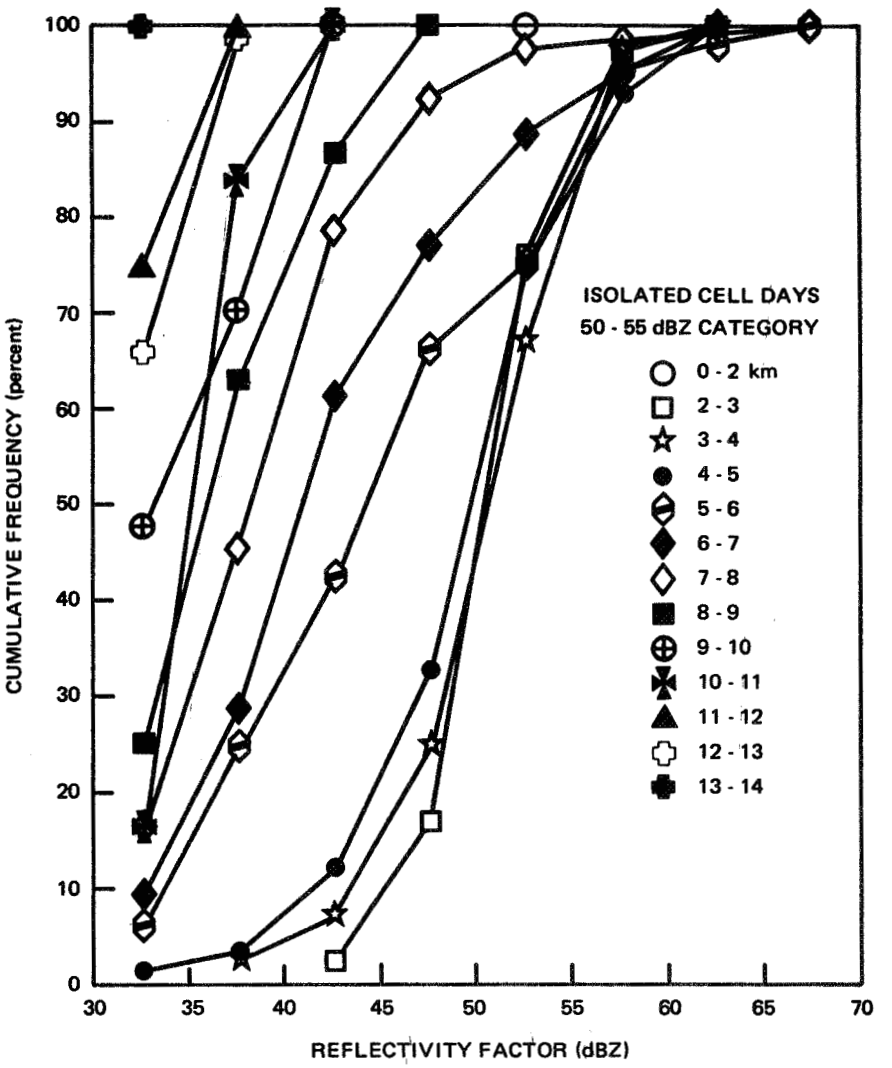

Figure 10.40. Cumulative Frequency Distributions of Peak Reflectivity Factor for 50 - 55 dBZ Category Cells for Isolated ROG Cell Days

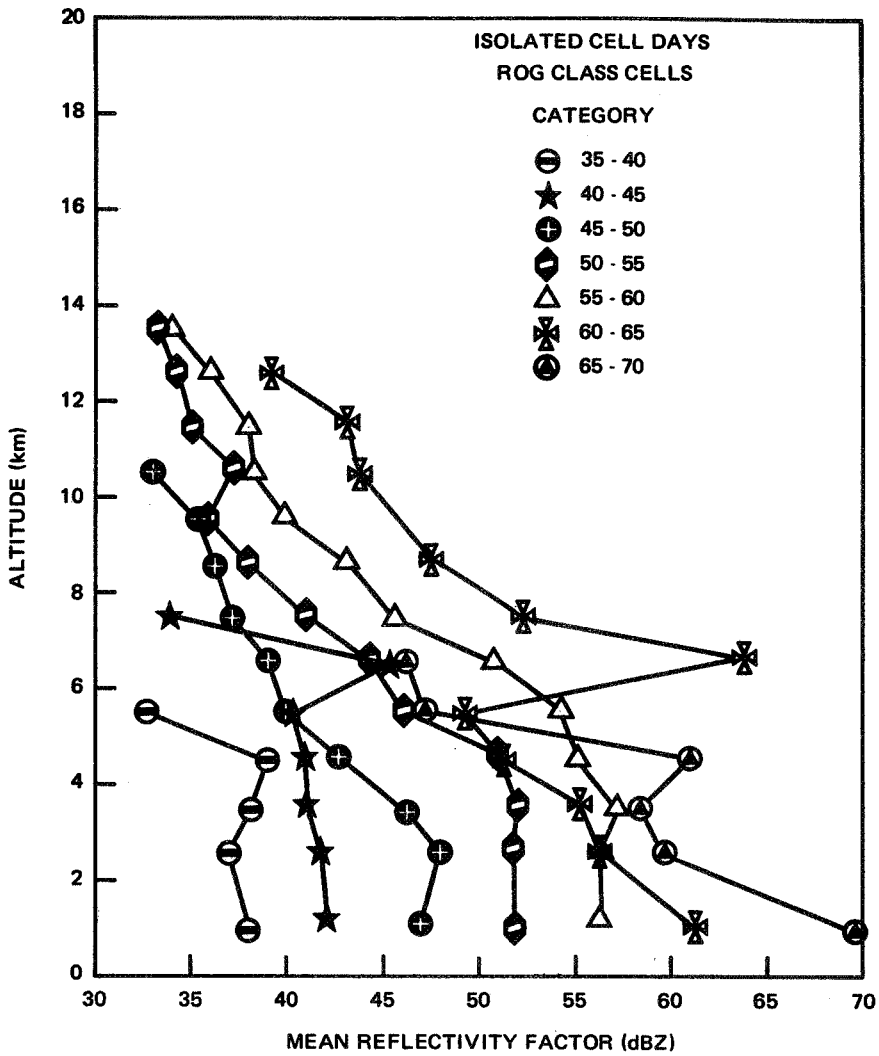

Figure 10.41. Profile of Mean Reflectivity Factor for Isolated Cell Days

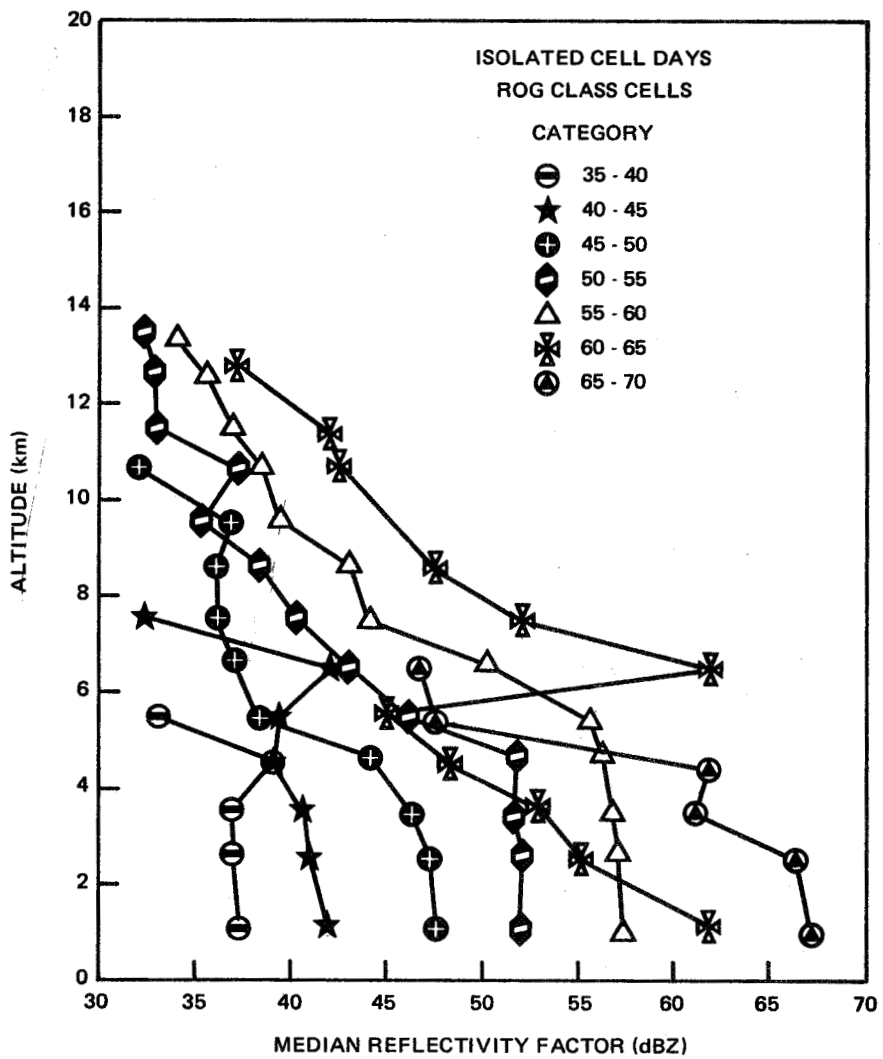

Figure 10.42. Profile of Median Reflectivity Factor for Isolated Cell Days

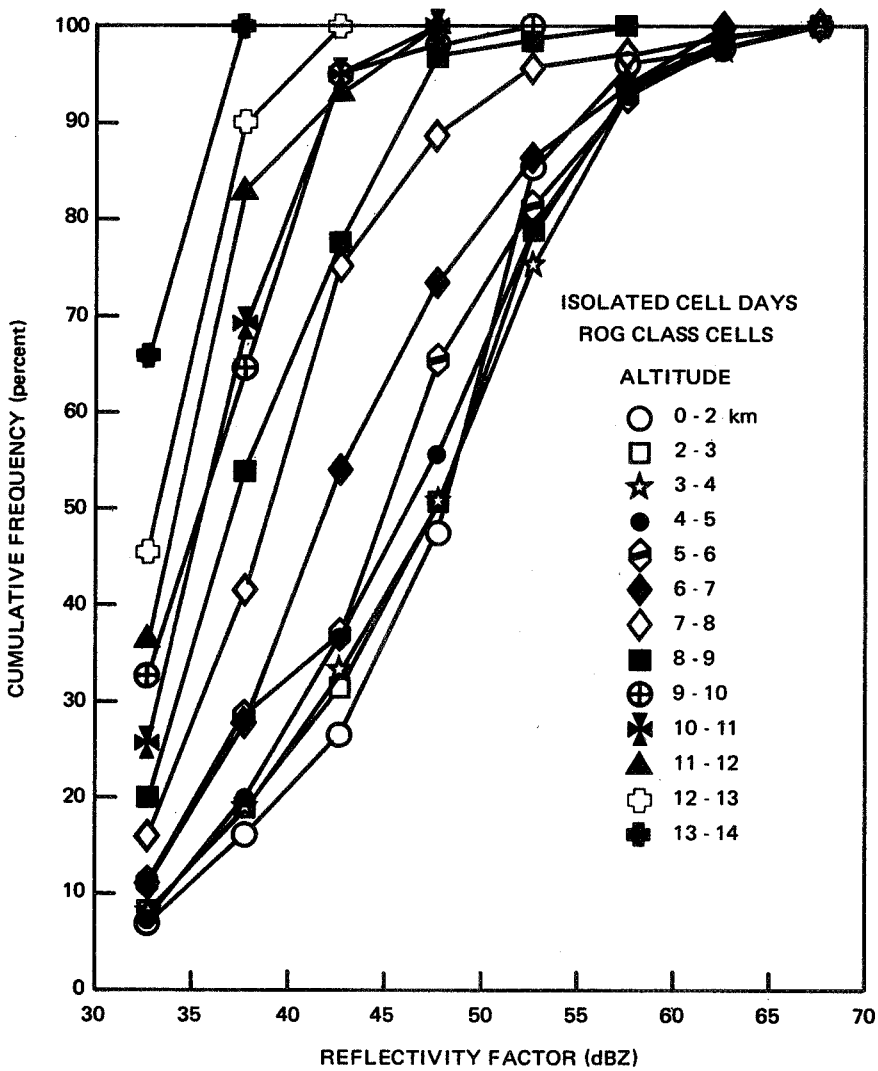

Figure 10.43. Cumulative Frequency Distributions of Peak Reflectivity Factor for All ROG Class Cells on Isolated Cell Days

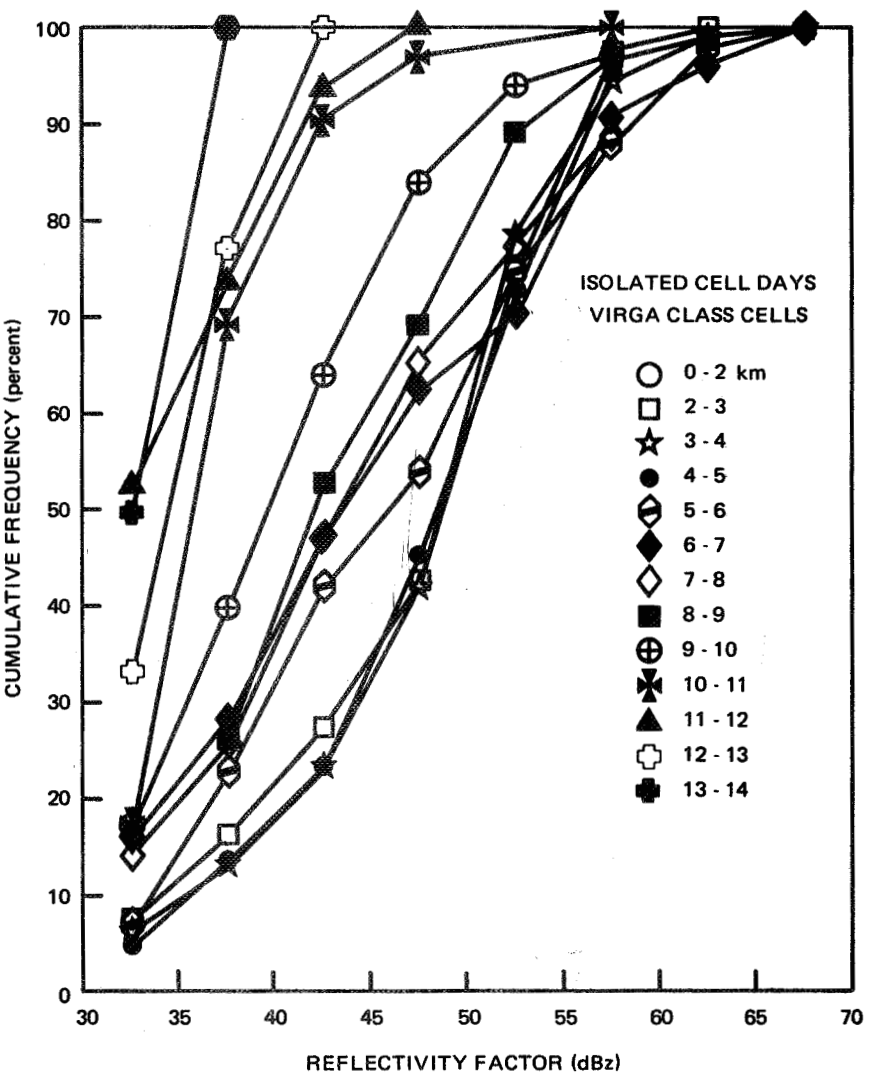

Figure 10.44. Frequency Distribution of Peak Reflectivity Factor for Virga Class Cells on Isolated Cell Days

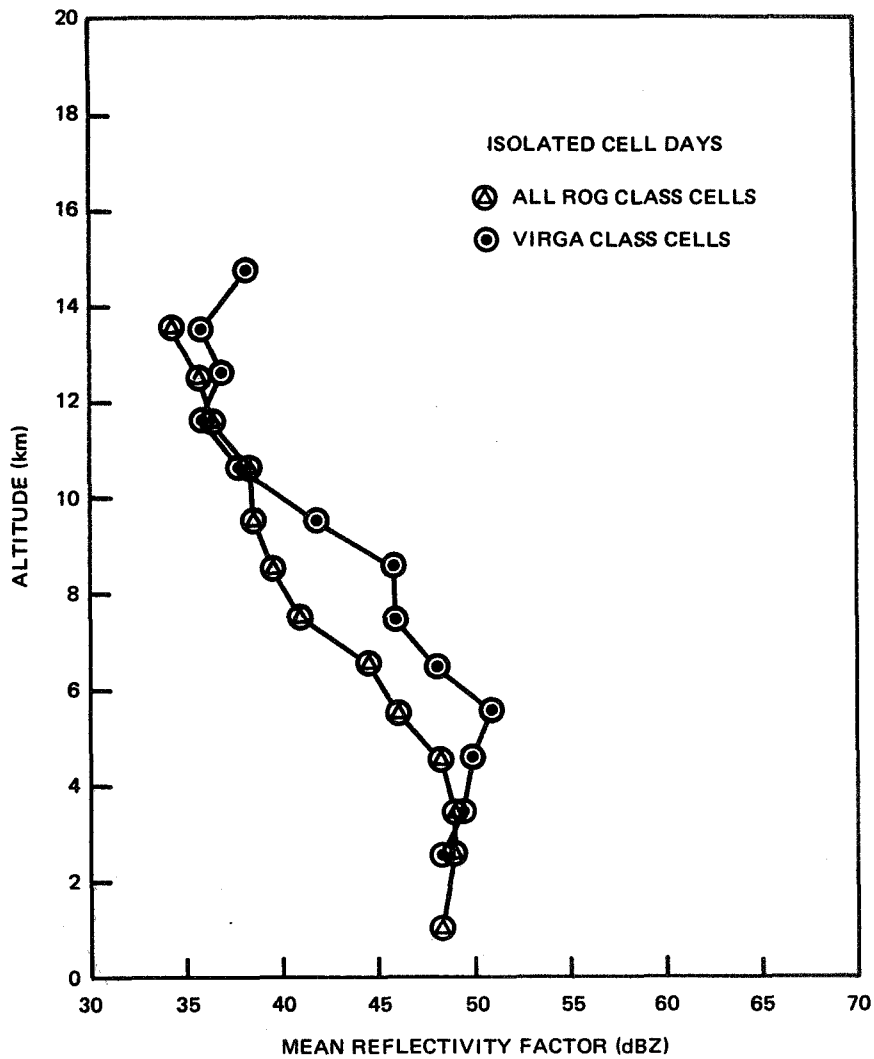

Figure 10.45. Profile of Mean Core Reflectivity for All ROG Class Cells and for Virga Class Cells on Isolated Cell Days

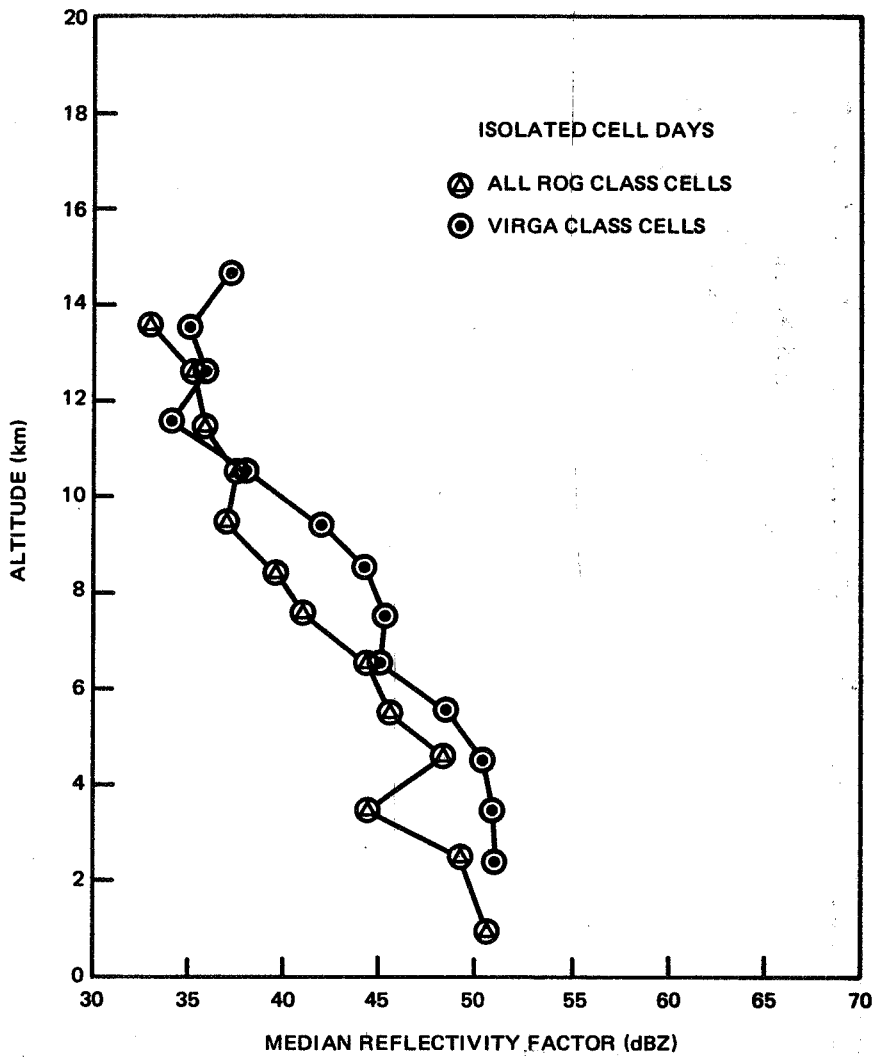

Figure 10.46. Profile of Median Core Reflectivity for All ROG Class Cells and for Virga Class Cells on Isolated Cell Days

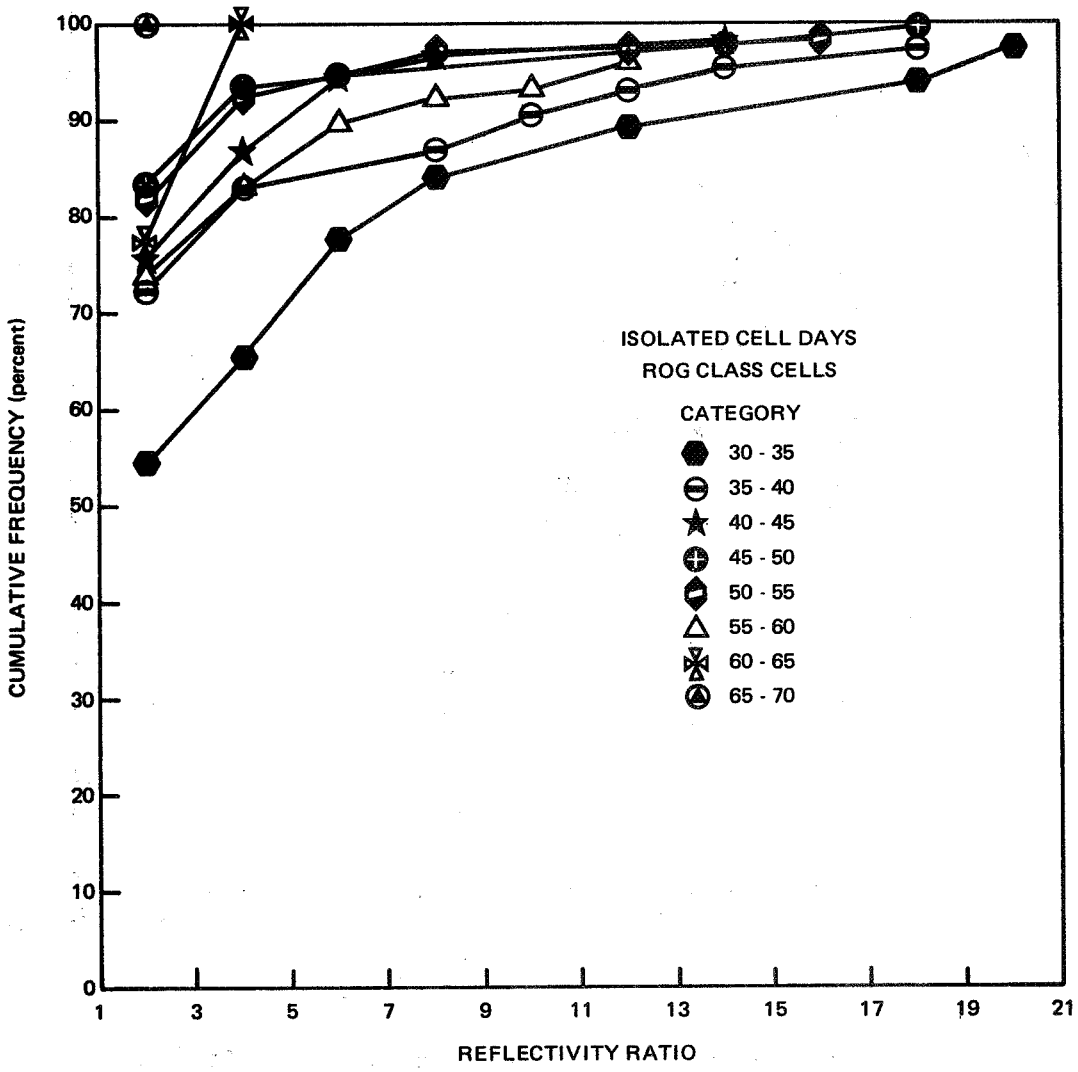

Figure 10.47. Cumulative Frequency Distribution of Reflectivity Ratio According to Category of ROG Cells on Isolated Cell Days

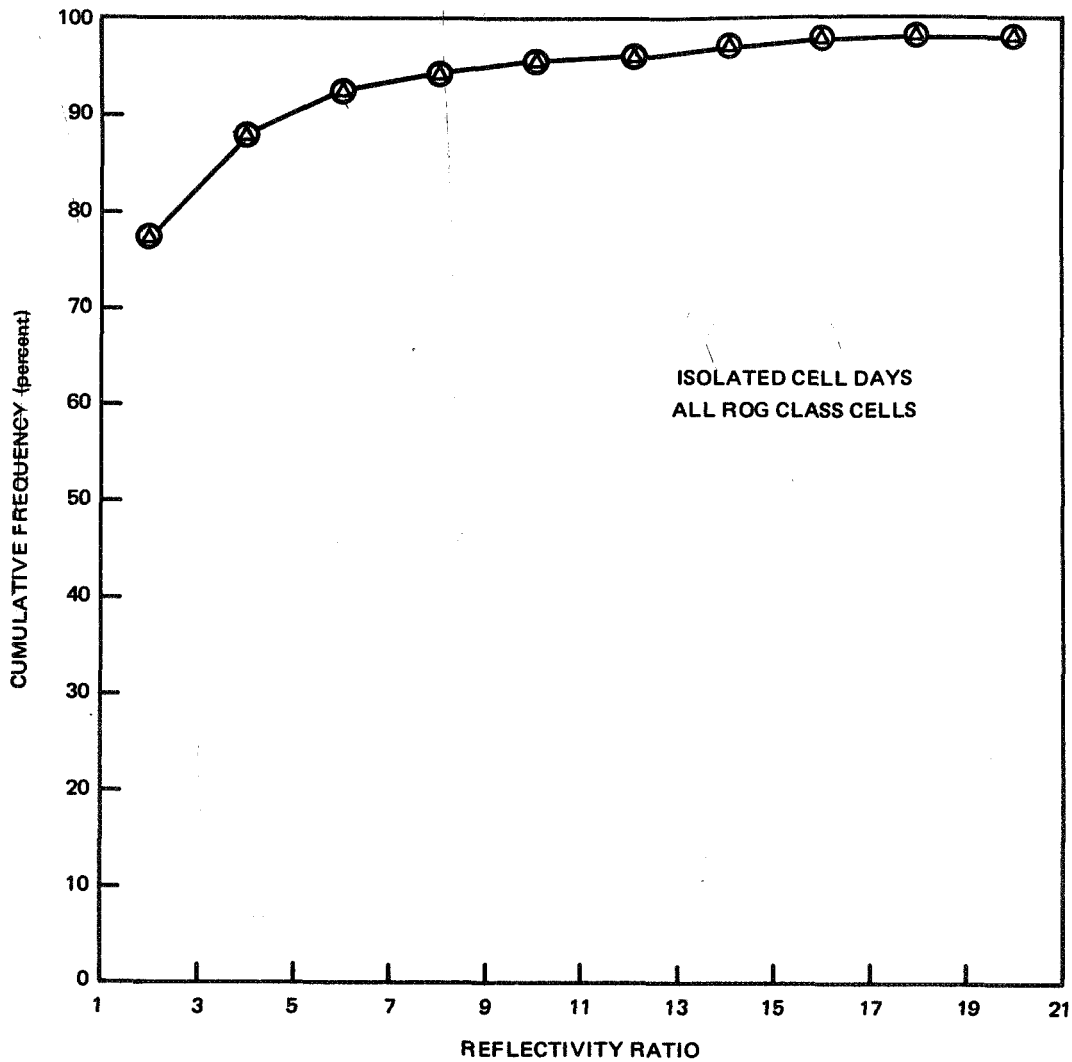

Figure 10.48. Cumulative Frequency Distribution of Reflectivity Ratio for All ROG Cells on Isolated Cell Days

10.3.1.3 Height of Maximum Reflectivity. Figure 10.49 shows the height of the maximum reflectivity as a function of ROG cell category and Figure 10.50 shows the height for all ROG class cells. The mean and median values are presented in Figure 10.51.

10.3.2 Embedded Cell Days

10.3.2.1 Peak Reflectivity. An example of the peak reflectivity distributions for those days in Table 10.1 classified as embedded cell days are presented in Figure 10.52 for the 50-55 dBZ category of ROG class cells in given altitude intervals. Figures 10.53 and 10.54 show the mean and median reflectivities for each category as a function of altitude. The cumulative frequency distributions and profiles of the mean and median reflectivities for all ROG class cells and for the Virga class are shown in Figures 10.55 through 10.58.

10.3.2.2 Reflectivity Ratio. The distributions of reflectivity ratio for the various categories of ROG class cells is shown in Figure 10.59 and the curve for the "all" category is shown separately in Figure 10.60. Again, note that the ratio in every case is concentrated heavily in the first interval, i.e., 1 to 3.

10.3.2.3 Height of Maximum Reflectivity. The height of the maximum reflectivity as a function of ROG cell category is shown in Figures 10.61 and 10.62. Mean and median values are shown in Figure 10.63.

10.3.3 Comparison of Statistical Descriptions

The comparison of the peak reflectivity, reflectivity ratio, and the height of the reflectivity maximum for the three cell populations, i.e., all summer, isolated cells and embedded cells, does not indicate any significant, consistent difference in the statistical descriptions. The distributions and statistical descriptors are different, i.e., the values are not identical for the three populations, but no identifiable trend is evident. This result should be taken with some reservations, however. As noted in Section 10.3, the separation of the 21 days into embedded and isolated cell days was done on a gross basis, i.e., a subjective generalization for a whole day. No attempt was made to identify, separate and classify individual cells. Such a procedure may very well produce more positive results in terms of significant differences in the statistical descriptions and properties.

10.4 CELL SPACINGS

The first problem in attempting to analyze the distance between cells is to define where the center of the cell is located.

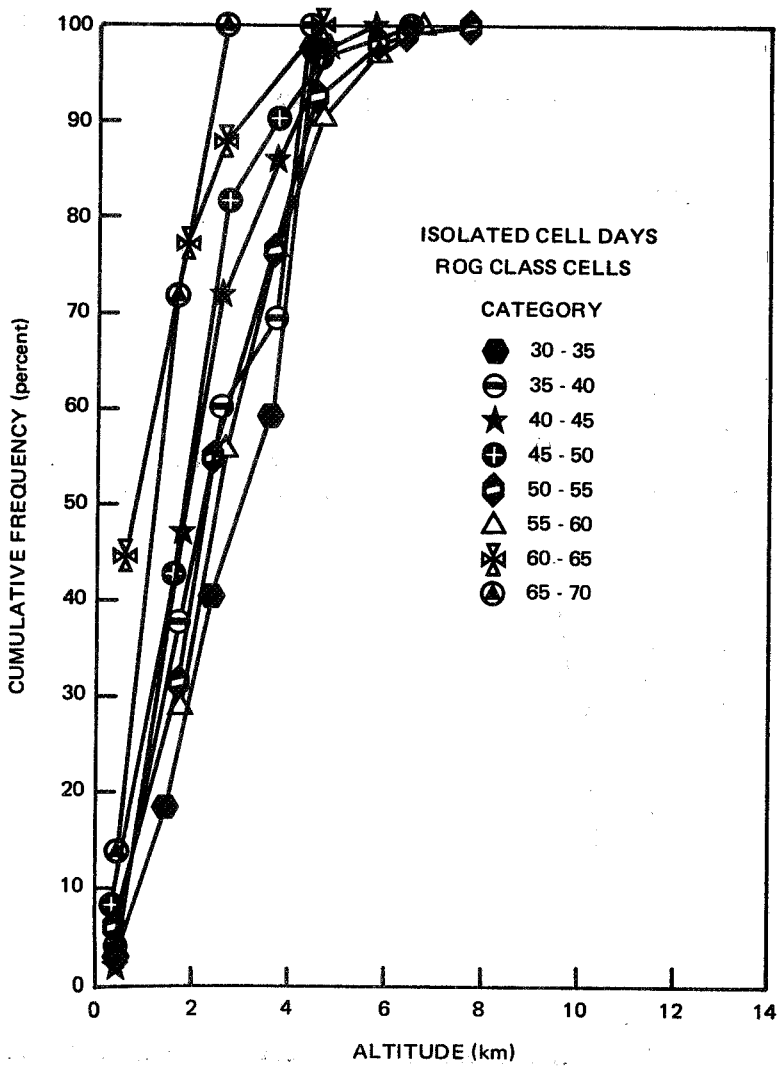

Figure 10.49. Distribution of the Height of the Maximum Peak Reflectivity for Isolated Cell Days by Category

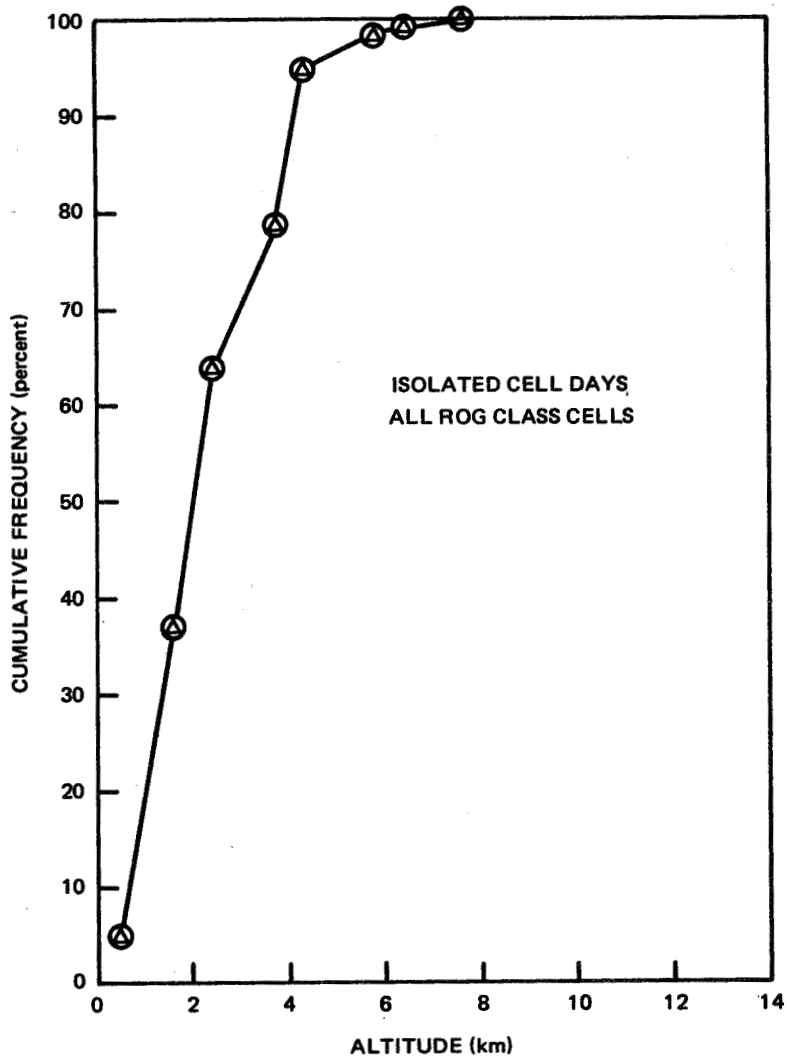

Figure 10.50. Distribution of the Height of the Maximum Peak Reflectivity for All ROG Class Cells on Isolated Cell Days

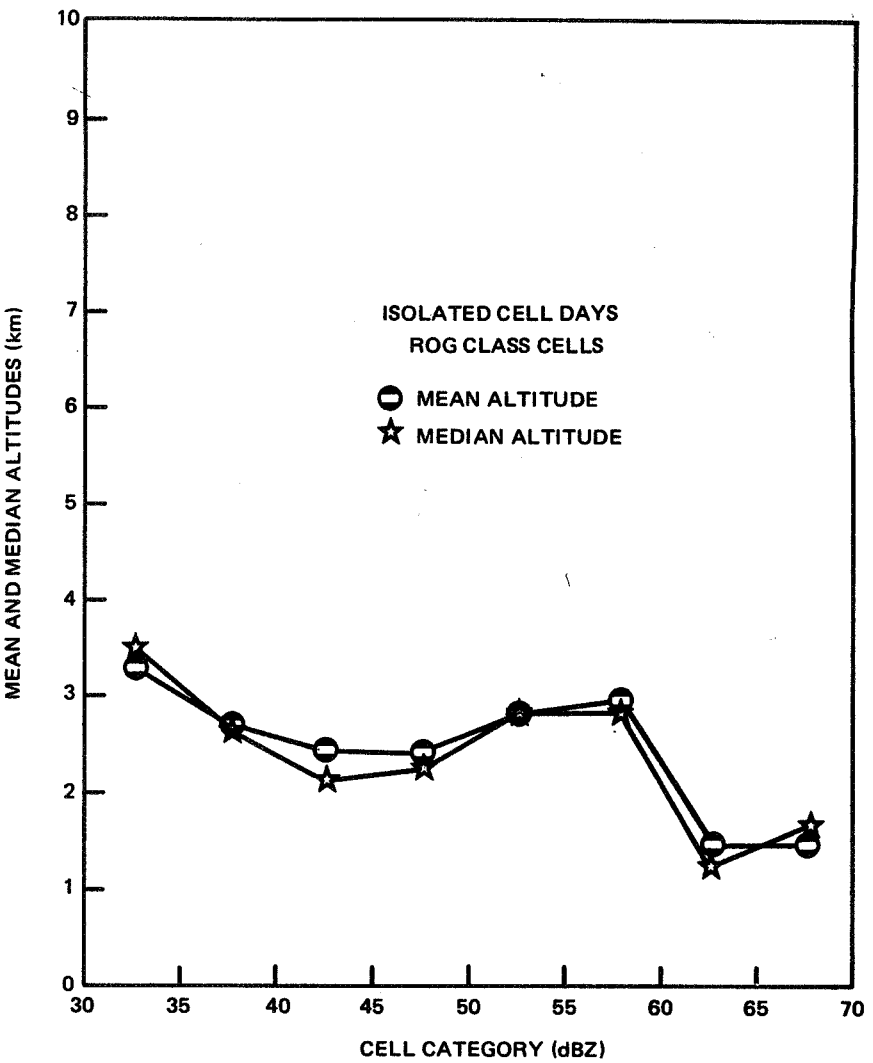

Figure 10.51. Mean and Median Heights of the Maximum Reflectivity According to Category for Isolated Cell Days

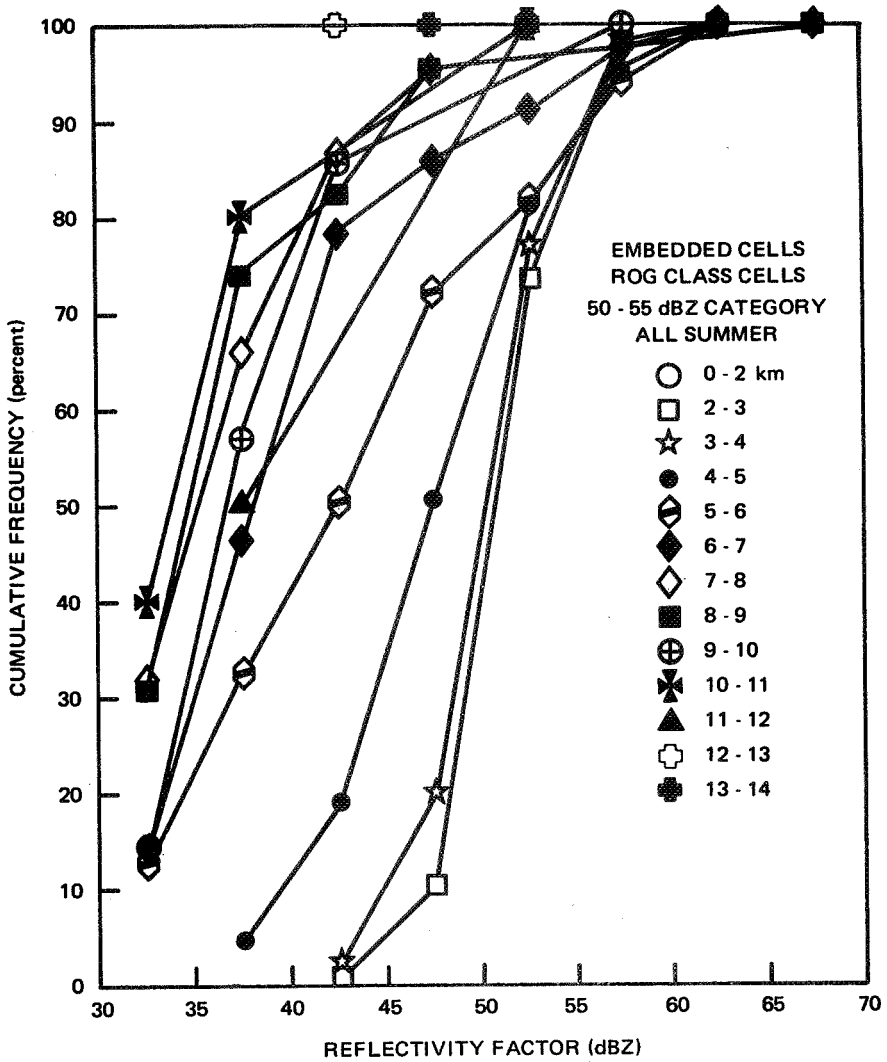

Figure 10.52. Cumulative Frequency Distribution of Peak Reflectivity Factor for 50 - 55 dBZ Category of ROG Class Cells on Embedded Cell Days

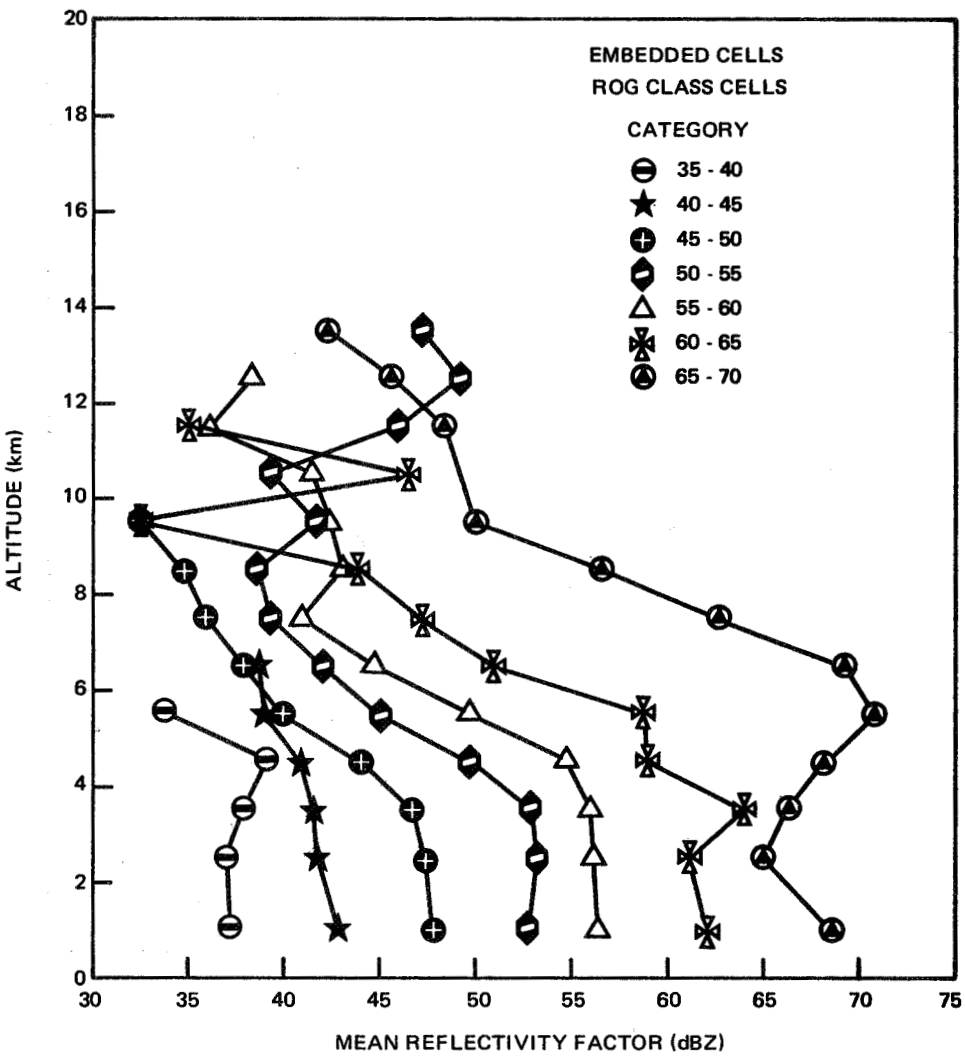

Figure 10.53. Profile of Mean Reflectivity Factor for Embedded Cell Days

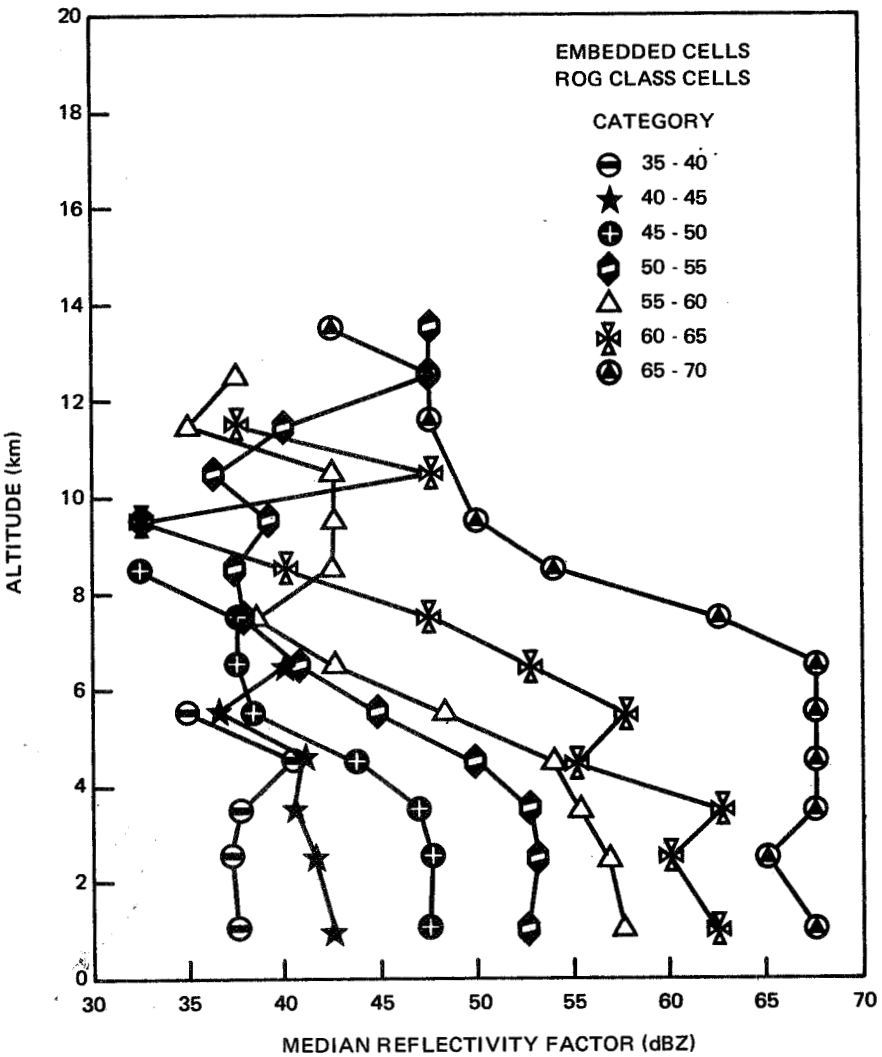

Figure 10.54. Profile of Median Reflectivity Factor for Embedded Cell Days

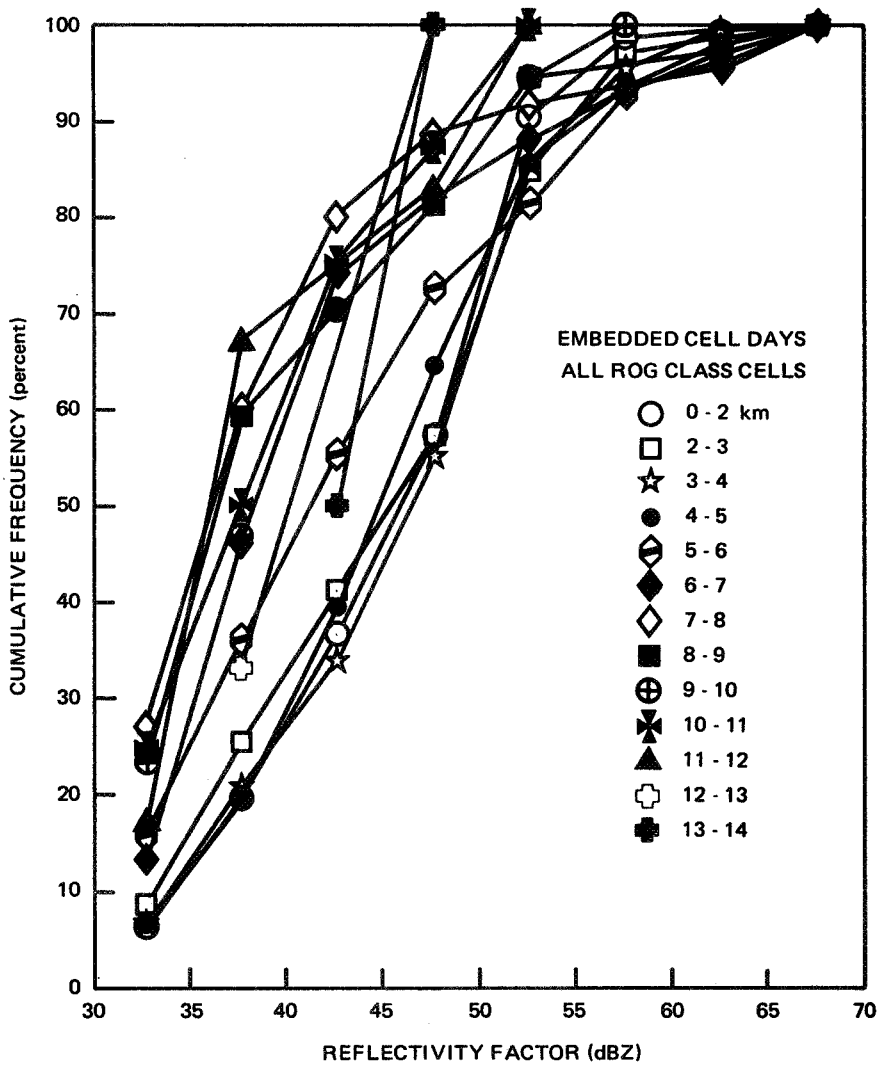

Figure 10.55. Cumulative Frequency Distribution for All ROG Class Cells on Embedded Cell Days

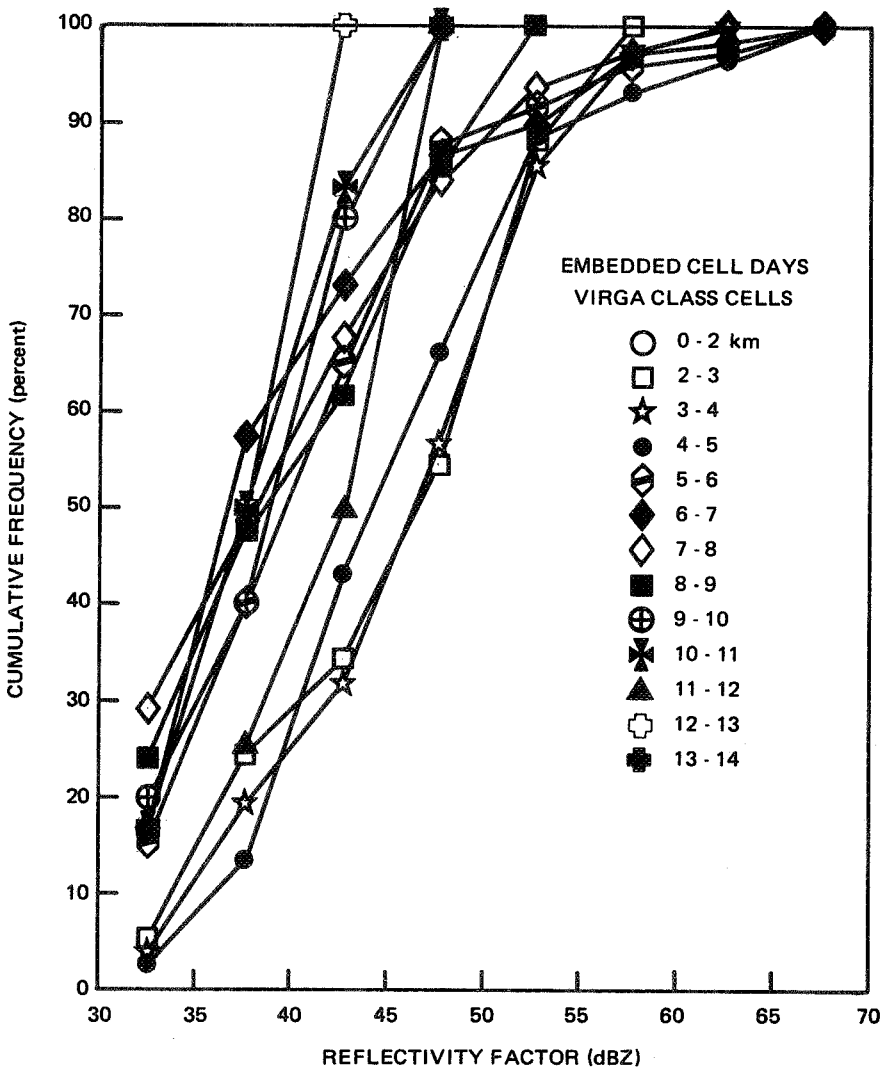

Figure 10.56. Cumulative Frequency Distribution for Virga Class Cells on Embedded Cell Days

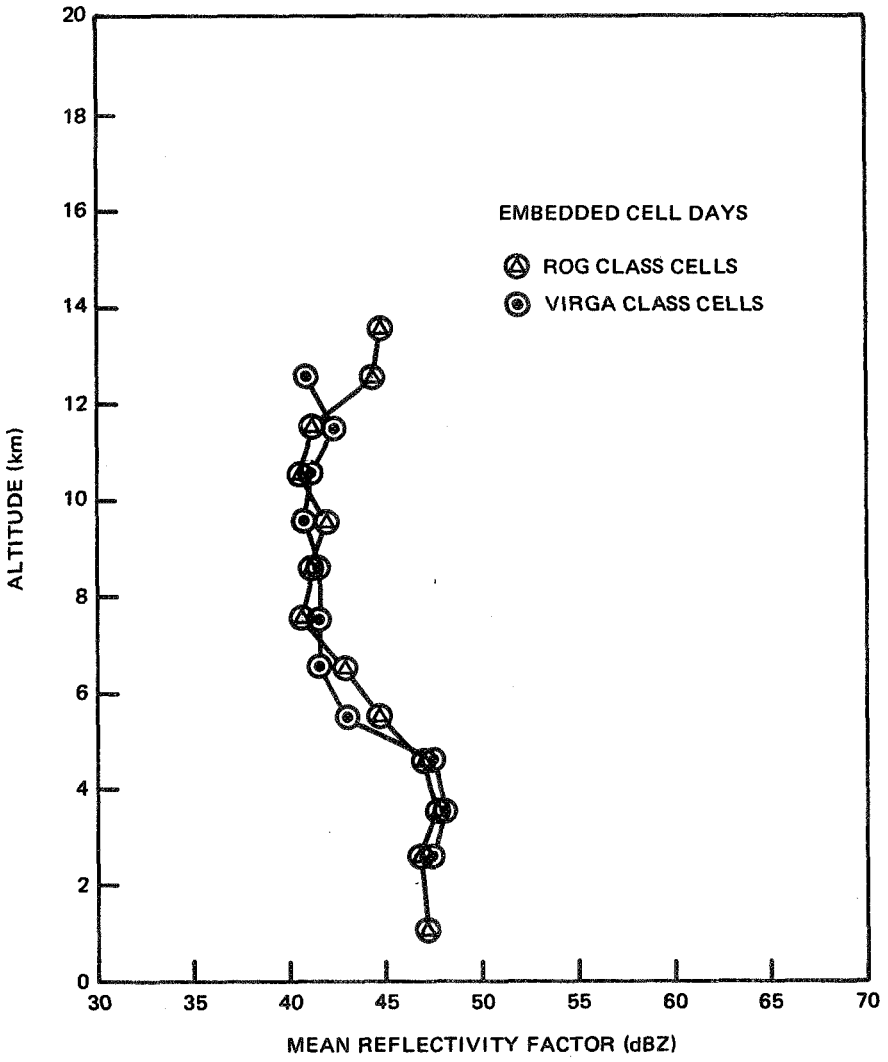

Figure 10.57. Profile of Mean Reflectivity Factor for All ROG Class Cells on Embedded Cell Days

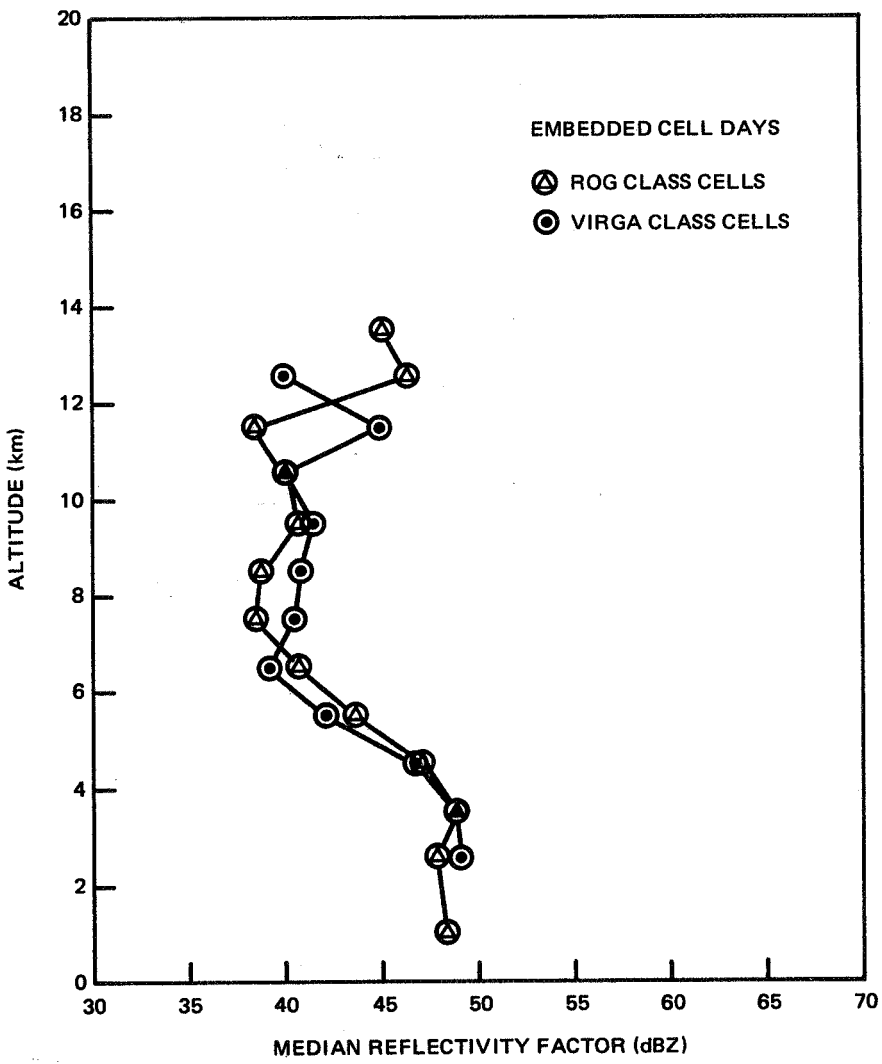

Figure 10.58. Profile of Median Reflectivity Factor for Virga Class Cells on Embedded Cell Days

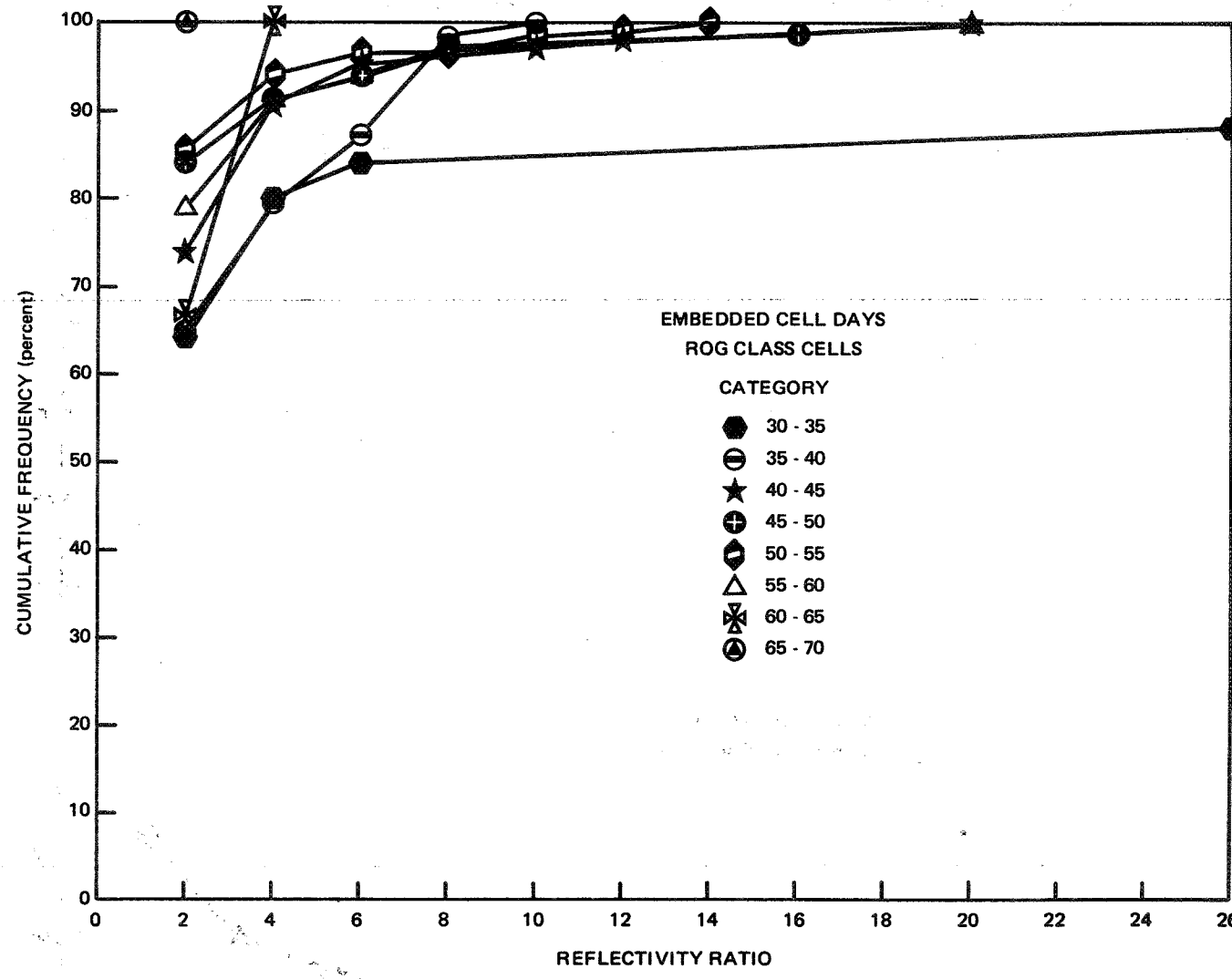

Figure 10.59. Cumulative Frequency Distributions of Reflectivity Ratio by Category for ROG Class Cells on Embedded Cell Days

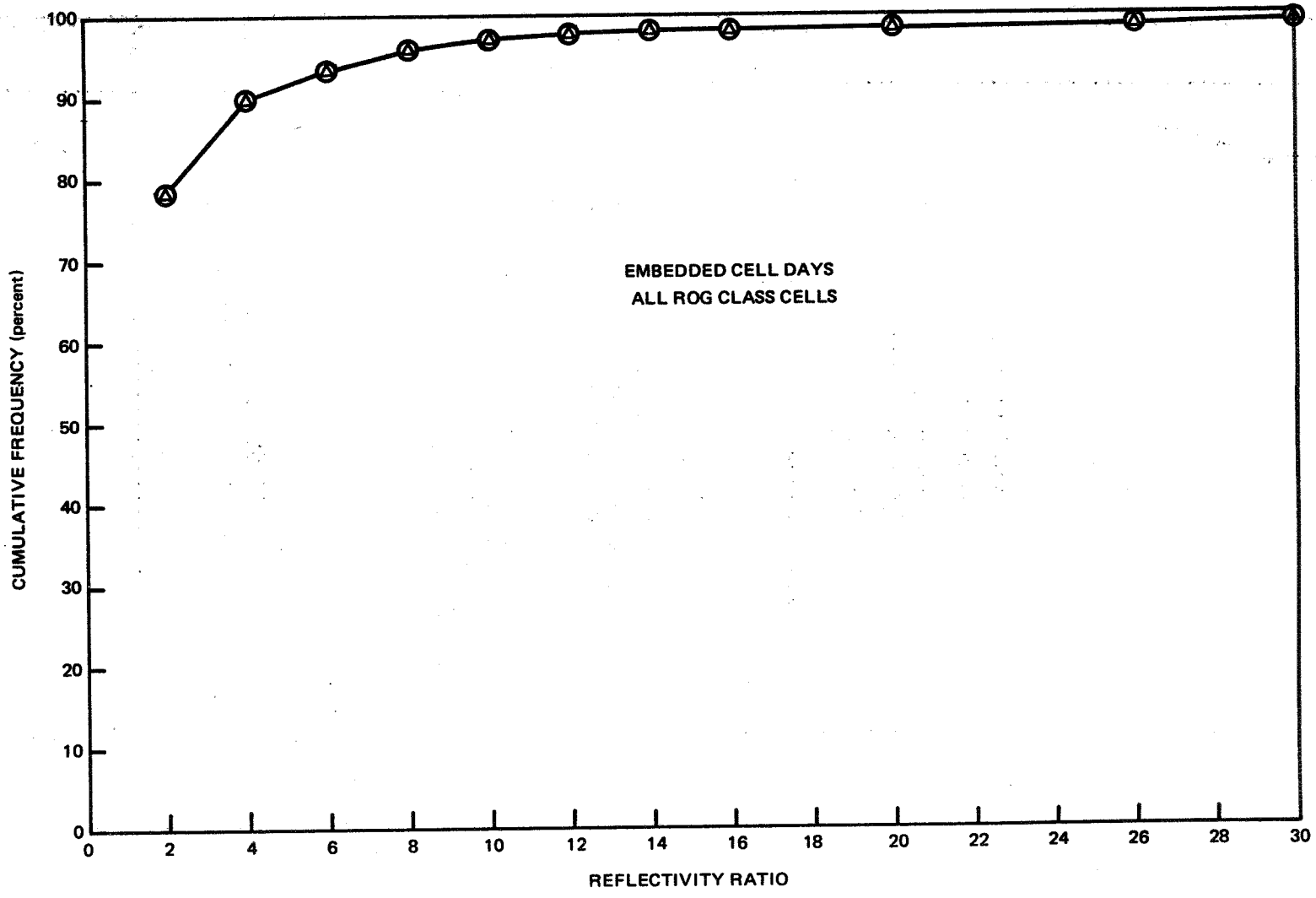

Figure 10.60. Cumulative Frequency of Reflectivity Ratio for All ROG Class Cells on Embedded Cell Days

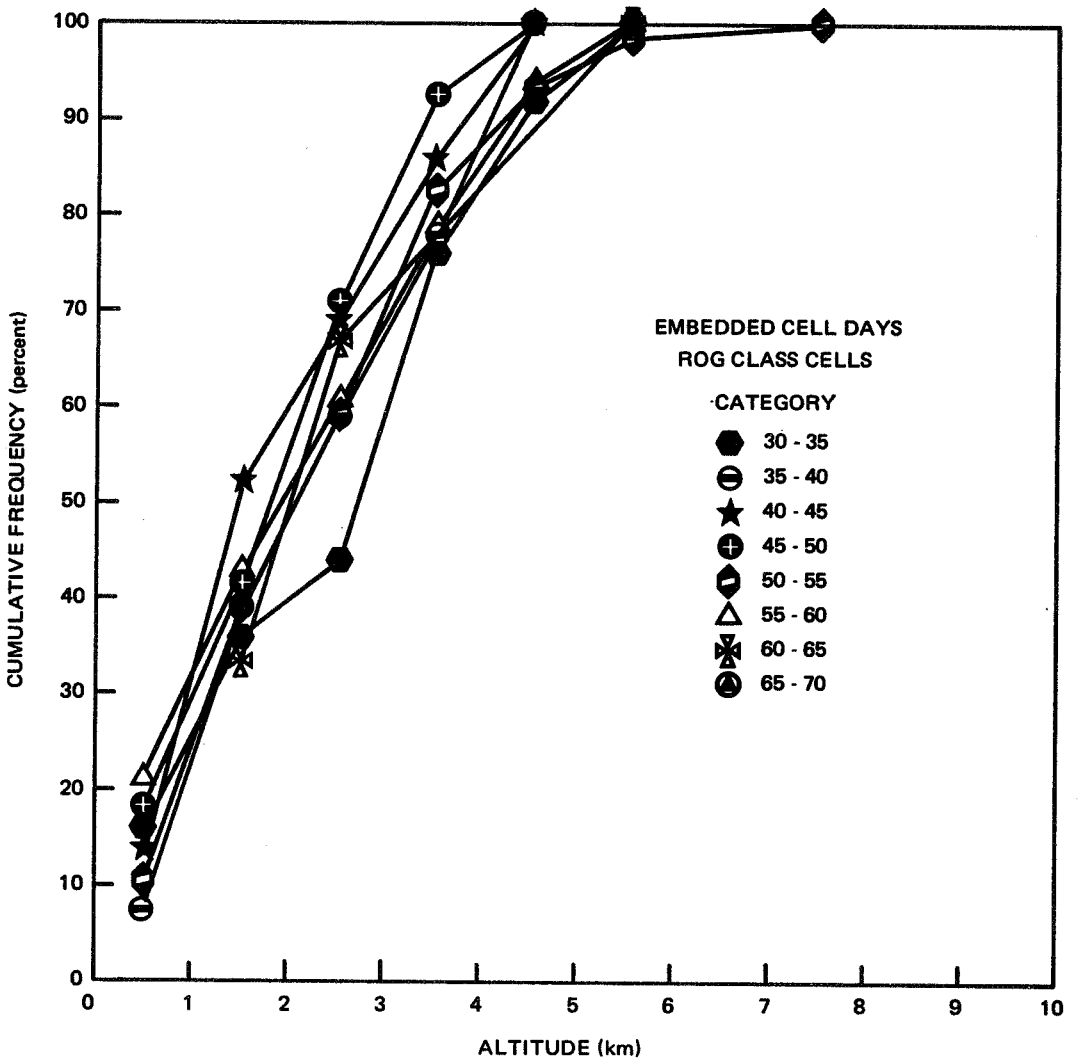

Figure 10.61. Distribution of the Height of the Maximum Peak Reflectivity for Embedded Cell Days by Category

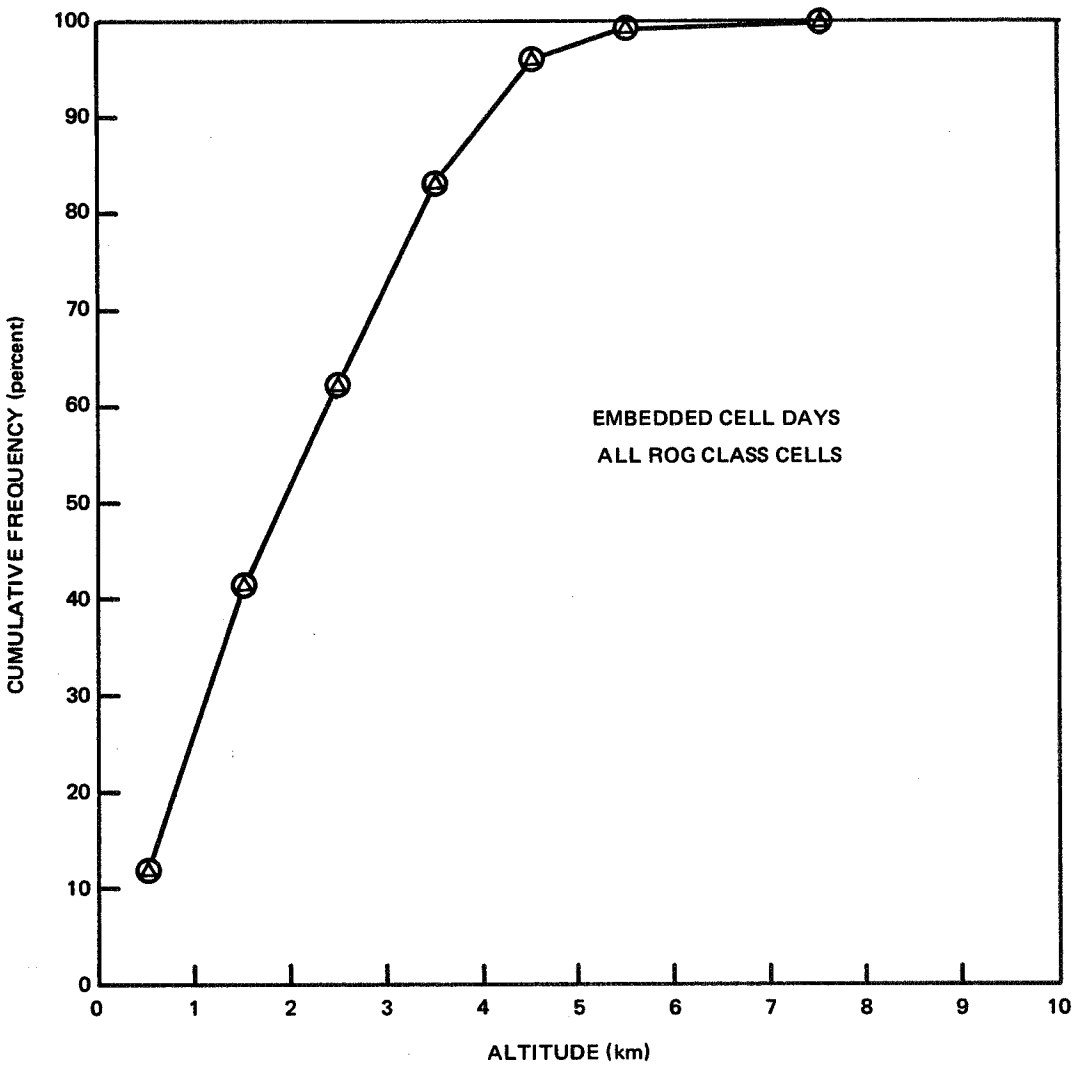

Figure 10.62. Distribution of the Height of the Maximum Peak Reflectivity for All ROG Class Cells on Embedded Cell Days

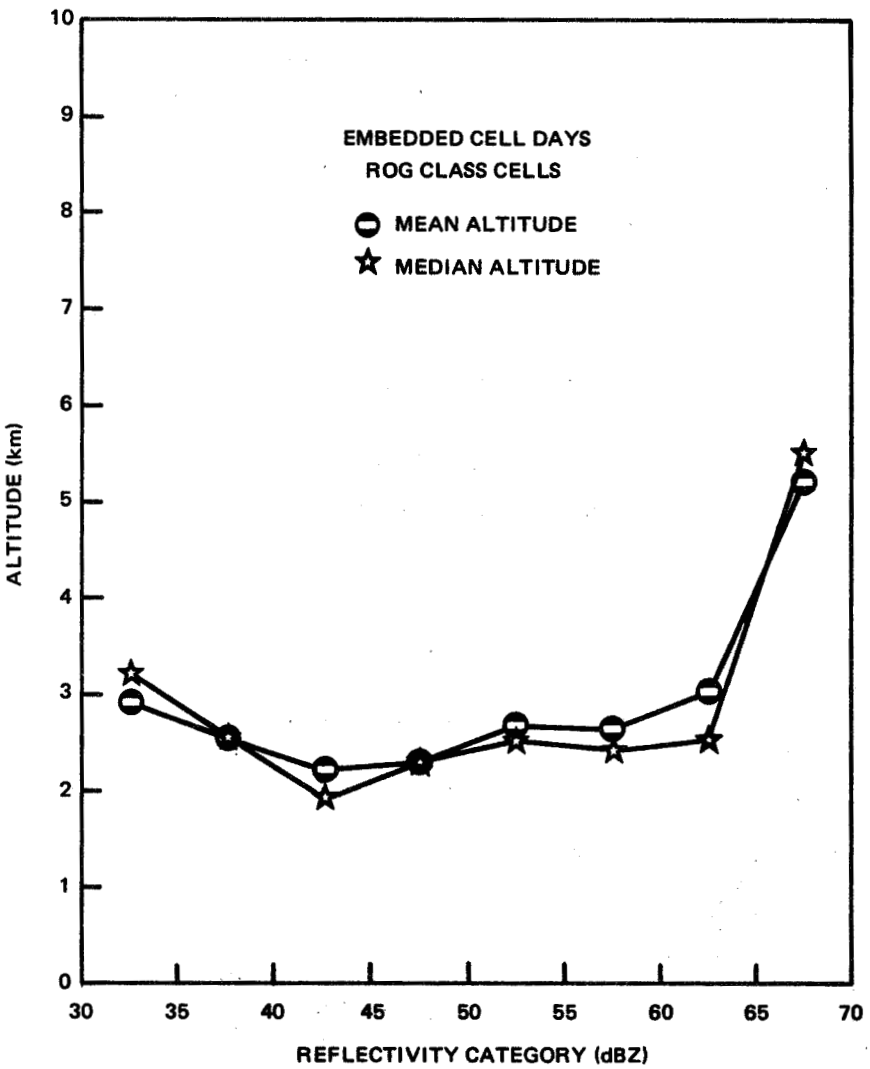

Figure 10.63. Mean and Median Heights of the Maximum Reflectivity According to Category for Embedded Cell Days

Referring to Figure 6.1, the locations of the peak or core reflectivities plotted for each cell in each scan are for different altitudes. The question arises, therefore, whether the distance between cells must be defined as a function of altitude. As discussed in Section 10.2.8, some cells do not extend as high as other cells so that the distribution of cell spacings is dependent on the distribution of cells by class and category, i.e., according to their intensity.

Rather than attempt to define a complex cell spacing which may be difficult to interpret and apply, a simple straightforward approach was used. The "center" of a cell was defined to be the center of the cluster of peak or core locations as determined by eye using the plots, such as Figure 6.1. This "center" is simply an eyeball average center location for all altitudes. Distances between these centers were then measured taking two cells at a time. The distance between any two cells was counted only once, however, That is, the distance between cell A to B is the same as from cell B to A. The population of scans, sweeps and cells included all cells regardless of class or category. The data were from the PPI sector scans of 60 deg or greater described in Volume I of this report. This finite azimuthal (or areal) coverage limits the maximum distances between cells which will be observed and measured. It was felt, however, that the lower end of the resulting frequency distribution would not be significantly affected. That is, the smaller distances, which are of interest, lie well within the dimensions of the area covered.

The frequency distribution and cumulative frequency of cell spacings are shown in Figure 10.64. The increment or bin size for distance was 2 nmi. Although the curves are rather smooth they do not follow any simple mathematical function such as log normal or Rayleigh. This is not too surprising, however, in light of the qualifications to the data discussed above which modify the distribution at larger values of spacing. The most probable distance between the cells is around 12 nmi with a median value of 18 nmi. Again, due to the bias in the data or lack of high values for cell separation, the median is questionable, but the mode should not be affected significantly. The 12 nmi dimension is well within the dimensions of the 60 deg or greater by 75 nmi radius quadrants used.

11. CONCLUSIONS

11.1 CORE REFLECTIVITY

Profiles of the mean and median core reflectivity for cells classified and categorized according to the rain intensity on the ground are, in general, well behaved and exhibit an orderly fall-off of reflectivity with altitude. The increase in altitude extent with increasing

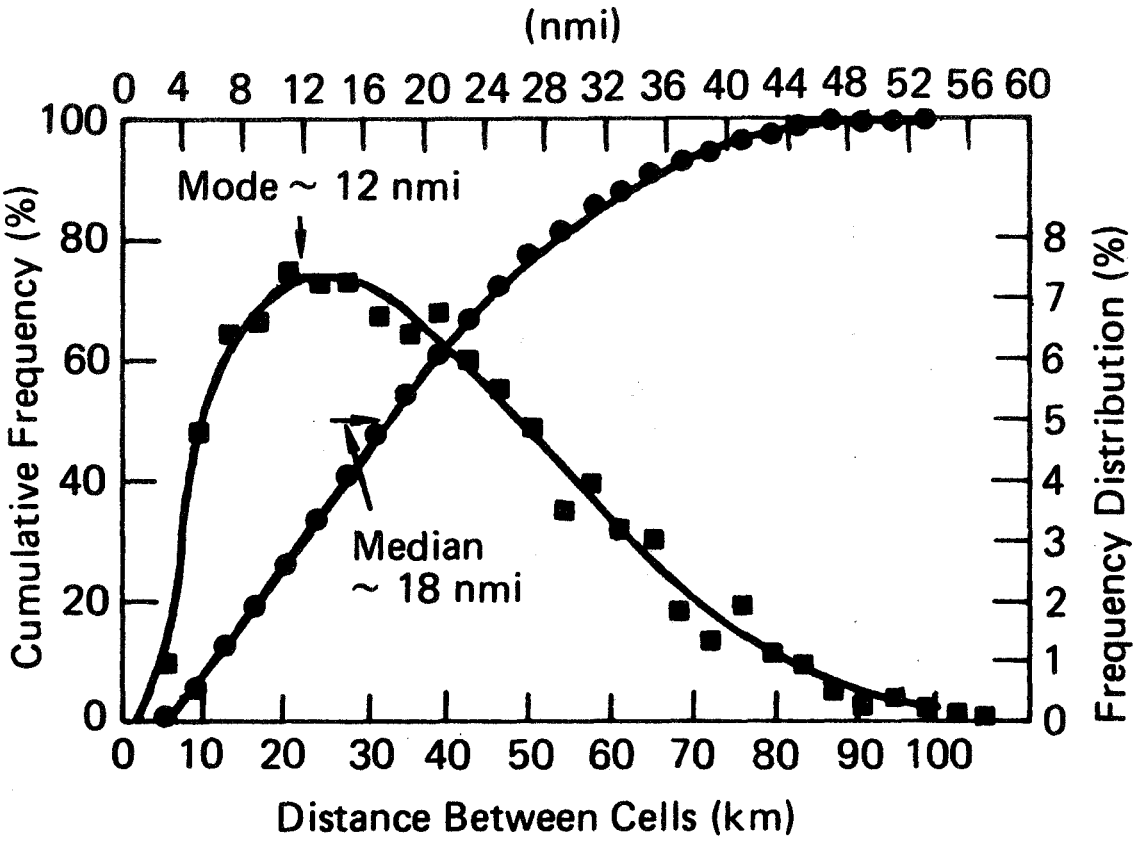

Figure 10.64. Distribution of Distance Between Rain Cell Centers

cell category is also evident. When all the rain cells observed during the summer are taken together, the resulting profile of reflectivity is in good agreement with that presented by other investigators such as Donaldson (Ref. 10).

11.2 REFLECTIVITY RATIO

No significant concentration of water at altitude is evident based on the reflectivity ratio distributions for the various categories of ROG class cells. More than half the cells had reflectivity ratios in the first interval, i.e., a ratio between 1 and 3. The distributions do indicate that cells with low reflectivities below 2 km, i.e., low category cells, have somewhat higher reflectivity ratios than the high category cells. This might be expected in that when rain on the ground

is heavy, one does not generally expect a larger rain rate aloft. The data also suggest that the effect of the bright band is not great in convective summer storms. Again, this is consistent with existing models of rain cells, especially thunderstorms. Further discussion of this point is contained in Section 11.3.

11.3 ALTITUDE OF THE MAXIMUM REFLECTIVITY

Distributions of the altitude of the maximum reflectivity substantiates the fact that the bright band is not strong in this type of rain cell. During the summer, the average altitude of the zero degrees isotherm occurred around 5 km. Over 90 percent of the altitudes for maximum reflectivity were below this altitude. In fact, 50 percent were in the lowest altitude interval, 0-2 km, i.e., the maximum reflectivity occurred essentially at ground level.

11.4 CELL AREA

Distributions of the area of the 10 dB contour relative to the peak reflectivity follow an exponential form but are independent of cell category, altitude, or local peak reflectivity value (effectively the contour reflectivity value). The distributions have a high standard deviation and suggest that cell area is not easily represented even in statistical terms. The most physically consistent and orderly relationship is between the mean contour area and the contour value (alternatively the liquid water content). This relationship shows the expected fall-off of contour area with increasing contour reflectivity, i.e., rain intensity.

11.5 LENGTH-TO-WIDTH RATIO

In general, the cumulative distributions show that 50 percent of the cells have a length-to-width ratio of three or less regardless of reflectivity interval, category or altitude. Roughly 80 percent have ratios of six or less. However, no consistent identifiable variation in the length-to-width ratio was found with any of the sorting parameters. There is some indication that the cells at lower altitudes have higher ratios than those cells at altitude. Such conclusions, however, must be tempered by the fact that there are fewer cells at altitude and as such the statistical confidence is low. It should be remembered that the length-to-width ratio calculated is not the result of any fitting by an ellipse or any other shape. It is simply the ratio of the maximum dimension through the centroid of the 10 dB contour area to the minimum dimension. It was intended only as a rough indicator of the contour shape.

11.6 CONTOUR ORIENTATION

The distributions of the orientation of the contour major axis show all directions from zero to 180 deg are equally probable. This is also shown in the cumulative frequency curves which are approximately a straight line between zero and 180 deg. The orientation was found to be independent of altitude, category, or peak reflectivity. Note that no comparison or sorting was made based on wind or frontal direction, however.

11.7 NUMBER OF CELLS BY CATEGORY FOR GIVEN ALTITUDE

The distributions of a number of cells at each altitude according to category may be used in a variety of ways by communicators. The distribution in the lowest altitude interval is more useful. It shows the probability of occurrence of rain cell intensity at any point in an area. Somewhat surprisingly, the most probable rain intensity is the 50-55 dBZ category or from 35 to 100 mm/hr rain rate. The distribution follows closely that found by Donaldson (Ref. 10) in the New England states but with a slightly higher mode. A somewhat related question may also be answered using these distributions, namely, given it is raining at a given altitude, what is the probability it is raining on the ground?

11.8 NUMBER OF CELLS BY HEIGHT FOR GIVEN CATEGORY

The distributions of cells by height for given categories is also quite useful in that they show the altitudes to which cells of given intensities may be expected to extend. The probability of rain cells reaching some altitude for known rain cell core intensity on the ground is of interest both to meteorologists and to communicators using earth-satellite links. The results show an orderly increase in the altitude extent for given probability with increasing category of cells up to the 50-60 dBZ category. For rain intensities greater than this value the altitudes remain essentially constant.

11.9 ISOLATED VS EMBEDDED RAIN CELLS

The attempt to analyze the characteristics of rain cells according to the type of rain pattern did not reveal any consistent, identifiable differences between those cell days which were identified as having isolated cells and those where the cells were embedded in larger, mesoscale systems such as fronts.

12. RECOMMENDATIONS

The experiment was initially designed to provide rain cell data which could be used for many purposes, e.g., to determine probability of occurrence of cells, cell intensity vs altitude, time histories, etc. For practical reasons much of the proposed analysis was cut short thus leaving much yet to be done. Described here are five subjects considered vitally important. It is recommended that they be pursued actively in a follow-on analytical effort:

1. Cell life history study
2. Cell intensity vs cell size
3. Attenuation statistics for space diversity
4. Extrapolating statistics to other geographic areas
5. Development of an objective meteorological characterization related to the radar derived characteristics.

The life cycle of rain storm systems and individual rain cells are determined by the dynamics of the meteorological process. A wide variety of weather data were gathered during the experiment consisting of surface and upper air observations from many of the surrounding weather stations. In addition to the routine PPI raster scans through the depth of the rain cells, time histories of cells were documented by repeatedly scanning as fast as possible an area of rain cells with the antenna at a constant elevation. With this combination of weather and radar data one can find how cells move relative to the wind, how long individual cells last, how individual cells behave in comparison to the motion of the entire storm, among other things. Also, since Wallops Island fortuitously encompasses land-water boundaries, cell development can be studied as a function of the surface over which the storm is moving. The planning of communications links near shore lines would obviously be helped by results of this study.

The relationship between rain intensity and cell size has two aspects. One is how does the intensity vary with distance out from the core of the rain cell? Previous research has shown a square root or cube root relationship. The other view is how does the area of a selected level of intensity down from the core vary with the core intensity

level? It was this latter question which was analyzed in the present study. Verification of the first question was not attempted and remains unanswered. It is recommended that the tapes be rerun with the appropriate program to look for cell size vs intensity out from the cell core. Answers to this question bear strongly on calculations of scatter interference and attenuation.

The data base accumulated in this experiment are invaluable in providing fading statistics and space diversity data. Work along these lines has already begun to study the fading statistics and space diversity for frequencies above 10 GHz and for satellite path angles 30 to 90 deg. These are part of a separate analytical and experimental program involving the ATS-6 satellite and is reported elsewhere. However, much remains to be done in this direction. For example, one should also examine the data to find fading statistics and path diversity for zero degree elevation, applicable to terrestrial link placement. Also this analysis should take angular orientation into account. In this way the effects of frontal precipitation and random air mass rains can be evaluated. As mentioned before, the weather data are available for this study.

The fourth recommendation is perhaps the most important and has not yet been attempted. This study concentrated on summer showers occurring in an east coast, mid-latitude area. Any attempt to extrapolate to other areas must be linked to ground rainfall measurements made at a point. Thus the statistics of cells in which the rain data were accumulated at 20 to 30 min sampling intervals should be related to the point rainfall measurements made at Wallops Island during the experiment. With this accomplished it is anticipated that one could extrapolate to other areas in which the point rainfall statistics are similar.

Finally the rain cell model for microwave scattering and attenuation varies with "climatic regions." However, the classifications developed by climatologists were not prepared for the communicators - rather, they are more pertinent to agronomists and hydrologists, neither of whom are particularly interested, for example, in the vertical extent of rain. There is the need to derive a suitable rain descriptor for communication purposes. With such a parameterization, a world-wide communications-oriented map can be prepared from existing meteorological data. It is proposed that the data taken in this program be blended with the concomitant meteorological data for the purpose of obtaining an objective meteorological characterization related to the measured reflectivities. There now exists several such parameters, used in severe storm forecasting, for example. These parameters, computable from

radiosonde data, have been related successfully to occurrence or non-occurrence of radar echoes - but this is not quantitative. It is proposed that a quantitative (numerical) assessment be made. There is promise that such quantities as probability of high reflectivity, areal extent, etc., can be obtained.

13. REFERENCES

1. Kropfli, R.A., "Radar Data Reduction Plan for the CLC Experiment," APL/JHU Memo MPD73U-036, 30 April 1973.

2. Kropfli, R.A., "Specification and Logic for Reflectivity Contouring Program," APL/JHU Memo MPD72U-15, 3 May 1972.

3. Lawson, M.W., "Description of the FORTRAN IV Program to Analyze High Resolution Radar Scans Through Severe Thunderstorms," APL/JHU Memo BCP-598 (Rev 1), 25 October 1973.

4. Kropfli, R.A., "Second Pass Program Specifications," APL/JHU Memo MPD72U-050, 14 November 1972.

5. Goldhirsh, J., "Measured Radar Parameters and Error Budget Associated with SPANDAR and the CLC Program," APL/JHU Memo MPD73U-054, 9 July 1973.

6. Goldhirsh, J., and Kropfli, R.A., "Inclusion of Atmospheric Attenuation Contribution in Radar Equation," APL/JHU Memo MPD73U-014, 26 February 1973.

7. Blake, L.V., "Ray Height Computation for a Continuous, Non-linear Atmospheric Refractive Index Profile," Radio Science, Vol. 3, 1968, pp. 85-92.

8. Sellers, S.J., "Description of PL/1 Computer Program to Perform Statistical Analysis of Data Collected Through High Resolution Radar Scans of Rain Showers," APL/JHU Memo BCP4-007, 5 August 1974.

9. Altman, F.J., Elliptical Storm Cell Modeling of Digital Radar Data, NASA Report X-752-72-438, March 1972.

10. Donaldson, Ralph J., "Radar Reflectivity Profiles in Thunderstorms," J. Meteor., Vol. 18, June 1961, pp. 292-305.

*U.S. GOVERNMENT PRINTING OFFICE: 1975 - 635-275/28